# Design of a Large-Scale Electrochemical $CO_2$ Reduction Process

## Master's Thesis

Matthijs Kroes

TU Delft

# Design of a Large-Scale Electrochemical $CO_2$ Reduction Process

By


## Matthijs Kroes


In partial fulfilment of the requirements for the degree of

**Master of Science**
In Chemical Engineering

At the Technical University of Delft,
To be defended publicly on Thursday April 20, 2023 at 2:15 pm.

| | |
|---|---|
| Supervisor: | Prof. Dr. Ir. W. de Jong |
| Thesis committee: | Prof. Dr. Ir. W. de Jong |
| | Dr. R. Kortlever |
| | Dr. Ir. A. Somoza-Tornos |
| | Prof. Dr. Ir. A. Urakawa |


An electronic version of this thesis is available at http://repository.tudelft.nl/.



TU Delft Delft University of Technology

# Abstract

The rise of $CO_2$ concentration in the atmosphere is a leading cause of global warming. Utilizing $CO_2$ obtained from point sources, such as chemical industries, as a feedstock to produce high energy density fuels and chemicals could mitigate the emission of $CO_2$ as well as provide various economic benefits. One promising technology is the electrochemical reduction of $CO_2$, however, the presence of contaminants in the industry-supplied feedstock and the separation of products downstream would be challenging in a continuously operated large-scale plant. To address these challenges and indentify the bottlenecks involved, it is important to study which pre-treatment and post-treatment steps are required and how to integrate these in a large-scale electrochemical $CO_2$ reduction process.

The gas and liquid feed streams to the $CO_2$ electrolyzers are first cleaned to the desired levels. The liquid feed stream is water from the river Rhine that is purified so the specifications of the water meet the requirements for type 1 water (ultrapure water). The gas feed stream is the flue gas stream of an average steel-producing plant in Europe and is cleaned to remove sulfur and nitrogen compounds. A two-step electrolysis process is used where $CO_2$ is first reduced to CO, followed by the reduction of CO to $C_{2+}$ products. The electrolyzer for the first step is a membrane electrode assembly-based flow cell with a current density of 300 $mA\ cm^{2-}$ and a faradaic efficiency (FE) of 96% to CO. In the second step, a gas diffusion electrode-based flow cell with a current density of 300 $mA\ cm^{2-}$ and a faradaic efficiency of 9.35%, 15.49%, 45.57%, and 16.38% towards acetic acid, ethanol, ethylene, and propanol, respectively, is used. The anolyte and catholyte in the reactors are recycled 3,500 and 2,000 times, respectively, to reduce the size of purification of the liquid feed stream section and increase the liquid product concentration. In both steps, unreacted $CO_2$ and CO are recycled. The gaseous and liquid products are separated and purified to meet the industry standards using established separation techniques.

The total capital investment for a process with an industrial gas feed of 381.678 tons per hour is 4,053.5 million dollars with a daily operating cost of 7.403 million dollars. The daily income from selling the products is 2.363 million dollars, but this could increase if the FE towards acetic acid is increased since this product has the highest income per electron consumed. The net present value (NPV) for the base case, assuming current technological and market conditions, is -19.4 billion dollars after 15 years. To analyze which parameters have the most influence on the NPV, a sensitivity analysis is also performed with a better and optimistic scenario. It was found that the economic feasibility of the currently designed process is not limited by the technological progress, but mainly by the market conditions.

The target of this process is to reduce the emission of $CO_2$, however, the operation of the plant itself contributes to some $CO_2$ emissions. Therefore the process should consume more $CO_2$ than it emits. The units that consume most energy and emit the most $CO_2$ are the CO to $C_{2+}$ products electrolyzer and the first distillation column in the liquid product separation section to remove acetic acid. It was found that the process is only carbon negative when the consumed energy is generated by nuclear, wind, or solar energy. The net $CO_2$ emission is the lowest when nuclear or wind is used as an energy source. Generating all the required energy from these sustainable sources brings another challenge since the total installed capacity of these sources are currently not sufficient to cater to the needs of such a large-scale continuously operating $CO_2$ electrolysis plant.

**Keywords:** Electrochemical $CO_2$ reduction, large-scale, pre-treatment, post-treatment, techno-economical analysis, energy analysis

# Acknowledgement

First of all, I want to express my gratitude to all members of the defense committee for offering their time and reviewing my thesis.

Furthermore, I want to thank Asvin Sajeev Kumar and Isabell Bagemihl for guiding and helping me during my thesis. They helped me with all the struggles and questions I had and they also provided me with useful comments and tips to improve my report.

I would also like to thank all my colleagues at the Large-Scale Energy Storage and Product and Process Engineering group. They provided me with helpful input for my thesis project during group and personal meetings.

Lastly, I want to thank my family and friends who always supported me and where I could go for relaxation.

# Contents

# List of Figures

# List of Tables

# Abbreviations

**AC** Activated Carbon.

**AEM** Anion Exchange Membrane.

**BPM** Bipolar Membrane.

**CapEx** Capital Expenses.

**CD** Current Density.

**CE** Chemical Engineering.

**CEM** Cation Exchange Membrane.

**$CO_2$** Carbon Dioxide.

**$CO_2$RR** Carbon Dioxide Reduction Reaction.

**ED** Electrodialysis.

**EDI** Electrodeionization.

**EDTA** Ethylenediaminetetraacetic Acid.

**ENR** Engineering News-Record.

**EROEI** Energy Return On Energy Investment.

**f.o.b.** Free On Board.

**FE** Faradaic Efficiency.

**GDE** Gas Diffusion Electrode.

**MDEA** Methyl diethanolamine.

**MEA** Membrane Electrode Assembly.

**MFC** Microfluid Flow Cell.

**MS** Marshall and Swift.

**NF** Nelson-Farrar.

**NPV** Net Present Value.

**OOR** Organic Oxidation Reaction.

**OpEx** Operating Expenses.

**PEM** Polymer Electrolyte Membrane.

**PEMFC** Proton Exchange membrane Flow Cell.

**PSA** Pressure Swing Adsorption.

**PV** Pervaporation.

**Redox** Reduction and Oxidation.

**RHE** Reversible Hydrogen Electrode.

**RO** Reverse Osmosis.

**ROI** Return On Investment.

**SCR** Selective Catalytic Reduction.

**SHE** Standard Hydrogen Electrode.

**SOEC** Solid-oxide Electrolysis Cell.

**TCI** Total Capital Investment.

**TEA** Techno-Economic Analysis.

**TRL** Technology Readiness Level.

**UF** Ultrafiltration.

**UPW** Ultrapure Water.

**UV** Ultra Violet.

# Symbol list

| Greek letter | Description | Unit |
|---|---|---|
| $\alpha$ | Charge Transfer Coefficient | $[-]$ |
| $\eta$ | Overpotential | $V$ |
| $\pi$ | pi | $[-]$ |

| Symbol | Description | Unit |
|---|---|---|
| $C_B$ | Base Cost | \$ |
| $C_{P_i}$ | Free on Board Price of Unit i | \$ |
| $C_P$ | Free on Board Price | \$ |
| $C_P$ | Cost for Platforms and Ladders | \$ |
| $C_T$ | Cost for Installed Trays | \$ |
| $C_{BT}$ | Base Cost for Installed Trays | \$ |
| $C_V$ | Cost for Vertical Tower | \$ |
| $C_{TCI}$ | Total Capital Cost | \$ |
| $D$ | Diameter | $m$ |
| $E^0$ | Thermodynamic Reaction Voltage | $V$ |
| $E$ | Electrode Potential | $V$ |
| $E$ | Fractional Weld Efficiency | $[-]$ |
| $E_{eq}$ | Equilibrium Potential | $V$ |
| $EE$ | Energy Efficiency | % |
| $f_{L_{TCI}}$ | Lang factor | $[-]$ |
| $F$ | Faraday Constant | $A\ s\ mol^{-1}$ |
| $F_t$ | Type Factor | $[-]$ |
| $F_{nt}$ | Number of Trays Factor | $[-]$ |
| $F_{tt}$ | Tray Type Factor | $[-]$ |
| $F_m$ | Material Factor | $[-]$ |
| $FE$ | Faradaic Efficiency | % |
| $H$ | Height | $m$ |
| $i$ | Current Density | $A\ m^{-2}$ |
| $i_0$ | Exchange Current Density | $A\ m^{-2}$ |
| $I$ | Index | $[-]$ |
| $I_i$ | Updated CE Index | $[-]$ |
| $I_{b_i}$ | Base CE Index | $[-]$ |
| $L$ | Length | $ft$ |
| $m$ | Number of Moles of Product | $mol$ |
| $n$ | Number of Electrons Transferred | $[-]$ |
| $N_T$ | Number of Trays | $[-]$ |
| $P_b$ | Break Power | $Hp$ |
| $P_D$ | Design Pressure | $psi$ |
| $P_G$ | Gauge Pressure | $psi$ |
| $q$ | Total Applied Charge | $A\ s$ |
| $Q$ | Flow Rate | $gal\ min^{-1}$ |
| $R$ | Universal Gas Constant | $J\ K^{-1}\ mol^{-1}$ |
| $iR_s$ | Ohmic Loss | $V$ |
| $R$ | Gas Constant | $J\ K^{-1}\ mol^{-1}$ |
| $S$ | Size Factor | $[-]$ |
| $t_p$ | Wall Tickness to Withstand Internal Pressure | $inch$ |

| | | |
|---|---|---|
| $T$ | Temperature | $K$ |
| $V$ | Volume | $m^3$ |
| $W$ | Weight | $lb$ |
| $z$ | Number of Electrons Involved | $[-]$ |

# Assumptions

**Process**

1. ASPEN Plus V12 Template Electrolytes with Metric Units is used to design the model
2. NRTL method is used to model the upstream and downstream liquid phase processes and the electrolyzers in ASPEN Plus V12
3. ELECNRTL method is used to model the upstream gas phase processes in Aspen Plus V12
4. PENG-ROB method is used to model the downstream gas phase processes in Aspen Plus V12
5. The process is a fluid processing plant
6. The pressure drop in the gas and liquid phase downstream product separation units are negligible

**Feed streams**

7. The average water concentration of the Rhine is used at the measuring station near Nieuwegein, Utrecht, The Netherlands from 2021
8. The concentration of ions in the liquid feed stream to the ultrapure water production is constant
9. The gas feed composition entering the gas purification part is constant
10. The gas feed is 381,678 ton/hr and the flow rate is constant
11. The feed water from the river has a constant temperature of 13.3°C

**Electrolyzers**

12. Only carbon monoxide, ethylene, hydrogen, and methane are formed in the electrolyzers in the gaseous phase and will leave the electrolyzer in the gaseous phase
13. Only acetate, ethanol, and propanol are formed in the liquid phase and will leave the electrolyzer in the liquid phase
14. The large-scale electrolyzers operate at the same current density, faradaic efficiency, and single pass conversions as mentioned in the reference article
15. The average residence time in an electrolyzer for the electrolyte is 1 minute
16. All $OH^-$ that passes through the electrolyzer membrane is consumed immediately
17. No loss of $CO_2$ due to carbonate formation or other side reactions
18. Recycling electrolyte does not influence the electrolyzer specifications if the water mole fraction is 0.8 or higher
19. pH in the electrolyzers remain the same as mentioned in the articles
20. The transport phenomena in all channels and all cells are the same and scalable
21. Acetic acid will only leave the CO electrolyzer in deprotonated form

**Units**

22. All the units function identically on a large scale as indicated in the referenced articles
23. All the components not mentioned in the reference articles pass through the membranes unaffected.
24. The pressure after a membrane separation unit is 1 bar
25. Pump efficiency is obtained from ASPEN PLUS V12 and is 86%
26. Pumps have an open, drip-proof type of enclosure
27. Flash drums have an average residence time of 5 seconds
28. COS to $H_2S$ reactor is an autoclave
29. The average residence time in the COS to $H_2S$ reactor is 1 minute
30. Ions are perfectly removed before liquid products separation for modelling purposes, but this does not influence the separation
31. In pervaporation units, 98% of the diffusing compounds pass through the membrane
32. All gas impurities leave the PSA unit in the product stream
33. Heat exchangers are floating head heat exchangers
34. All units are made from stainless steel 304

**Techno-economic and energy analysis**

35. Prices for utility streams and $CO_2$ emission data from ASPEN PLUS V12 is used
36. $CO_2$ emission in ASPEN PLUS V12 used for heating is based on natural gas as energy source
37. The maintenance costs for each unit are assumed to be 2.5% of the CapEx of the unit
38. The f.o.b. purchase price for all PSA units are based on the price of a $H_2$ PSA unit
39. Flash drums are pressure vessels
40. Flash drums have a height 4 times its diameter with a cylindrical shape

# 1

# Introduction

Since the start of the industrial revolution, the concentration of $CO_2$ and other greenhouse gasses in the atmosphere has increased[1]. The rise of $CO_2$ in the atmosphere is causing global climate change with more extreme weather conditions, rising sea levels, and fewer ice caps at the poles, consequently[2–4]. International treaties, such as the Paris Agreement, have led to deals to reduce or completely stop the emission of $CO_2$ to mitigate the impacts of climate change[5]. Transitioning the world into a low-carbon economy, where resources are used efficiently, is the main target to fulfil the objectives agreed upon in climate treaties.

One of the largest contributor to $CO_2$ emissions is the chemical industry. Two proposed routes to reduce the emission of $CO_2$ in this sector is to shift from fossil fuel based processes to electrified processes or to capture the emitted $CO_2$ to decrease the emission into the atmosphere. Capturing $CO_2$ from industrial point sources is an established technology where $CO_2$ can either be used directly or as a feedstock for other chemical processes. Some applications for direct use of $CO_2$ on a large scale are enhanced gas or oil recovery and enhanced geothermal systems, but $CO_2$ can also be used directly for small-scale applications, such as in the beverage industry or fire extinguishers[6, 7]. Other technologies where $CO_2$ is converted to value added chemicals include homogeneous, heterogeneous, photochemical, electrochemical, catalytic, and biochemical conversion[8–15]. These indirect methods have the potential to close the carbon cycles, which is considered the core strategy, and generate a circular carbon economy where fossil resources are superfluous. Before these technologies can be deployed on an industrial scale, they have to be able to produce chemicals and fuels more sustainably in terms of environmental requirements, economic requirements, market size, and social perspective[16, 17].

The previously mentioned conversion technologies are not as elaborated as equivalent fossil-based techniques and are still at a low technology readiness level (TRL). The commercial viability of these techniques is low, due to high investment costs and the absence of an all-considering $CO_2$ emission tax which promotes the research towards these techniques[18]. Using $CO_2$ as a feedstock is an opportunity to have an inexpensive or negatively priced carbon source but requires a considerable energy input to reduce to a more valuable compound. The availability of a low-cost energy source that is also renewable is essential for this route to become economically feasible as well as carbon-negative. Nowadays, the cost of renewable electrical energy is competitive with the cost of electricity generated by coal[19]. A downside of renewable energy is that the surplus of energy fluctuates more than energy generated by fossil fuels which can influence the processes.

One technique that has drawn a large deal of attraction from the industry and the research world is the electrochemical reduction method to reduce $CO_2$ into higher-value compounds. Since renewable energy sources mainly produce electricity as a source of energy, this technique has great potential and it is carried out at room temperature and atmospheric pressure. Together with the fluctuation of surplus in electrical energy, electrochemical $CO_2$ reduction can store the excess energy which can be used later. Additionally, electrochemical $CO_2$ reduction can reduce the net carbon footprint of chemical production, as the $CO_2$ used in the process is captured from the atmosphere or industrial processes.

It has the potential to transform the industry and create new economic opportunities by generating value from a product that is now considered a waste product.

This method has achieved large development in the past years and there are even small pilot plants built[20]. In order for the electrochemical reduction of $CO_2$ to become feasible on a large, industrial scale, a number of challenges must be addressed. One such challenge is ensuring that the streams entering the electrolyzer have a high concentration of $CO_2$ and are free from harmful contaminants, including $H_2S$, $SO_2$, $NO_2$, and heavy metals, to maintain the performance and prevent deactivation of the catalyst[21, 22]. The feed streams consist of a flue gas stream and a liquid stream of water that need to be purified to ultrapure water. Various techniques for separation are used to achieve the required level of purity and eliminate undesired substances to an acceptable concentration. The allowable concentration of unwanted compounds in the feed stream is dependent on the influence these compounds have on the catalyst performance and deactivation. $CO_2$ is converted in two steps. First, $CO_2$ is converted in CO and in the second step CO is converted in $C_{2+}$ products. In both steps, the electrolyzers operate at atmospheric pressure and temperature. The streams leaving the the electrolyzers consist of both unreacted $CO_2$ or CO and the desired products. The unreacted $CO_2$ or CO is removed to be recycled and the electrolyte is reused to reduce cost and increase the liquid products concentration. The products are separated and purified to the industrial-required specifications using well-established separation methods.

The purpose of this thesis is to design an industrial-scaled electrochemical $CO_2$ reduction process and finding the answers to the research questions stated below.

1. What pre-treatment and post-treatment steps are required for the gas and liquid phases for the continuous operation of a large-scale, low-temperature electrochemical $CO_2$ reduction process?
2. Design an integrated large-scale electrochemical $CO_2$ reduction process to maximise the production of $C_{2+}$ products.
3. What are the bottlenecks in scaling-up an electrochemical $CO_2$ reduction process from a techno-economic and energy point of view?

In Chapter 2, the theory that is needed to understand this thesis is explained. This is followed by the Basis of Design (Chapter 3) where the battery limit, feed streams composition, and the requirements and specifications of the process are stated. In Chapter 4, the process is modelled and design specifications are described. In Chapter 5, the stream results from the liquid and gas purification section are discussed and a techno-economical and energy analysis on the process is performed. In the last two chapters the conclusions and recommendations of the thesis are given.

# 2

# Theory

In this chapter, the theory of the design of the process and the processes that are taking place are explained.

## 2.1. Electrochemistry

Electrochemistry is the use of electricity as a driving force to proceed a chemical reaction by transferring electrons. It encompasses the study of the behavior of electrons in chemical reactions, as well as the design and development of devices that use or produce electricity through chemical reactions. The chemical reaction in electrochemistry, which is called an oxidation-reduction (redox) reaction, is a combination of two half reactions. During these reactions, the oxidation states of the compounds change with the addition or loss of an electron. These half reactions occur at the anode and the cathode, which are called the electrodes.The oxidation reaction takes place at the anode and the reduction reaction takes place at the cathode. The electrons are transferred from the anode to the cathode by an electron-conducting medium between the two electrodes. The electrodes are separated by an ion conducting and a non electron-conducting electrolyte that exchanges ions, and an ion exchange membrane. This is to avert the reduced products from oxidizing again. Membranes used typically are anion exchange membrane (AEM), cation exchange membrane (CEM), or bipolar membrane (BPM) depending on the formed products and pH[23].

### 2.1.1. Electrolyzer

An electrolyzer is a device that uses electrical energy to drive a chemical reaction that would otherwise be non-spontaneous. This is the opposite of a galvanic cell where an electric current is produced by a spontaneous redox reaction. The Gibbs free energy of the $CO_2$RR in an electrolyzer is positive, so an additional electrical energy input is required for the reaction to occur. The basic components of an electrolyzer include an anode and a cathode, which are separated by an electrolyte, and an external circuit that supplies the electrical energy. The cell design and type of cell have a large influence on the Faradaic efficiency, current density, and stability. There are two types of electrolyzers that are commonly used: h-cell and flow cell[24, 25]. Another type of electrolyzer that has drawn attention recently are membrane electrode assembly (MEA) cells[26].

H-type cells are the most used and well-known cells in lab-scale reactors for the $CO_2$RR, because of their low cost, simple usage, and easy product separation. The reactor owes its name to the shape of the reactor as is observable in Figure 2.1. In an H-cell, there are two compartments that are connected by an ion exchange membrane. One chamber is the cathodic chamber, where the $CO_2$ is reduced. The other chamber is the anodic chamber, where the counter reaction takes place. The downside of this reactor is the low solubility of $CO_2$, which is caused by mass transfer limitations leading to performance insufficient for industrial application[27].

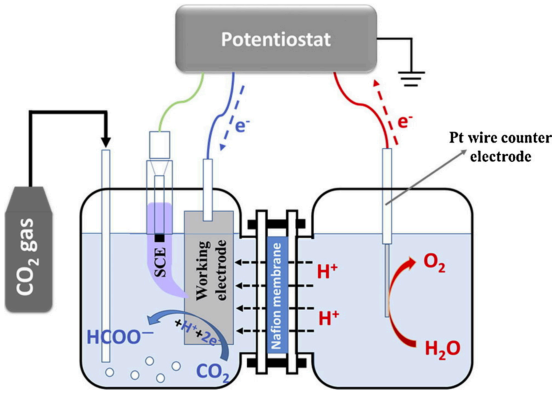


Figure 2.1: Schematic image of a H-type electrochemical cell[23]

Flow cells have drawn a lot of attention due to their efficient mass transfer efficiency and high possible current densities[27]. The reason is that the flow cell can continuously circulate reactants and products, so a higher $CO_2$ concentration is achieved at the electrode surface. Next to the increased mass transfer efficiency, the flow cell can also performs $CO_2$RR in the gas phase which deals with the low solubility of $CO_2$ in water. There are three different kinds of flow-cell type electrolyzers; polymer electrolyte membrane (PEM) flow cells, microfluidic flow cells (MFC), solid-oxide electrolysis cells (SOEC).

PEM flow cells resemble proton exchange membrane fuel cells (PEMFC) and are the most extensively studied type of flow cell[23, 28–30]. The configuration of a PEM flow cell is also almost the same as a PEMFC and consists of a cathode and anode current collector, a flow plate, and a membrane electrode assembly (MEA) as shown in Figure 2.2a. The MEA is a composition of the PEM, cathode gas diffusion electrode (GDE), and anode GDE. A GDE is an electrode with a gas, liquid, and solid interface and a catalyst where the reaction between the liquid and gas phase occurs. The GDE is typically made of carbon fiber and a microporous layer (MPL) with the coated catalyst[31].

Microfluid flow cells are used to research the catalyst performance on $CO_2$RR. They consist of a cathode gas channel, a cathode current collector, a cathode GDE, an electrolyte channel, an anode GDE, an anode current collector, and an anode gas channel as shown seen in Figure 2.2c. The reason why MFC is used to research different catalysts is that conditions, such as pH and composition, are easily adaptable.

Besides the previously discussed flow type cells, the solid-oxide electrolysis cell (SOEC) operates at higher temperatures to improve the kinetics of the reaction[23]. the SOEC is usually made of three components; solid electrolyte, anode, and cathode. The solid electrolyte is used for ionic transport and is an oxygen ionic conductor or protonic conductor. The product range of this type of flow cell is quite small and mostly CO is formed because of the high temperatures[32].

Another type of electrolyzer is a MEA-cell electrolyzer. The benefit of these types of cells are that they have shown excellent stability for thousands of hours and demonstrated promising activity and selectivity towards electrochemical $CO_2$ reduction products. In a MEA-cell, the electrodes are only separated by an ion exchange membrane and the electrolyzer operate as solid electrolyte as can be seen in Figure 2.2d, whereas in flow cells the electrodes are also separated by electrolyte. This increases the energy efficiency and reduces the resistance because the gap between the electrodes is reduced to only the thickness of the membrane.[26]

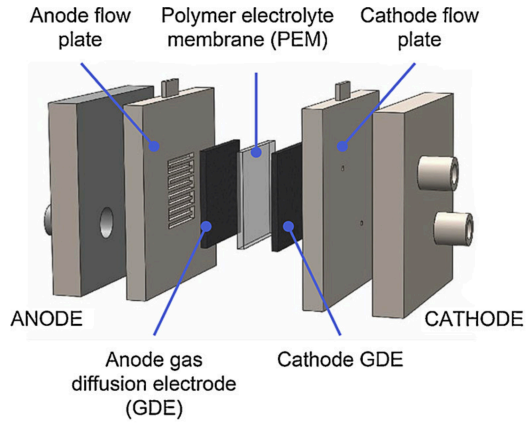


(a) Schematic image of a polymer electrolyte membrane electrochemical flow cell[33]

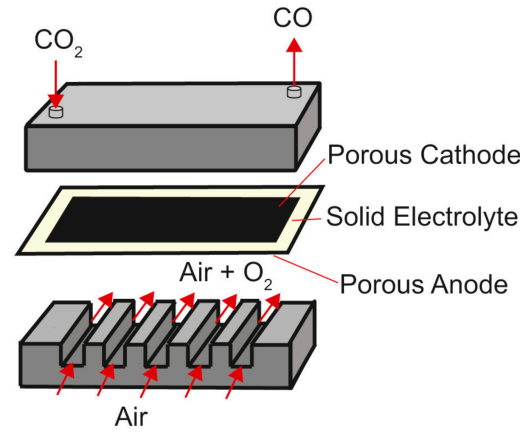


(b) Schematic image of a solid-oxide electrochemical flow cell[34]

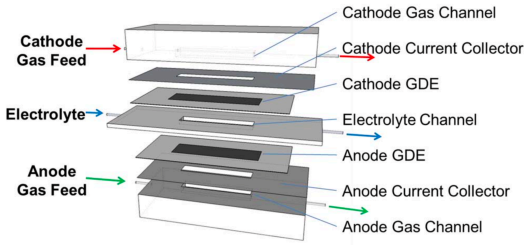


(c) Schematic image of a microfluidic electrochemical flow cell[35]

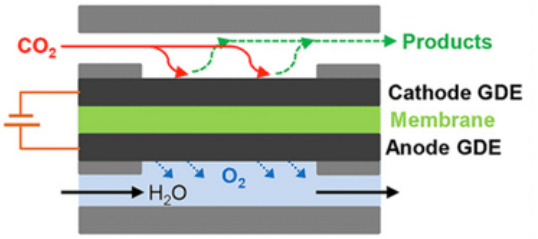


(d) Schematic image of a membrane electrode assembly[26]

Important performance indicators for an electrolyzer are current density, overpotential, faradaic efficiency, energy efficiency, and stability. Some of these parameters are used in the Tafel equation that relates the reaction rate to the required overpotential which is shown in Equation 2.2.

### Tafel Equation

The Tafel equation is a fundamental relationship in electrochemistry that describes the relationship between the current density and the overpotential of an electrode[36]. It is derived from the Butler-Volmer equation, which describes the current density at an electrode as a function of the electrode potential as shown in Equation 2.1. The Butler-Volmer equation is a more general equation that describes the current density at an electrode in the presence of a concentration gradient of the reactant and product species.

$$i = i_0 \left\{ exp\left[ \frac{\alpha_{anode} z F}{RT} (E - E_{eq}) \right] - exp\left[ -\frac{\alpha_{cathode} z F}{RT} (E - E_{eq}) \right] \right\} \tag{2.1}$$

With $i$ the current density in $A\ m^{-2}$, $i_0$ the exchange current density in $A\ m^{-2}$, $\alpha$ the charge transfer coefficient, $z$ the number of electrons involved, $F$ the Faraday constant of 96,485.332 $S\ A\ mol^{-1}$[37], $R$ the universal gas constant, $T$ the temperature in $K$, $E$ the electrode potential in $V$ and $E_{eq}$ the equilibrium potential in $V$. The Tafel equation is obtained by assuming that the concentration of the reactant and product species is constant at the electrode surface and that the rate of charge transfer is controlled by the overpotential[38]. With these assumptions and rewriting the equation, the Tafel equation for a single electrode is obtained and it is shown in Equation 2.2.

$$\eta = a + b * log(i) = 2.303 \frac{RT}{\alpha F} log\left( \frac{i}{i_0} \right) \tag{2.2}$$

Where $R$ is the universal gas constant of 8.31446 $J\ K^{-1}\ mol^{-1}$[39], $T$ is the temperature in $K$, $\alpha$ is the charge transfer coefficient, $F$ is the Faraday constant of 96,485.332 $S\ A\ mol^{-1}$[37], $i$ is the current density in $A\ m^{-2}$ and $i_0$ is the exchange current density in $A\ m^{-2}$. Plotting this equation gives a Tafel plot. The exchange current density is obtained by calculating the intersect of the plot. The exchange current density is a value that indicates the catalytic activity and the kinetics of the reaction[40]. Using

the slope of the plot, the charge transfer coefficient is obtained which has a value between 0 and 1. A rapid change in the slope can indicate a changing reaction mechanism. This is why the Tafel equation is useful by getting to know the rate determining step and elementary steps. The Tafel equation however gets less reliable at higher overpotentials, which makes it harder to use this equation for products, such as ethylene and methane, that use a high overpotential.

### Current Density

Current density (CD) is a measure of the flow of electric charge per unit area in a conductor. It is defined as the current ($I$) flowing through a conductor divided by the cross-sectional area ($A$) of the conductor with units amperes per square meter ($A\ m^{-2}$) or milli amperes per square centimeter ($mA\ cm^{-2}$). The CD indicates the reaction rate of all products or a certain product depending on if the current density or partial current density is used. This is because the extent of the reaction is proportional to the number of electrons transferred, which means that the reactants are consumed faster if more current is applied. The rate of the reactions is related by the Tafel equation as shown in the previous equation, which describes the relationship between the current density and the overpotential of the electrode.

### Overpotential

Overpotential is a measure of the difference between the electrode potential and the equilibrium potential of an electrode in an electrochemical system. It is defined as the difference between the potential required to drive a specific electrochemical reaction and the thermodynamic potential of that reaction[41]. Overpotential is caused by a lot of factors but is classified into two groups; activation overpotential and concentration overpotential[42]. The first category is the activation polarization required to overcome the activation energy barrier for a reaction to occur at the surface of the electrodes and membrane[43]. The second category is the mass transfer limitation of the reactants.

### Faradaic Efficiency

Another important parameter is the faradaic efficiency (FE). Faradaic efficiency is a measure of the efficiency of an electrochemical reaction in which electrons are exchanged between a substance and an electrode. It is used to determine the selectivity and the efficiency of a given electrochemical reaction, such as the oxidation or reduction of a substance at an electrode. It is defined as the ratio of the number of electrons exchanged in the desired reaction to the total number of electrons exchanged in all reactions occurring at the electrode. This efficiency is calculated using Equation 2.3[42, 44].

$$FE = \frac{mnF}{q} * 100\% \tag{2.3}$$

Where $FE$ is the faradaic efficiency in $\%$, $m$ is the number of moles of the product, $n$ is the number of electrons transferred per mole product, $F$ is the Faraday constant of 96,485.332 $A\ s\ mol^{-1}$[37], and $q$ is the total applied charge in $A\ s$. The faradaic efficiency says something about the selectivity towards a particular product. It is desirable to have a high faradaic efficieny towards the desired products to decrease the cost of product separation and lower the total energy required for the process.[45]

### Energy Efficiency

The energy efficiency is a combination of the faradaic efficiency, overpotential, and other energy losses and is determined for individual species or the entire cell. It represents how much of the applied electrical energy is stored in newly formed chemical bonds. Using Equation 2.4 the energy efficiency is calculated[42].

$$EE = \frac{E^0}{E^0 + \eta + iR_S} * FE \tag{2.4}$$

Where $EE$ is the energy efficiency in $\%$, $E^0$ is the thermodynamic reaction voltage in $V$, $\eta$ is the overpotential in $V$, and $iR_S$ is the ohmic loss in the cell in $V$. The energy efficiency determines how much energy an electrolyzer uses and thus is a large contributor to the operational cost. A high energy and faradaic efficiency is needed for an economically feasible electrolyzer and process[46].

#### Stability

Next to improving the performance of the electrolyzer, the stability of the electrolyzer is also important. A reliable and durable electrolyzer is necessary for an economically feasible industrially scaled process. The stability is tested by applying a constant current and measuring the change in potential. If the electrolyzer is stable, the potential is constant for more than thousand hours[47].

### 2.1.2. Chemical Reactions

An electrolyzer is connected to an electrical energy source and the electrons are transported by the electrodes. $CO_2$ and CO are reduced at the cathode where it forms different compounds depending on the conditions and used catalyst. All the possible reactions for the reduction of $CO_2$ and CO that can occur at the cathode are shown in Equations 2.5 to 2.13 and 2.14 to 2.18[48]. What reactions take place at the cathode is dependent on the used catalyst and Section 2.2.3 it is elaborated which reactions take place with different types of catalysts. CO and $CO_2$ can also react with $H^+$ instead of $H_2O$, but the local pH near the catalyst is commonly basic, so only the alkaline reactions will take place.

$$CO_2 + 2H_2O + 2e^- \longrightarrow HCOOH + 2OH^- \tag{2.5}$$
$$CO_2 + 2H_2O + 2e^- \longrightarrow CO + 2OH^- \tag{2.6}$$
$$CO_2 + 2H_2O + 4e^- \longrightarrow C + 4OH^- \tag{2.7}$$
$$CO_2 + 3H_2O + 4e^- \longrightarrow HCHO + 4OH^- \tag{2.8}$$
$$CO_2 + 5H_2O + 6e^- \longrightarrow CH_3OH + 6OH^- \tag{2.9}$$
$$CO_2 + 6H_2O + 8e^- \longrightarrow CH_4 + 8OH^- \tag{2.10}$$
$$2CO_2 + 2e^- \longrightarrow C_2O_4^{2-} \tag{2.11}$$
$$2CO_2 + 8H_2O + 12e^- \longrightarrow C_2H_4 + 12OH^- \tag{2.12}$$
$$2CO_2 + 9H_2O + 12e^- \longrightarrow C_2H_5OH + 12OH^- \tag{2.13}$$

$$2CO + 6H_2O + 8e^- \longrightarrow C_2H_4 + 8OH^- \tag{2.14}$$
$$CO + 5H_2O + 4e^- \longrightarrow CH_4 + 6OH^- \tag{2.15}$$
$$3CO + 10H_2O + 12e^- \longrightarrow C_3H_7OH + 12OH^- \tag{2.16}$$
$$2CO + 7H_2O + 4e^- \longrightarrow C_2H_5OH + 8OH^- \tag{2.17}$$
$$2CO + +4H_2O + 4e^- \longrightarrow CH_3COOH + 4OH^- \tag{2.18}$$

Next to the conversion of $CO_2$, $H_2O$ also reacts at the cathode. This side reaction is unavoidable and hydrogen is also formed as a product in an electrolyzer. The half reaction of water at the cathode is given in the equation below.

$$2H_2O + 2e^- \longrightarrow H_2 + 2OH^- \tag{2.19}$$

At the anode, the counter half reaction occurs which is the oxidation of water[49]. The reaction equations for the oxidation of water is given in Equation 2.20[50, 51].

$$4OH^- \longrightarrow O_2 + 2H_2O + 4e^- \tag{2.20}$$

## 2.2. Electrolyzers

Electrochemical $CO_2$ reduction systems are a promising technology for the utilization of $CO_2$, but several challenges must be overcome to scale up these systems for industrial applications. These challenges exist in the devices and catalyst used and the process itself.

### 2.2.1. Scale-up Challenges

The main challenges that lie in the electrolyzer include low current density and pH gradient. In aqueous electrolytes, the solubility of $CO_2$ is only 34 mM, which limits the conversion, current density, and energy efficiency[52]. Therewith, the transfer rate of $CO_2$ from the bulk phase to the surface of the electrode is limited at high current densities in an H-type cell and dissolved $CO_2$ can react with $OH^-$ to form ${CO_3}^{2-}$ in alkaline electrolytes[23, 49]. Alongside the need for a high current density (higher than 200 $mA\ cm^{-2}$), the electrolyzer also needs to be stable at high current densities for a long period of time (more than 20,000 hours)[42]. Although an H-type cell is typically used because of its simplicity as described in Section 2.1.1, the stability of these types of electrolyzers is not reasonable at high current densities. This makes a H-cell type electrolyzer not suitable for a large-scale industrial process and a continuous flow cell is preferred since it is more stable at high current densities.

To avert reoxidation of the formed products and make the separation of the products less complicated by avoiding the mixing of gaseous products, an ion exchange membrane is used. Using a membrane will cause a pH gradient in the membrane due to internal mass transfer which increases the resistance and will lower the energy efficiency and damage the process. To cope with this problem a strong acidic or basic environment is needed because then the charge is carried entirely by $H^+$ or $OH^-$ which has a high concentration in a acidic or basic environment. However, at a high or low pH another problem arises, because catalysts perform optimally in a neutral to slightly basic environment and these conditions lead to a potential loss[53]. Next to a pH gradient, the optimal pH for the $CO_2$RR is different than the oxidation of water or OOR and by using a CEM or AEM it is hard to have the optimal pH at both the anode and cathode. The pH at which the electrolyzer operates also affects the catalyst performance. This can cause a different and more expensive catalyst to be needed, so a compromise needs to be made to determine the optimal pH.

### 2.2.2. Process

As mentioned previously, $CO_2$ has a low solubility in aqueous electrolytes and a low conversion of only 30% as shown by L.C. Weng et al.[49]. The unreacted $CO_2$ leaves the electrolyzer in the gas stream with the gaseous products. A lot of $CO_2$ needs to be separated to obtain these products and recycle the unreacted $CO_2$ which increases separation costs. The large $CO_2$ recycle also causes an increase in the size and cost of the electrolyzer and gas separation units. Next to the gaseous phase, the formed liquid products are mixed with the electrolyte used in the electrolyzer. Normally, the single-pass amount of liquid product formed is small compared to the amount of electrolyte. Separating products with low concentrations is quite energy intensive and expensive. Recycling the electrolyte until a significant concentration of products is reached can reduce the cost and amount of energy required to separate the products. Nonetheless, if the concentration of the products is too high, the performance of the electrolyzer can decrease[54].

The majority of the operating expenses (OpEx) are the cost of electricity, so a cheap electricity source is required for an economically feasible process[42, 55]. M. Rumayor et al. determined the contribution of electricity to the OpEx in an electrochemical $CO_2$ reduction to formic acid process[56]. Two scenarios, $E_{min-21}$ and $E_{min-82}$, were considered, and in both scenarios, it was assumed that there was not an overvoltage loss. In the $E_{min-21}$ and $E_{min-82}$ scenario, the weight percentage of formic acid concentration in the product stream was 21 wt% and 81 wt%, respectively. In the $E_{min-21}$ scenario, they found that the variable cost is €0.26 per kg formic acid from which electricity was €0.15 per kg formic acid[56]. Even though they assumed a perfect electrical energy consumption, the electricity takes up 57.7% of the OpEx. Beside the techno-economic analysis for the production of formic acid, M. Jouny et al. performed a techno-economic analysis for n-propanol, formic acid, carbon monoxide, ethanol, ethylene, and methanol. Also in this research, the electricity cost was always in the top three of the biggest contributor to the OpEx. The high electricity cost is also caused by the high overpotential that is required to reduce $CO_2$ into energy-rich $C_{2+}$ compounds[57, 58]. Next to a high overpotential, a large variety of compounds are formed which increases the cost of separation. This makes it hard to design a large-scale process that is economically feasible. A solution to tackle this problem is to use a two-step process where $CO_2$ is reduced to CO followed by the reduction of CO to $C_{2+}$ compounds[59].

Another challenge in designing an economically feasible process is that the various components

and parameters are examined separately, but the different factors affect each other. This requires the development of a large-scale process that includes all aspects of small-scale systems.

### 2.2.3. Catalyst

Catalysts lose their catalytic activity over time, but the time scale in which catalysts deactivate is different. This is highly dependent on the process design, the contamination the catalysts are exposed to, and the intermediate compounds[46]. Catalysts are deactivated by poisoning, fouling, vapor compound formation, vapor-solid and/or solid/solid reactions, thermal degradation, and crushing/attrition[60]. Since the feed streams not only contain $CO_2$ and ultrapure water, but also other compounds that can damage the catalyst, it is vital to remove these compounds. It is, next to nearly impossible, also very expensive to remove all impurities, so a compromise needs to be made for an acceptable deactivation rate.

The feedstocks of this process are the exhaust gasses from the industry and surface water from a nearby river or harbour or wastewater streams from the industry. The compounds that are present in these feed streams that deactivate the catalysts are $Zn^{2+}$, $Fe^{2+}$, $Pb^{2+}$, $SO_2$, $NO_2$, COS, and $H_2S$[46, 61–68]. The metal ions poison the catalysts because the metal ions are reduced and deposited on the surface of the catalyst which deteriorates the catalytic activity. The sulfur and nitrogen compounds have a corrosive effect on the catalysts by reacting with the silver and copper catalysts[65–67]. All necessary information information including technical and health & safety data of the substances that are present in the gaseous and liquid feed streams and the product streams are stated in Table F.1.

The reactants are converted using a catalyst. The metallic elements Cu, Au, In, Sn, Pb, Zn, Ag, Hg, Pd, Bi and some carbon-based materials have shown catalytic activity to reduce $CO_2$[69–77]. Nonetheless, the products and composition of products formed are dependent on the catalyst used. The catalysts can be classified into three classes based on the formed products and the composition of the products. The first class of catalysts is compounds such as Sn, Pb and In that produce formate or formic acid as major product[70, 78, 79]. The second class is metals like Au, Ag, and Zn which produce CO as their main product[78, 79]. The third class consists of only one metal. Cu is the only metal that can reduce $CO_2$ or CO into hydrocarbons ($C_{2+}$) and oxygenates using electrochemistry with a high Faradaic efficiency[78–80].

## 2.3. Separation Methods

As mentioned in the previous section, impurities in the feed streams can poison the catalyst and damage the electrolyzer. These impurities need to be removed from the streams by using different separation methods. Next to the purification of the feed stream, the formed products need to be separated and purified to the required purity. Chemical separation methods are a set of techniques used to separate and purify chemicals and chemical compounds.

### 2.3.1. Gas Feed Stream

Before the gas feed stream can enter the electrolyzer, $SO_2$, $NO_2$, COS, and $H_2S$ need to be removed as explained in Section 2.2.3. In this section techniques to remove these compounds are elaborated.

#### NO and $NO_2$

Reducing the NO and $NO_2$ concentration in the flue gas stream can be achieved by reducing $NO_x$ to $N_2$. This reaction can be carried out with or without the presence of a metal oxide based catalyst[81]. Ammonia is used as reducing agent and reacts with $NO_x$ as shown in Equations 2.21 and 2.22.

$$4NO + 4NH_3 + O_2 \longrightarrow 4N_2 + 6H_2O \tag{2.21}$$

$$6NO_2 + 8NH_3 \longrightarrow 7N_2 + 12H_2O \tag{2.22}$$

#### $SO_2$

As can be seen in Table 3.2, $SO_2$ has the highest molar fraction of the impurities that need to be removed. $SO_2$ is removed by using an absorbent that absorbs and captures $SO_2$. There are two types of desulphurization systems for the removal of this gas. The first is a once-through system where the absorbent containing $SO_2$ is considered a waste product and is discharged. In the other type of process, the absorbed $SO_2$ is processed further into different forms of sulphur, but this type of process is very cost intensive[82]. Some once-through technologies that are already proven on industrial scale are wet scrubbing, spray dry scrubbing, and sorbent injection. In a wet scrubber, the gas stream is run through a liquid which contains an absorbent to remove the impurities. The most used absorbent in wet scrubbing for the removal of $SO_2$ is limestone ($CaCO_3$)[83, 84]. $SO_2$ reacts with limestone in a chemical reaction to form $CO_2$ and $CaSO_3$ as shown in Equation 2.23. The sulphur is captured in the solid limestone and cannot leave the system. The other industrially proven system are spray dry scrubbing and sorbent injection and both these methods use a solid absorbent to capture $SO_2$[83].

$$CaCO_3 + SO_2 \longrightarrow CaSO_3 + CO_2 \tag{2.23}$$

#### COS

COS can be removed using separation methods, but the proven systems, such as acid gas removal systems, do not have a high efficiency. Another way to remove COS from a gas stream is to convert it to $H_2S$. Since $H_2S$ is already present in the stream and also needs to be removed, this is a useful method to remove COS. Converting COS to $H_2S$ can be done by hydrogenation or hydrolysis as shown in Equations 2.24 and 2.25 using a metal oxide catalyst[85].

$$COS + 4H_2 \longrightarrow H_2S + CH_4 + H_2O \tag{2.24}$$
$$COS + H_2O \longrightarrow H_2S + CO_2 \tag{2.25}$$

#### $H_2S$

The most used technique to remove hydrogen sulphide or acid gas (mixture of $H_2S$ and $CO_2$) is absorption using a solvent, but this techniques has some drawbacks[86]. Most solvents are corrosive on the equipment or foaming of the solvent occurs and some of the $CO_2$ is removed as well. Another method is caustic washing where $SO_2$ reacts with NaOH in two reaction steps to form $Na_2S$ and $H_2O$ as shown in Equations 2.26 and 2.27[86, 87]. The downside of this method is that $CO_2$ also reacts with NaOH to form $Na_2CO_3$ and $H_2O$ when present in high concentrations as shown in Equation 2.28[87]. Using an amine-based solvent prevents the reaction with $CO_2$ and increases the selectivity to the adsorption of $H_2S$.

$$H_2S + NaOH \longrightarrow NaHS + H_2O \tag{2.26}$$
$$NaHS + NaOH \longrightarrow Na_2S + H_2O \tag{2.27}$$

$$CO_2 + 2NaOH \longrightarrow Na_2CO_3 + H_2O \tag{2.28}$$

### 2.3.2. Liquid Feed Stream

As mentioned previously, electrolyzers use electrolyte to conduct electrical charge from the electrodes. Electrolyte is made from water with the addition of ions, so the solution can conduct charge through the movement of the ions. Not every water feed can be directly used to prepare an electrolyte. There are four types of water purity's with each having different purposes. The purity of water is determined by the resistivity and the concentration of some compounds. The four types include feed water or raw water, primary grade water (type 3), general laboratory grade water (type 2), and ultrapure water (type 1). The water required to make a electrolyte is type 1 water and the requirements for water to be called ultrapure water are listed in Table 2.1. To go from industrial wastewater or surface or river water to ultrapure water, multiple cleaning technologies are needed. To produce 1 $m^3$ of ultrapure

water, about 1.5 $m^3$ of surface water is required[88]. This is due to water losses in purification steps. The production of ultrapure water consists of three stages. The first stage is the pretreatment part to remove solid particles, organics, and microorganisms. This is done by ultrafiltration and UV treatment. This is followed by a make-up stage to remove salts and dissolved gasses with reversed osmosis, gas filter, and softener. At last, the polishing stage raises the water quality to the required specification using electrodeionisation[89]. The requirements for the water purity and purification steps are based on the purification of electrolytes for water electrolysis which uses ultrapure water for electrolytes.

Table 2.1: Requirements for ultrapure water (type 1) at 25°C[90]

| **Parameter** | **Value** |
|---|---|
| Resistivity | 18.2 $M\Omega\ cm$ |
| Particles: | |
| >0.05 $\mu m$ | <200 $count\ L^{-1}$ |
| >0.1 $\mu m$ | <50 $count\ L^{-1}$ |
| >0.2 $\mu m$ | <20 $count\ L^{-1}$ |
| >0.5 $\mu m$ | <1 $count\ L^{-1}$ |
| Bacteria | <1 cfu/100 $mL$ |
| Total organic carbon (TOC) | <1 $\mu g\ L^{-1}$ |
| Dissolved oxygen | ≤10 $\mu g\ L^{-1}$ |
| Calcium | <2 $\mu g\ L^{-1}$ |
| Cations (each) | <0.01 $\mu g\ L^{-1}$ |
| Boron | <0.05 $\mu g\ L^{-1}$ |
| Chloride | <0.1 $\mu g\ L^{-1}$ |
| Ammonium | 0.05 $\mu g\ L^{-1}$ |
| Anions (each) | <0.05 $\mu g\ L^{-1}$ |
| Silica (dissolved) | 0.5 $\mu g\ L^{-1}$ |
| Silica (total) | 0.5 $\mu g\ L^{-1}$ |

### Ultrafiltration

Ultrafiltration (UF) is a separation process that uses a semipermeable membrane to separate immersed particles and macromolecules in the range of 1 $nm$ to 0.1 $\mu m$ from a liquid based on their sizes[91]. The membrane allows small molecules, such as water and dissolved ions, to pass through, while larger molecules and particles are retained[92]. The membrane permeability is measured by the molecular weight cut off and it is the lowest molecular weight that is retained for 90% by the membrane. For the UF membrane, the molecular weight cut-off is between 1,000 and 1,000,000 $Da$[93, 94].

### UV Treatment

UV treatment is a method for disinfecting water, air, and surfaces by exposing them to ultraviolet (UV) radiation. UV radiation is a type of electromagnetic radiation with a wavelength range of 100-400 nanometers. When microorganisms such as bacteria, viruses, and fungi are exposed to UV radiation, the energy from the UV light damages their DNA and RNA, preventing them from reproducing and killing them[95, 96]. UV light with a wavelength of 265 $nm$ has the highest efficiency towards killing microorganisms[97]. The benefit of this method to kill bacteria, viruses, and fungi is that it is a chemical-free technique that does not produce harmful by-products.

### Active Carbon Filter

Active carbon filters are used to remove a wide range of contaminants such as organic compounds and ions[98]. The filter consists of a bed of activated carbon granules or pellets, which are made from materials such as coconut shells, peat, or wood[99]. The carbon is treated with oxygen to create a large number of tiny pores between the carbon atoms, which increases its surface area and adsorption capacity. The impurities are adsorbed onto the surface which means that the filter has a maximum adsorption capacity and needs to be renewed to maintain the removal efficiency.

### Softener

Water softening is a process that reduces the concentration of dissolved minerals, particularly $Ca^{2+}$ and $Mg^{2+}$, in water. This is accomplished by exchanging cations that cause hard water with sodium ions and the exchange of ions is performed using either lime softening or ion exchange resin[100]. The exchange of $Ca^{2+}$ and $Mg^{2+}$ with $Na^{+}$ is caused by the fact that multivalent ions bind more strongly to the lime or resins than $Na^{+}$[101]. Reducing the water hardness is necessary to reduce scaling on membranes and pipelines.

### Reverse Osmosis

Reverse osmosis (RO) is a separation method that uses a membrane to separate ions and other dissolved molecules, such as silica, from water. Due to the fact that ions are stopped by the membrane, a pressure difference between the two sides of the membrane arises. This pressure difference is called the osmotic pressure and is the minimum pressure that needs to be applied to stop fresh water from flowing through a semipermeable membrane. When a higher pressure to the side of the membrane with high ion concentration is applied, water molecules are forced to pass through the membrane and leave the ions behind. This leaves an ions rich and poor stream[102, 103].

### Degasser

Dissolved $O_2$ in water causes corrosion to the electrolyzer and is removed using a degasser. The maximum oxygen concentration in water is 40 $mg\ L^{-1}$ at 25°C, but it needs to be lower than 1 ppb to prevent corrosion[104]. Degassers are used to remove dissolved gases from liquids using physical and/or chemical methods, such as vacuum, centrifugal, and bubble stripping. The efficacy of a degasser depends on the concentration of dissolved gases, the temperature and pressure of the liquid, and the flow rate of the liquid[105, 106].

### Electrodeionization

Electrodeionization (EDI) uses electricity, resins, and ion exchange membranes to remove ions from water and is used to upgrade the water after reverse osmosis to the required specifications. EDI is a continuous process that automatically regenerates itself. Dissolved ions have a negative or positive charge and by applying a charge the cations and anions move to the positive or negative electrode, respectively. A cation exchange membrane is used near the cathode to block anions and only let cations move to the other side. An anion exchange membrane is used near the anode, so only anions can pass. This process, however, only works when the concentration of ions is large enough because the electrical resistance increases with decreasing ion concentration. As a consequence, the ions move more slowly through the water. To cope with this problem, cation and anion selective resins are added between the ion exchange membranes and reduce the resistance as shown in Figure 2.3. The ions are transported over the surface of the resins to the electrodes. When the ion concentration reaches a ppt level, a potential difference arises that splits water into $OH^{-}$ and $H^{+}$. These ions replace other ions on the resin surface and the resins are regenerated so a continuous process is possible[107, 108].

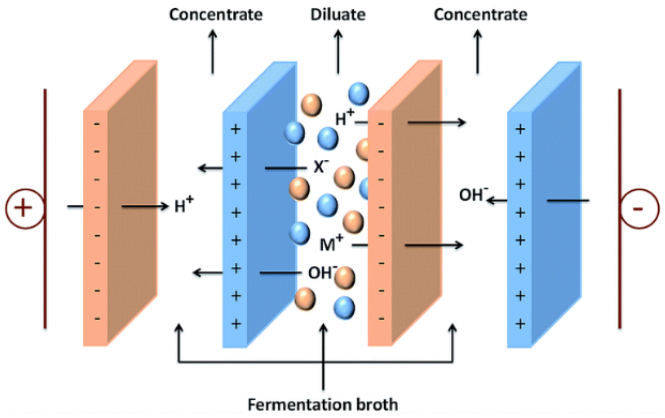


Figure 2.3: Schematic of the stack configuration for an electrodeionization unit[109]

### 2.3.3. Gas Product Stream

Next to unreacted CO or $CO_2$ and inert compounds, also ethylene and hydrogen leave the electrolyzer in the gas phase at the cathode side. These two compounds are separated and isolated from the gas stream using pressure swing adsoprtion (PSA) and cryogenic distillation.

#### Pressure Swing Adsorption

Pressure swing adsorption (PSA) is separation technique that is already used in the industry for gas separation and purification. The separation is based on the difference in adsorption of gases on a solid adsorbent at different pressures, allowing for the separation of gases in a mixture. The advantage of this separation technique compared to other techniques include less energy consumption, simplicity, and high purity of the separated gas[110]. PSA, however, also has some downsides, such as frequent absorbent regeneration, adsorbent degradation, and the high cost of the adsorbent material[111].

The efficiency of PSA depends on the used adsorbent and the target gas that needs to be removed. Various types of adsorbents can be used in PSA, such as zeolites, activated carbon, molecular sieves, and metal-organic frameworks (MOFs)[112]. The effectiveness of PSA also depends on the operating parameters, such as pressure, temperature, and flow rate[113].

#### Cryogenic Distillation

Cryogenic distillation is a separation technique that separates gaseous compounds based on the differences in their boiling points at very low temperatures. The gas mixture is cooled down to a temperature where the component with the highest boiling point condenses, and then the remaining gas mixture is cooled further until the next component with a higher boiling point condenses. This process is repeated until all components have been separated or the desired component can be removed from the other compounds[114, 115]. Cryogenic distillation, just as normal distillation, uses a distillation column with multiple stages, but also a refrigeration system to cool down the gas stream. The refrigeration system consists of a compressor, a heat exchanger, and a cooling system that uses a cryogenic fluid such as $N_2$ or He[115].

### 2.3.4. Liquid Product Stream

In addition to the electrolyte leaving the electrolyzer, the liquid products also leave the reactor. To separate and isolate the products, several separation techniques are used; distillation, extractive distillation, electrodialysis, and pervaporation.

#### Distillation

Distillation is a separation technique that separates compounds from each other using a difference in boiling point and thus can be separated by controlling the temperature of the mixture. When a mixture

is heated, the components with lower boiling points will vaporize first, leaving behind the components with higher boiling points. The separation takes place in a column that consists of several stages. Each stage operates at a different temperature and has a different composition. At the top stage, the compound or mixture with the lowest boiling point emerges and at the bottom stage, the compound or mixture with the highest boiling point emerges. The vapor at the top stage is condensed, so two liquid streams exit the distillation column.

### Extractive Distillation

Extractive distillation also separates compounds from each other by the difference in the boiling point using a column. The difference is that extractive distillation uses an entrainer. The entrainer interacts with one of the components of the mixture by changing its boiling points to make it easier to separate it from the other components. This separation technique is often used to separate mixtures of liquids that are difficult to separate using traditional distillation methods, due to their close boiling points or similar vapor pressures[116].

### Electrodialysis

Electrodialysis (ED) uses, just as EDI, an applied electrical potential difference and ion-exchange membranes to transport ions from one solution to the other. The difference between these two techniques is that ED does not use selective resins. The diffused ions will either be leaving the unit with a higher concentration or react with other ions[109].

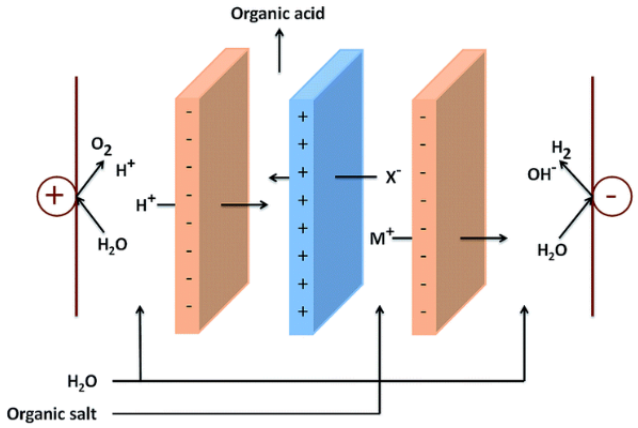


Figure 2.4: Schematic of the stack configuration for an electrodialyzer unit[109]

### Pervaporation

Some mixtures form an azeotrope and are impossible to separate from each other by simple distillation. Pervaporation (PV) is a method where azeotropes can be separated by vaporisation using a permeable membrane. The driving force is a pressure difference across the membrane causing the more volatile components of the mixture to evaporate and pass through the membrane into the permeate stream. The benefits of PV are that it has a low energy consumption and produces minimal waste because it is often performed at low temperatures and is a chemical-free technique.

## 2.4. Techno-Economic Analysis

To determine if the designed electrochemical $CO_2$ reduction process is economically feasible, a techno-economic analysis (TEA) is performed. In this analysis, the capital cost (CapEx), operating cost (OpEx), and revenue are estimated by combining engineering, business, and research and development. Different methods to effectuate a TEA are used, but for this thesis, the method described by Seider et al. is used which is called the Lang method[117]. The advantage of this method is that it takes inflation into account by using an index parameter and it includes all additional costs by multiplying with the Lang factor. The indexes that are used for present-day prices are the Chemical Engineering (CE) Plant

Cost Index, Marshall and Swift (MS) Equipment Cost Index, Nelson-Farrar (NF) Refinery Construction Cost Index, and Engineering News-Record (ENR) Construction Cost Index depending on the industry of the designed process. The CE and MS indexes both consider the entire plant with the cost for materials and labor and installation of the plant. The difference between these indexes is that the NF index is only suitable for the petroleum industry, whereas the CE index is an average of all chemical industries. The ENR index pertains to an average of industrial construction that consists of the cost of raw materials and labor to construct the process. The MS index pertains to the average all-industry purchase cost. For the design of the electrochemical $CO_2$ reduction process, the CE index is used, because units from a variety of industries are used and it considers all costs. The CE Plant Cost Index is published every month in the *Chemical Engineering* magazine with its base year in 1957-1959 (CE-index = 100). The CE index is used to calculate the total capital investment ($C_{TCI}$). This is a one-time expense for the design, construction, and start-up of a production plant and is calculated using Equation 2.29[117]. This equation has an accuracy of $\pm$35% of the final total capital investment. The free on board (f.o.b.) purchase cost is the price that has to be paid before shipment of the component and to account for the shipment cost the total price is multiplied by 1.05. The Lang factor is dependent on the type of process and is 4.67, 5.03, and 5.93 for a solid processing plant, solid-fluid processing plant, and fluid processing plant, respectively. The electrochemical $CO_2$ reduction process is assumed to be a fluid processing plant, so the process has a Lang factor of 5.93.

$$C_{TCI} = 1.05 f_{L_{TCI}} \sum_i \left( \frac{I_i}{I_{b_i}} \right) C_{P_i} \tag{2.29}$$

With $f_{L_{TCI}}$ the Lang factor, $I_i$ the updated CE Index, $I_{b_i}$ the base CE Index, and $C_{P_i}$ the f.o.b price of unit i.

For each unit, the f.o.b. price is calculated using a unit-specific equation with size-dependent parameters. Next to size-dependent parameters, the f.o.b. purchase price depends on the material used and a material factor is added. These equations are derived from the base equation $C_P = aS^b$ with S the size factor and a and b constants. Taking the natural logarithm from the base equation and adding higher-order polynomial terms gives a final expression for the f.o.b. purchase cost:

$$C_P = exp\left(A_0 + A_1[ln(S)] + A_2[ln(S)]^2 + A_3[ln(S)]^3 + \ldots\right) \tag{2.30}$$

Next to the total capital investment, the annual revenue, annual production cost, and total earnings are other important parameters to calculate. These parameters are calculated using a cost and income sheet. With these parameters, the return on investment (ROI) and payback time are calculated as shown in Equation 2.31. For an investment to be interesting, the ROI needs to be higher than the commercial interest rate. The commercial interest rate is the rate investors receive on their low-risk investments. The payback time is the time it takes before the total capital investment is earned back.

$$ROI = \frac{Annual\ revenue}{C_{TCI}} * 100\% \tag{2.31}$$

The prices are calculated using the Lang method in the dollar and all prices and money flows are calculated in the dollar.

# 3

# Basis of Design

The process is considered to be located at an average steel producing plant in Europe with a lifetime of 15 years[118]. This location is chosen because it uses the emissions of a steel producing plant and the gas flow rate of the plant determines the size of the designed process. The process will operate 24 hours a day for 350 days a year. It is aimed to design an integrated large-scale electrochemical $CO_2$ reduction process and analyze which are the most capital- and energy-intensive units in such a process.

## 3.1. Battery Limits

The Battery limits of the process include the purification of the liquid and gas feed streams, electrolyzers, and the gas and liquid product separation units. The liquid and gas feed stream enter the battery limit and the products and purge streams exit the battery limit. Only the products formed at the cathode of the electrolyzers are included in the product separation and economical and energy analysis. The storage of the products and treatment of purge and waste streams are not included in the scope this study.

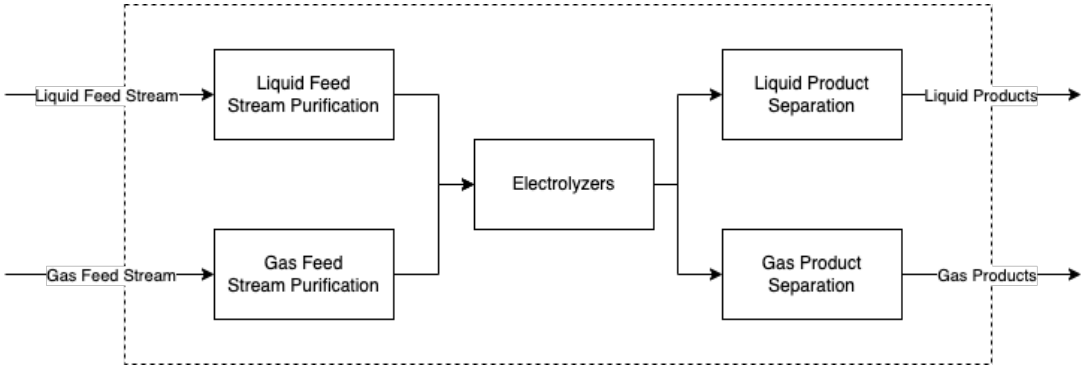


Figure 3.1: Battery limits of the project

## 3.2. Liquid Feed Stream

The liquid feed is water obtained from the river Rhine near Nieuwegein. The average concentrations of compounds present in the water are shown in Table 3.1 and are the average from 2021. For the concentrations of metal ions, only ions with an average concentration higher than 0.050 $mg\ L^{-1}$ or that have a large influence on the process are considered. The water has an average temperature of 13.3°C and a pH of 8.1

Table 3.1: Average concentration of metal ions in The Rhine near Nieuwegein in 2021[68]

| **Compounds** | **Symbol** | **Minimum concentration** ($mg\ L^{-1}$) | **Average concentration** ($mg\ L^{-1}$) | **Maximum concentration** ($mg\ L^{-1}$) | **Average concentration** ($mmol\ L^{-1}$) |
|---|---|---|---|---|---|
| Aluminium | $Al^{3+}$ | 0.157 | 0.379 | 0.585 | 0.0140 |
| Barium | $Ba^{2+}$ | 0.0577 | 0.0658 | 0.0764 | 0.000479 |
| Calcium | $Ca^{2+}$ | 54.6 | 66 | 74 | 1.65 |
| Iron | $Fe^{2+}$ | 0.239 | 0.527 | 0.863 | 0.00944 |
| Lead | $Pb^{2+}$ | 0.000526 | 0.00128 | 0.00198 | 0.000000618 |
| Magnesium | $Mg^{2+}$ | 8.78 | 10.2 | 11.3 | 0.420 |
| Sodium | $Na^{+}$ | 25 | 37.3 | 46.2 | 1.622 |
| Potassium | $K^{+}$ | 3.21 | 4.09 | 5.48 | 0.105 |
| Strontium | $Sr^{2+}$ | 0.344 | 0.428 | 0.471 | 0.004885 |
| Zinc | $Zn^{2+}$ | 0.00456 | 0.00899 | 0.0133 | 0.000138 |
| Oxygen | $O_2$ | 7.2 | 9.32 | 10.8 | 0.291 |
| Carbon dioxide | $CO_2$ | 1.9 | 2.54 | 3.1 | 0.0577 |
| Bicarbonate | $HCO_3^-$ | 148 | 171 | 189 | 2.80 |
| Carbonate | $CO_3^{2-}$ | 1.9 | 2.54 | 3.1 | 0.0423 |
| Chloride | $Cl^-$ | 0.00456 | 0.00899 | 0.0133 | 0.000138 |

## 3.3. Gas Feed Stream

The gas feed is the flue gas stream from a steel producing plant and has a temperature and pressure of 160°C and 1 bar. The composition of this gaseous stream is listed in Table 3.2 which is based on in-house knowledge of the flue gas composition of a typical steel producing plant in Europe. The mass flow rate of this stream is the size-determining factor of the process and has a flow rate of 381.678 tons per hour.

Table 3.2: Composition of the gas feed stream

| **Component** | **Symbol** | **Molar fraction** |
|---|---|---|
| Carbon dioxide | $CO_2$ | 0.23600 |
| Carbon monoxide | CO | 0.29600 |
| Hydrogen | $H_2$ | 0.06200 |
| Oxygen | $O_2$ | 0.00180 |
| Nitrogen | $N_2$ | 0.39700 |
| Argon | Ar | 0.00620 |
| Methane | $CH_4$ | 0.00024 |
| Ethene | $C_2H_4$ | 0.00001 |
| Ethane | $C_2H_6$ | 0.00001 |
| Propane | $C_3H_8$ | 0.00001 |
| Butane | $C_4H_{10}$ | 0.00001 |
| Isobutane | $C_4H_{10}$ | 0.00001 |
| Hydrogensulfide | $H_2S$ | 0.00001 |
| Carbonyl sulfide | COS | 0.00002 |
| Sulfur dioxide | $SO_2$ | 0.00040 |
| Nitrogen dioxide | $NO_2$ | 0.00028 |

## 3.4. Electrolyzers

Two electrolyzers are used to convert $CO_2$ into more valuable compounds. In the first electrolyzer, $CO_2$ is converted to CO and in the second electrolyzer, CO is converted into high-value compounds. The requirements for the both electrolyzer are that they need a high current density and a good stability. The first electrolyzer that converts $CO_2$ needs a high faradaic efficiency towards CO and the second electrolyzer needs a high faradaic efficiency towards the products described in Section 3.5.

Several compounds that are present in the liquid and gas stream can harm the process and these need to be removed below a certain concentration to reduce the risk of damage. Impurities that are present in the liquid stream are removed to an acceptable level with the purification of water to ultrapure water. The requirements for ultrapure water are shown previously in Table 2.1. The catalyst poisoning sulphur and nitrogen compounds are removed to a concentration where the faradaic efficiency of the electrolyzers matches that achieved when a pure stream is used. These concentrations are based on experimental data.

## 3.5. Gas and Liquid Products

The products with the most interest can be divided into liquid products and gas products. The liquid products are ethanol, n-propanol, and acetic acid. The required purity for ethanol depends on the application ethanol will be used for. This purity ranges from 96% to 99.9%, but most suppliers mention that high purity ethanol has a purity of 99%[119–121]. n-Propanol could be used as a solvent in the paint and ink industry, cosmetics, and fuels. Dependent on the application a purity of 95% to 99.9% is needed[122–124]. Large manufacturers of acetic acid produce acetic acid with a purity of 80%, so this is the target purity for acetic acid[125–127].

The gaseous products are ethylene, hydrogen, methane, and oxygen. Ethylene is sold with two different purities and the purities are polymer grade and chemical grade where polymer grade has a purity of >99.9% and chemical grade >95%[128]. There are three grades of hydrogen used in the industry with different purities and these three grades are qualified, first and excellent grade with purities of 99.0%, 99.5%, and 99.95%, respectively[129]. Methane requires a purity between 99.5% and 99.999% for chemical pure grade and ultrapure grade[130, 131]. Oxygen can be used for industrial applications as well as for medical applications and requires a purity of 99% to 99.5%.[132]

# 4

# Process Modelling and Design

In this chapter, the methodology of the design process and the designed process itself is modelled. The model scheme of the entire process can be found in Appendix A in Figure A.1.

## 4.1. Liquid Feed Stream Purification

As mentioned previously, electrolyzers require electrolyte that is made from ultrapure water. The design of the purification of the liquid feed stream is described in this section and the model scheme of this part of the process is shown in Figure 4.1. It is assumed that after each unit, the pressure is 1 $bar$, due to pressure drop. The separation techniques used is based on the separation techniques used in the purification of water to ultrapure water for the electrochemical production of hydrogen.

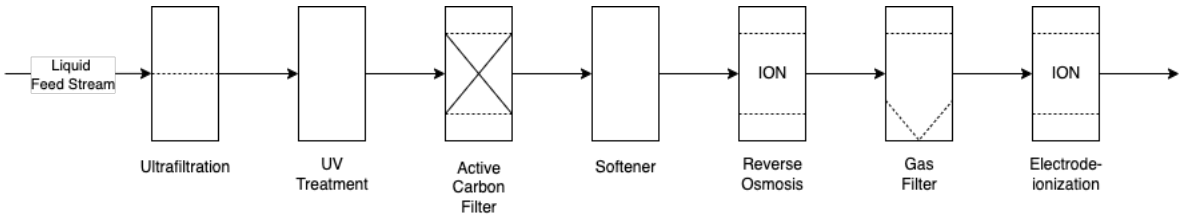


Figure 4.1: Model scheme for the purification of the liquid feed stream

### 4.1.1. Ultrafiltration

The first step in the purification steps for water is ultrafiltration. Before the feed water is run through a UF membrane, the water is pre-filtered to prevent clogging of the membrane using an automatic back-washable filter with 100 $\mu m$ sieve openings[133]. The membrane used for UF is a ceramic membrane because it is more effective, cheaper, and has a longer lifetime than polymeric membranes and it is also already proven in the industry[134, 135]. The lifetime of these membranes is around 20 years, so they do not need to be replaced during the lifetime of the process. The pore size of the membrane is 0.02 $\mu m$ and has the lowest total operating cost when a flux of 4,074.58 $l\ m^{-2}\ day^{-1}$ is used with an applied pressure of 7 $bar$[135]. The surface area of the ceramic membrane is calculated to be 3,095.85 $m^2$ as can be seen in Appendix B.1 and has a water recovery rate of 97%[135]. It is assumed that 99.9% of all solid particles are removed by UF[136].

### 4.1.2. UV Treatment

After the water is run through the UF unit, bacteria and viruses are killed by UV light. UV light with a wavelength of 265 $nm$ is used, since this has the highest efficiency towards killing microorganisms, with a UV dose of 40 $mJ\ cm^{-2}$[97, 137]. Using UV light results in a decrease in the total viable count by more than 99.9% and a 60% decrease in the total organic carbon concentration[89].

### 4.1.3. Activated Carbon

Activated carbon is used to filter contaminations from air or liquid. It is a form of carbon with a high surface area. The activated carbon filter used removes more than 95% of all chloride in water[138]. Besides removing chloride, activated carbon is also able to remove some metal ions, such as $Pb^{2+}$ and $Zn^{2+}$ with an efficiency of 83% and 83.6%, respectively[139]. This helps to reduce the concentration of heavy metal ions that deactivate the catalyst. Activated carbon has maximum adsorption capacity of 704.23 $mg\ g^{-1}$ and a density of 650 $kg\ m^{-3}$[140, 141]. The activated carbon filter is a fixed bed column with a height two times the diameter with a calculated bed volume of 818.63 and 40.94 $m^3$ for the first and second bed, respectively[117]. The calculations can be found in Appendix B.1. The velocity of the liquid through the column is 0.3048 $m\ s^{-1}$[142]. The lifespan of an activated carbon filter is 6 months to 1 year and to keep the efficiency of the filter to the required level, the filter is replaced every 6 months[143, 144]. The concentration of chloride need to be lower than 0.1 ppm because the membrane used in RO has a low resistance towards free chlorine ions[145]. For this reason, two activated carbon filters are used to meet the required chloride concentration.

### 4.1.4. Softener

The removal of multivalent ions to soften the water can either be done by lime softening or ion-exchange resins. Ion-exchange resins have proven to be the most effective method[146]. Ion-exchange resins are organic polymers with an anionic active site that contain sodium ions. The efficiencies of this method are 94% and 70.8% with adsorption capacities of 0.15 and 0.219 $g\ g^{-1}$ for $Ca^{2+}$ and $Mg^{2+}$, respectively. The resins can be easily recycled by washing them with a solution with a high NaCl concentration[101]. This needs to be done every 10 to 15 years[147]. Since the lifetime of the plant is 15 years, this is done 1 time after 7 or 8 years. The volume of resins needed is dependent on the flow rate and the volumetric flow rate should be between 5 and 50 times the bed volume of the ion exchange resins[148]. The volumetric flow rate entering the softener is 1,143.88 $m^3\ hr^{-1}$. A volumetric flow rate and bed volume ratio of 25 is chosen, so a bed volume of 45.76 $m^3$ is used.

### 4.1.5. Reverse Osmosis

The used membrane for reverse osmosis is a thin film composite polyamide membrane. It is made up of three different layers. The first part is a backing layer with pore sizes between 100 and 200 $\mu m$ and the second part is a microporous layer made from polysulfone with pore sizes of 20 to 50 $\mu m$. The third layer of the RO membrane is made of polyamide with pore sizes between 0.05 and 0.3 $\mu m$[145]. The membranes are produced by TORAY and have a surface area of 37 $m^2$ and a water permeability of 41.6 $m^3\ day^{-1}$. The operating pressure is 15.5 bar and it is able to remove 98% of salts present with a recovery of 90%[89, 149]. The lifetime of a reverse osmosis membrane is between 3 to 5 years, so the membrane is replaced every 4 years[150]. To meet the requirements for ultrapure water, four RO units are used, so the concentration of each ion is below the requirements. The membrane area of each unit is 21,960.7, 19,772.1, 17,802.2, and 16,028.5 $m^2$ for the first, second, third, and fourth unit, respectively, as calculated in Appendix B.1.

### 4.1.6. Degasser

As mentioned in Section 2.3.2, oxygen and carbon dioxide are the gasses that are dissolved. Carbon dioxide is used in the process, so this gas does not necessarily have to be removed, but oxygen needs to be removed. Oxygen in the system can react with metals and oxidize them[151]. It is hard to separate oxygen without separating carbon dioxide as well, so while separating $O_2$, a degasser removes both $O_2$ and $CO_2$. For the degasser, a chemical-free separation method is used that uses a membrane to remove the dissolved gasses. The membrane is a polymethylpentene hollow fiber membrane with a thickness of 35 $\mu m$ that operates with a liquid pressure of 8 $bar$[152]. One degasser unit has a maximum capacity of 50 $m^3\ hr^{-1}$. With a volumetric flow rate of 751.039 $m^3\ hr^{-1}$, 16 degasser units are required. A combination of a vacuum for the gas phase and a sweep gas is used to extract as much oxygen as possible. The used sweep gas is pure nitrogen with a counter-current flow towards the water flow. The concentration of the dissolved gasses is reduced to less than 1 ppb and 5 ppb for oxygen and carbon dioxide, respectively[153].

### 4.1.7. Electrodeionization

A multi-compartment EDI system is used with an operating pressure of 2 $bar$ and a voltage of 70 $V$. The applied current in each compartment is 5 $A$. The EDI system is able to remove the remaining 90% of the ions and has a water recovery rate of 98%.[154]. This unit acts as an extra safety barrier and can also be bypassed if the specifications of UPW are already met.

### 4.1.8. Pumps

Most of the separation units for the production of UPW use membrane separation techniques, which require pressure differences and cause large pressure drops. To increase the pressure to the requirements for each separation unit, pumps are used. The summary of each pump is listed in Table 4.1. It is assumed that after every membrane separation unit, the pressure is 1 $bar$, due to pressure drop.

Table 4.1: Specifications of the pumps in the water purification process

| Pump | From | To | Pressure increase $(bar)$ | Pump head $(m)$ | Energy consumption $(kW)$ |
|---|---|---|---|---|---|
| 1 | | Ultra filtration | 6 | 60.96 | 228.717 |
| 2 | Ultra filtration | Activated carbon 1 | 1 | 10.16 | 36.982 |
| 3 | Activated carbon 1 | Activated carbon 2 | 1 | 10.16 | 36.973 |
| 4 | Activated carbon 2 | Softener | 1 | 10.16 | 36.972 |
| 5 | Softener | Reverse osmosis 1 | 15 | 147.36 | 536.034 |
| 6 | Reverse osmosis 1 | Reverse osmosis 2 | 15 | 147.33 | 484.242 |
| 7 | Reverse osmosis 2 | Reverse osmosis 3 | 15 | 147.39 | 438.109 |
| 8 | Reverse osmosis 3 | Reverse osmosis 4 | 15 | 147.45 | 396.513 |
| 9 | Reverse osmosis 4 | Degasser | 7 | 71.21 | 173.305 |
| 10 | Degasser | Electrode-ionisation | 1 | 10.175 | 24.762 |

### 4.1.9. Storage Tank

Every so often, the units for the liquid feed stream purification require maintenance. To prevent the entire system being shut down when a unit needs maintenance, a storage tank is placed in front of the electrolyzers where UPW is stored. It is assumed that a storage capacity of one day is sufficient to cope with small maintenance stops. The flow rate of the liquid feed stream purification is 736.018 $m^3\ hr^{-1}$, so the volume of the storage tank is calculated to be 17,664.4 $m^3$ as shown in Appendix B.1. To prevent that oxygen can dissolve back into the UPW, a floating roof storage tank is used.

## 4.2. Gas Feed Stream Purification

Before the flue gas can enter the electrolyzers, impurities that damage the electrolyzer and influence the specifications of the electrolyzer need to be removed. Four impurities need to be removed from the flue gas. These four compounds are $NO_x$, $SO_2$, COS, and $H_2S$. First, $NO_2$ and $SO_2$ are removed, followed by, the conversion of COS to $H_2S$, and at last, $H_2S$ is removed. After the impurities are removed, $CO_2$ and CO are isolated to increase the concentrations of both compounds. The model scheme of the gas purification process can be seen in Figure 4.2.

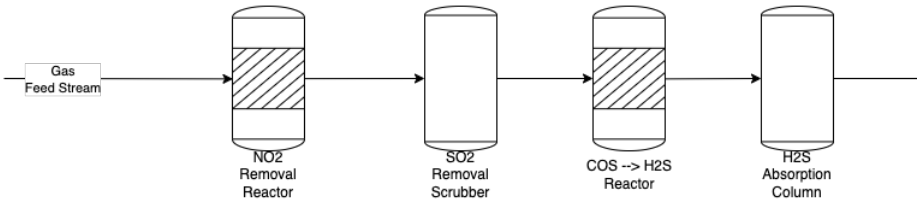


Figure 4.2: Model scheme of the gas purification process

### 4.2.1. NO and $NO_2$

Reducing NO and $NO_2$ in $N_2$ is an effective way to remove $NO_x$ from the flue gas. This reduction reaction can either be performed with or without the presence of a catalyst. Using a catalyst will increase the investment cost, but the reaction conditions are milder than compared to reaction conditions without the use of a catalyst. Without a catalyst, the reaction temperature needs to be 900 °C and with a catalyst a temperature between 250 and 500 °C is sufficient. Next to milder reaction conditions, the removal efficiency increases when a catalyst is used to 90%[81]. Since the reaction conditions are milder and the efficiency is higher, a catalyst is used to reduce $NO_x$. The used catalysts are metal oxide-based catalysts CaO, $SiO_2$, $Al_2O_3$, and MgO. Particulate matter that is present in the flue gas poisons the catalyst and causes problems in other downstream units, so the flue gas first needs to be removed using a particulate matter filter. The $NO_x$ are removed in a selective catalytic reduction (SCR) process[81]. A research on the removal of $NO_x$ and $SO_2$ from flue gasses using metal oxide-based catalysts stated that it is possible to remove $NO_x$ using a catalytic process without the $SO_2$ present poisoning the catalyst[81].

### 4.2.2. $SO_2$

$SO_2$ can be removed either by a once-through or regenerable processes. Since once-through processes are cheaper, more efficient, and already used in the industry, a once-through process is used to remove $SO_2$. Wet scrubbing is found to be the most effective technique. The other industrially proven systems are spray dry scrubbing and sorbent injection with an efficiency of 90% and 50%, respectively[83]. Both these methods use a solid absorbent to capture $SO_2$, but the high OpEx for spray dry scrubbing and low efficiency of sorbent injection makes these methods not usable for a large scale process[155] The used absorbent in wet scrubbing for the removal of $SO_2$ is limestone ($CaCO_3$) and it removes 99% of $SO_2$[83, 84]. The removal is performed using a column and the specifications of this column are shown in Figure 4.3 and Table 4.2. The column uses a liquid-to-gas ratio of 15 and a calcium-to-sulfur ratio of 1.05.

After the wet scrubbing column, the gas stream is cooled down and a flash drum is used to remove water that has left the column in the gas phase. It is assumed that flash drums are vertical pressure vessels which have a height 4 times the diameter with a cylindrical shape. The size and volume of the pressure vessel is calculated in Appendix B.2. The height and diameter are 20.88 and 5.22 $m$ and the flash drum has a volume of 447.04 $m^3$.

Table 4.2: Limestone scrubber column specifications to remove $SO_2$ from the gas stream

| | |
|---|---|
| Condenser duty | 0 $MW$ |
| Reboiler duty | 0 $MW$ |
| Tray height | 0.6096 $m$ |
| Tray diameter | 10.63 $m$ |

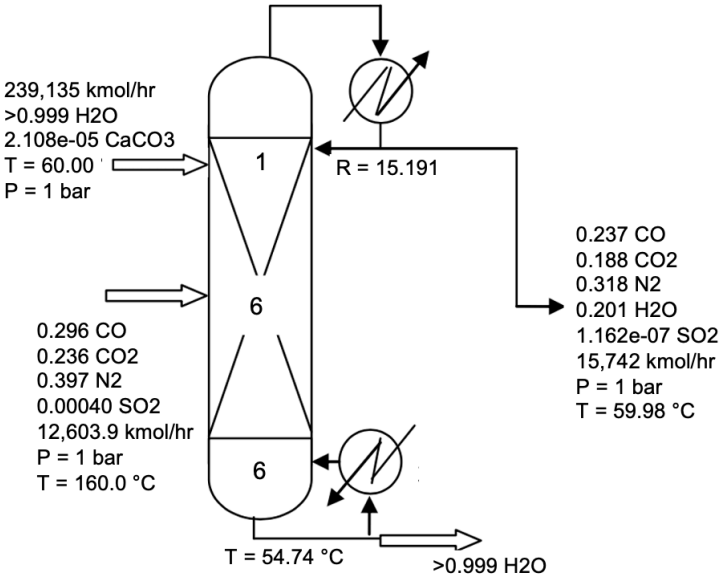


Figure 4.3: Scrubber column specifications to remove $SO_2$ using limestone

### 4.2.3. COS

There are two ways to remove COS from the gas stream. One is to directly remove COS using a separation technique and the other one is to convert COS into another compound. Directly removing COS is not a very effective technique, so converting COS to a different compound is chosen. As $H_2S$ also needs to be removed, converting COS in $H_2S$ is a logical reaction. This reaction can be done with hydrogenation or hydrolysis. It is proven by Zhang et al. that hydrolysis of COS is the preferred option due to milder reaction conditions and higher conversion compared to hydrogenation. Performing this reaction at 200 °C results in an almost complete conversion of COS using an oxysulfide catalyst and is independent of the applied pressure[85, 156]. This catalyst, however, is deactivated in the presence of $SO_2$, this is why $SO_2$ is removed before the conversion of COS[157]. The COS to $H_2S$ reactor is assumed to be an autoclave with an average residence time of 1 min. The flow rate at 200 °C is 8,522.36 $m^3\ min^{-1}$, so the reactor has a volume of 8,522.36 $m^3$.

### 4.2.4. $H_2S$

The last impurity in the gas feed stream that needs to be removed is $H_2S$. The $H_2S$ concentration is higher than stated in Table 3.2, due to the conversion of COS to $H_2S$. Removing this compound is already widely established in the industry using caustic washing with NaOH. To increase the selectivity towards the removal of $H_2S$, an amine-based solvent is used. It is found that sterically hindered amines are more effective compared to traditional amines and that a low temperature and high solvent concentration favoured the selectivity towards the removal of $H_2S$[158]. Even though sterically hindered amine solvents result in a higher selectivity, the conventional amine-based solvent MDEA is used due to the unavailability of certain substances in the ASPEN Plus V12 software. From a previous study it is know that the lowest $H_2S$ concentration is obtained when a mole fraction of 0.26 MDEA in water is used. The removal of $H_2S$ is done in an adsorption column and its specifications are shown in Figure 4.4 and Table 4.3.

During this separation step, a large amount of $CO_2$ is lost. To reduce this loss, the bottom stream that contains the lost $CO_2$ is run through a flash drum to recover most $CO_2$ and recycle it back to the column. The top stream is cooled down and a flash drum is used to remove water that has entered the vapor phase. It is assumed that the flash drum is a vertical pressure vessel with a height 4 times its diameter and an average residence time of 5 $min$. The flash drum has a calculated height and diameter of 20.31 and 5.08 $m$ and volume of 411.45 $m^3$ as calculated in Appendix B.2.

In the gas stream leaving the $H_2S$ scrubber, some $H_2O$ is present. A flash drum is used to remove

the excess water in this stream. The same assumptions for this flash drum are used as for the $CO_2$ recovery flash drum. In Appendix B.2, the size of the flash drum is calculated. The flash drum has a height and diameter of 3.37 and 0.84 $m$ and volume of 1.88 $m^3$.

Table 4.3: Absorber column specifications to remove $H_2S$ from the gas stream

| | |
|---|---|
| Condenser duty | 0 $MW$ |
| Reboiler duty | 0 $MW$ |
| Tray height | 0.6096 $m$ |
| Tray diameter | 8.977 $m$ |

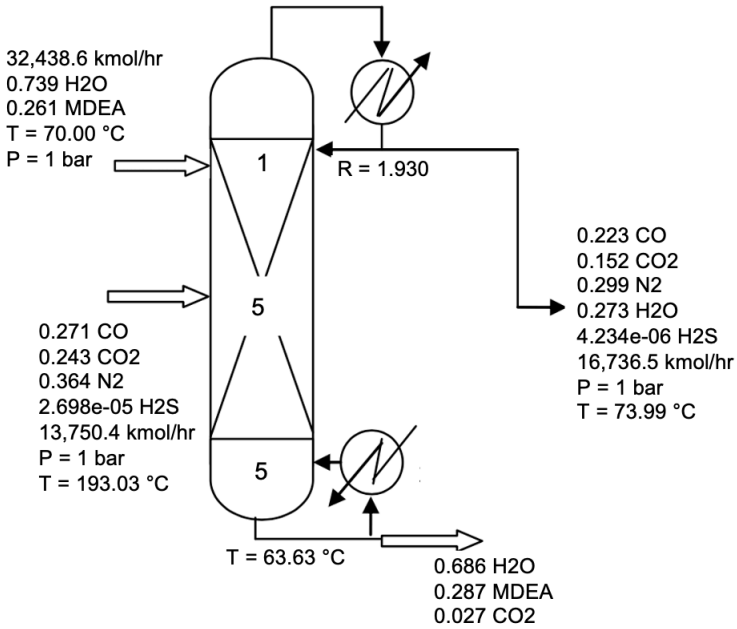


Figure 4.4: Scrubber column specifications to remove $H_2S$

### 4.2.5. $CO_2$

After the impurities are removed to the required level, $CO_2$ is isolated from the other gas compounds using pressure swing adsorption (PSA). It is assumed that all impurities leave the PSA units in the most important product stream. The PSA unit has a 90% $CO_2$ recovery and is able to produce a 95% pure $CO_2$ stream. The adsorbent used is a zeolite-based 5A and the operating pressure is 1 to 2 $bar$. The PSA unit can only be used when the $CO_2$ concentration is higher than 15%. After all impurity removal units and removal of water, the $CO_2$ concentration is 20.5%, so PSA can be used[159]. This isolated $CO_2$ stream is the gas input stream of the first electrolyzer.

### 4.2.6. CO

The other gas stream leaving the $CO_2$ PSA and the gas exit stream of the first electrolyzer are mixed and fed to the CO PSA. In this separation unit, CO is separated from the other gasses with a recovery of 96% using a cupric chloride on an activated carbon support. The CO stream leaving the PSA unit has a purity of 98% and has an operating pressure and temperature of 1 $atm$ and 27°C[160]. The CO-rich stream is fed to the second electrolyzer where it reacts to form $C_{2+}$ compounds.

## 4.3. Electrolyzers

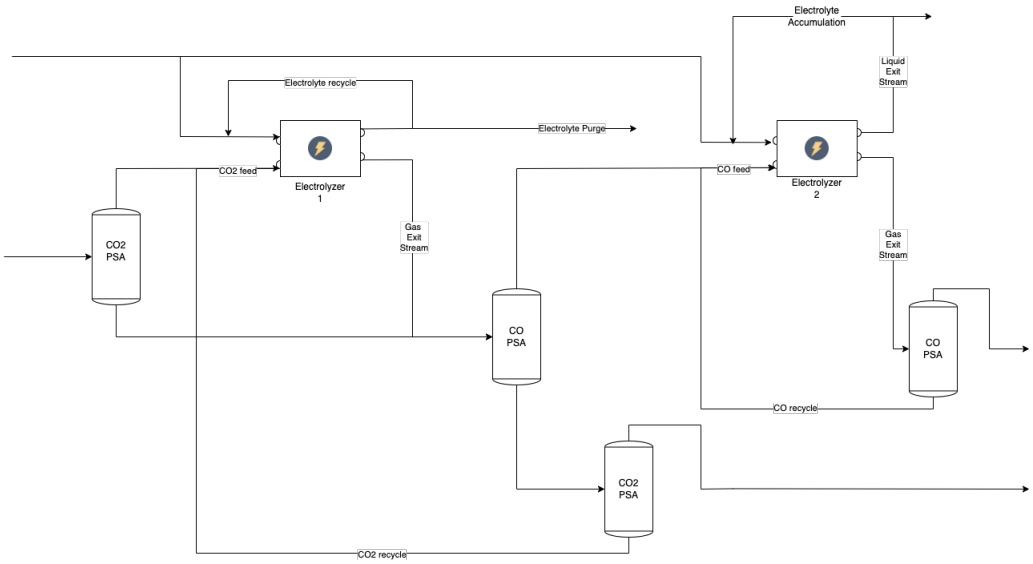


Figure 4.5: Model scheme for the electrolyzers

$CO_2$ is converted to $C_{2+}$ products in two steps using two types electrolyzers. The reason why two electrolyzers are used is that selective reduction of $CO_2$ on copper is challenging, due to various proton and electron transfers. First reducing $CO_2$ to CO yields a higher CO concentration at the electrode surface at the second electrolyzer, which favours C-C coupling[161, 162]. $C_{2+}$ molecules are favoured over C1-molecules as products because they have a higher energy density. The requirements for the electrolyzers are that they have a high CD, FE towards $C_{2+}$ products, high stability, and high single pass conversion. The model scheme of the two electrolyzer system is shown in Figure 4.5. The calculations for the electrolyzers can be found in Appendix B.3.

In the first electrolyzer, $CO_2$ is converted into CO and uses a volumetric flow rate ratio of 1:4 for the electrolyte-to-gas feed ratio in a membrane electrode assembly (MEA) electrolyzer[163]. The benefit is this type of electrolyzers for the first step is that they have high stabilities and only an anolyte is used. The half reactions taking place in the first electrolyzer are mentioned in Reactions 2.19 and 2.6 at the cathode and Reaction 2.20 at the anode. The total area of the electrode is calculated to be 7,239.48 $m^2$ and has a cell voltage of 3.2 $V$[163]. One electrolyzer cell has an electrode surface area of 1 $m^2$, so in total there are 7,240 electrolyzer cells for the conversion of $CO_2$ to CO. The total current and power of this electrolyzer is 21,718,440 $A$ and 69.50 $MW$ as calculated in Appendix C.1.1. The other specifications of the electrolyzer are mentioned in Table 4.4.

In the second electrolyzer, the formed CO from the first electrolyzer and CO that is already present are converted to $C_{2+}$ compounds with a volumetric electrolyte-to-gas feed ratio of 2:1[164]. The second electrolyzer type is a GDE flow cell with a total power of 977.06 $MW$ and a total current of 305,331,990 $A$. The benefit of a GDE flow cell is that the CO is directly supplied to the electrode. The other specifications of this electrolyzer are stated in Table 4.4. The half reaction that takes place at the anode of this electrolyzer is the same as the first electrolyzer (Reaction 2.20). The reactions that happen at the cathode are Reactions 2.19 and 2.14 to 2.18. The total area of the electrodes is calculated to be 101,777.33 $m^2$ and it is assumed that the same cell voltage of 3.2 $V$ as the first electrolyzer since this is not mentioned in the used paper. For the conversion of CO to $C_{2+}$ molecules, each cell also has an electrode surface area of 1 $m^2$, so 101,778 cells are needed.

The article used for the second electrolyzer mentions a faradaic efficiency of 0.50% towards formic acid, but the electrochemical reduction of CO towards formic acid is not possible. The reference paper also uses a two-step $CO_2$ reduction process and uses the gas exit stream of the first electrolyzer

as a feed stream for the second electrolyzer. This gas stream is purified before it enters the second electrolyzer, but due to the formation of formic acid, it is expected that there is still some $CO_2$ present which causes the formation of formic acid. Moreover, it is expected that the mentioned FE of 0.50% is a typo since the FE to formic acid decreases with increasing current density. However, only at 100% CO and 300 $mA\ cm^{-2}$ current density, the FE to formic acid increases 10 times compared to the 200 $mA\ cm^{-2}$ case. Due to the impossibility of the formation of formic acid from CO and a low FE, it is assumed that formic acid is not formed at all.

Next to the assumption to neglect the formation of formic acid, the electrolyte in both electrolyzers are recycled to reduce the cost of the production of UPW and to accumulate the liquid products in the catholyte of the second electrolyzer. The recycled rate is inversely proportional to the amount of fresh UPW needed, so a larger recycle rate will require less fresh UPW. The amount of fresh UPW, however, will not decrease much when the recycling rate becomes high. For this reason, the anolyte is assumed to be recycled for 3500 passes. Another reason why recycling can not be much larger is to prevent the accumulation of contingent present impurities. The accumulation of the liquid products in the second electrolyzer is done to make it economically and energetically feasible to separate the formed products from each other and water. Greenblatt et al.[165] did research on the technical and energetic challenges of separating the products formed in electrochemical $CO_2$ reduction. The research concluded that for the energy return on energy investment (EROEI) to be larger than 1, the required energy to separate the product should be less than half of the enthalpy of combustion[165]. For this reason, the liquid products containing catholyte is recycled 2,000 times. Using this recycling rate, $H_2O$ still has a mole fraction of 0.80. It is assumed that the efficiency of the electrolyzer is not affected when the $H_2O$ mole fraction is 0.80 or higher. To let the process run continuously, only 1/3500 part of both anolyte flows and 1/2000 part of the catholyte flow is removed and goes to the product separation part of the process. Normally when a recycle is used, a part is purged to prevent the accumulation of inert compounds or impurities. In this case, the purge contains the liquid products and goes downstream to the product separation part.

The recycled catholyte and anolyte are stored in a floating roof storage tank. It is assumed that the average residence time of the electrolyte in an electrolyzer is 1 $min$[166]. The volume of the storage tanks for the anolyte is based on the average residence time of the anolyte in the electrolyzer. A tank volume of two times the volume of anolyte that passes through the electrolyzer every minute is assumed to be adequate. The volume of the storage tank for the anolyte of the first and second electrolyzer is calculated in Appendix B.3 and has a volume of 937.75 and 20,336.2 $m^3$, respectively. Anolyte is not used in the downstream processes, but catholyte is used. Electrolyzers sometimes require small maintenance and need to be shut down for a short time. This can influence the downstream liquid product separation process, so a larger storage tank is used, so the downstream process is not influenced during maintenance of the electrolyzers. It is assumed that a storage tank should contain an extra volume of 1 day of downstream production besides the volume of two times the average residence time. Every day a volume of 7,402.12 $m^3$ flows to the liquid product separation. Since the catholyte and anolyte flow are equal for the second electrolyzer, the catholyte storage tank needs a volume of 27,768,32 $m^3$ as calculated in Appendix B.3.

Furthermore, the single pass conversion of $CO_2$ and CO in the first and second electrolyzer is 50% and 43%, respectively. To use as much $CO_2$ and CO, these compounds are separated from the other gas compounds in the exit streams using PSA and are recycled back to the electrolyzer. After the CO PSA isolates CO for the second electrolyzer, another $CO_2$ PSA unit is placed to recover unreacted $CO_2$. The unreacted and isolated $CO_2$ stream after the $CO_2$ PSA is mixed with the fresh $CO_2$ stream and goes to the first electrolyzer to react to CO. The gas stream exiting the second electrolyzer still contains a large amount of CO. A CO PSA unit is used to remove unreacted CO from this stream and the separated CO is mixed again with fresh CO to be fed to the second electrolyzer again. A storage tank for $CO_2$, CO, or gas products is not used, due to the large volume of the gas stream.

Table 4.4: Electrolyzers specifications[163, 164]

| Electrolyzer | Electrolyzer type | Current density ($mA\ cm^{-2}$) | Potential ($V$) | Catalyst | Catholyte | Anolyte | Faradaic efficiencies | Single pass conversion |
|---|---|---|---|---|---|---|---|---|
| $CO_2$ to CO | MEA flow cell | 300 | 3.2 | Ag coordination polymer | | 1M KOH | 96% to CO<br>4% to H2 | 50% of $CO_2$ |
| CO to $C_{2+}$ | GDE flow cell | 300 | 3.2 | Cu | 1M $KHCO_3$ | 2.5M KOH | 16.38% to PrOH<br>15.49% to EtOH<br>45.57% to Ethylene<br>9.35% to Acetic acid<br>10.92% to $H_2$ | 43% of CO |

## 4.4. Product Separation

As mentioned before, there are three liquid products and four gaseous products formed. The formed gas products that need to be separated are ethylene, hydrogen, methane, and oxygen. Methane, however, is only formed when sulfur and nitrogen impurities are present in the stream. In a previous study, it is found that removing gas impurities is the preferred option over not removing the impurities, due to the formation of more valuable products. For this reason, methane is not considered to be formed and separated. Currently, the oxygen that is formed at the anode side of the electrolyzer is assumed to leave the electrolyzer in a pure form and is purged. This is done due to how the electrolyzers are modelled and it is not known what the composition of the oxygen stream is. When it is known what the composition is, then oxygen can be purified and used and sold for industrial or medical applications. The liquid compounds are acetic acid, ethanol, and n-propanol. It is assumed that all liquid products are dissolved in the water phase and all gas products are in the gas phase. Furthermore, it is assumed that acetic acid is only present in deprotonated form as acetate, due to the high concentration of $OH^-$ in the stream. The model scheme of the gas and liquid products separation parts of the process are shown in Figure 4.6 and 4.8.

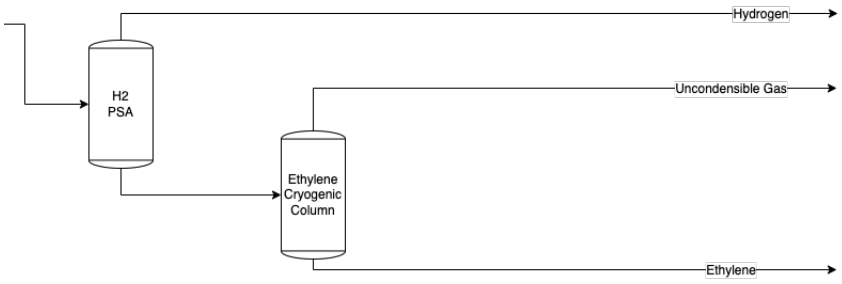


Figure 4.6: Model scheme for the gas separation process

### 4.4.1. Hydrogen

Two streams contain hydrogen. The first stream is the stream exiting the $CO_2$ PSA that recycles unreacted $CO_2$. This stream mainly contains $N_2$ and $H_2$. The mole fractions of $H_2$ and $N_2$ are 0.13 and 0.75, respectively. Since it is not possible to separate $H_2$ from $N_2$ with a low $H_2$ to $N_2$ ratio using PSA, another technique has to be used or another application for this stream has to be found. A possible method to remove $H_2$ from the gas streams is using a selective membrane separation technique. Graphene-based membranes have shown to be effective in selectively separating $H_2$ from $N_2$, but this technique is only proven on lab-scale so far[167]. Elaborating this technique can be a solution to obtain a high purity $H_2$ stream. Another possibility is to add extra hydrogen to this stream and use it in the Haber-Bosch process, but the influence of the other compounds present in the stream on the Haber-Bosch process has to be reseached.

The second stream which contains hydrogen has a higher hydrogen-to-nitrogen ratio, so PSA can be used as a separation technique to isolate $H_2$. This stream contains, next to $H_2$, also the other gas product ethylene. $H_2$ is chosen to be separated first because for the ethylene separation, the stream needs to be pressurized and cooled down. Removing $H_2$ first will decrease the cost of pressurizing and cooling down the stream, since it is smaller, and $H_2$ PSA is performed at room temperature. The $H_2$

leaving the PSA unit has a purity of 99.4%. Hydrogen is not further purified, since the purity higher than needed for qualified grade.

### 4.4.2. Ethylene

The next gas product is ethylene which is the main compound that is present after the removal of $H_2$. Other compounds that are present in noteworthy quantities are CO, $CO_2$, $H_2$, and $N_2$. Most of these compounds are hard to condense, but ethylene and $CO_2$ are condensable. To condense these compounds, the stream is cooled and pressurized. A trade-off has to be made between the pressure and temperature and it is found that pressures higher than 20 bar did not influence the increase in temperature and purity of ethylene that much anymore. The stream is first compressed to 20 bar and then cooled down to -80°C, to condense ethylene out as the liquid phase. The temperature is chosen so the required ethylene purity is reached. A cryogenic distillation column is used to separate the liquid phase from the gas phase. The specifications of the column are shown in Figure 4.7 and Table 4.5. The purity of ethylene is 98% which is already higher than required to be used for industrial applications and is chosen not to be purified further.

Table 4.5: Distillation column specifications to separate ethylene from non-condensible gasses

| | |
|---|---|
| Condenser duty | -0.737 $MW$ |
| Reboiler duty | 1.575 $MW$ |
| Tray height | 0.6096 $m$ |
| Tray diameter | 2 to 14: 0.7088 $m$<br>15 to 28: 1.3020 $m$ |

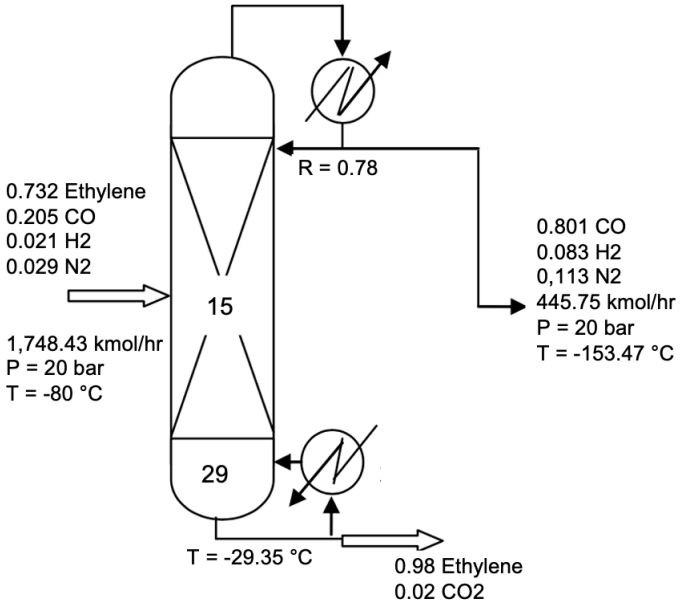


Figure 4.7: Distillation column specifications to separate ethylene from non-condensible gasses

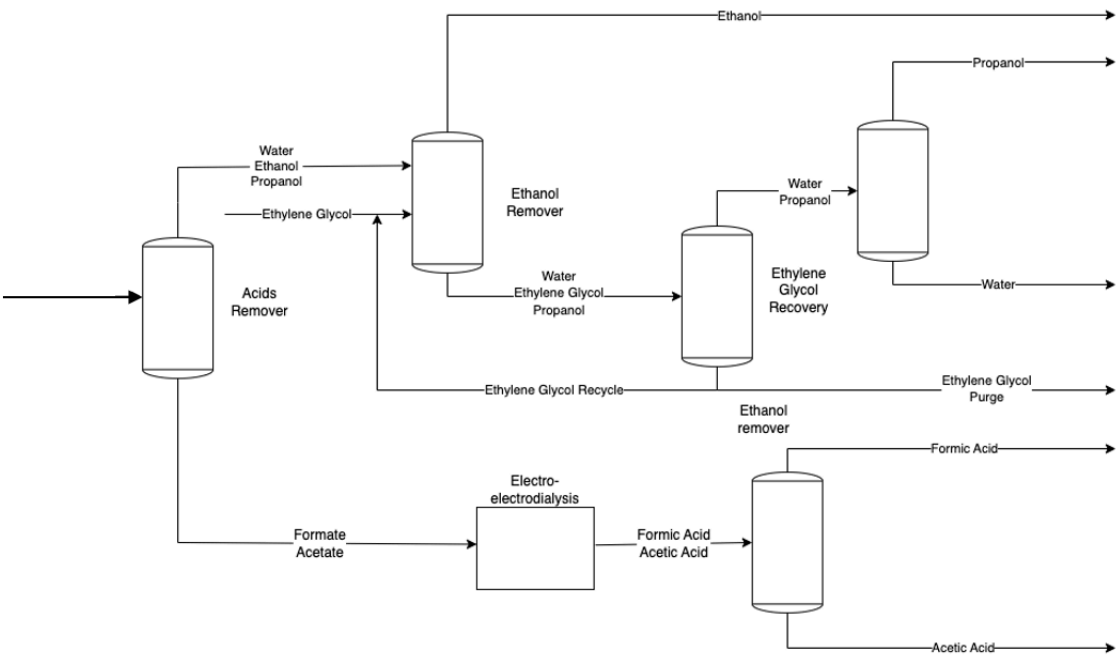


Figure 4.8: Model scheme of the product separation process

### 4.4.3. Acetic Acid

The first product that is separated from the liquid product stream is acetate. Acetate is removed first because ethanol and propanol form an azeotrope with water, so special separation methods are needed to isolate these compounds. Two separation methods are considered to separate acetate; distillation and electrodialysis. Since the stream is quite large and electrodialysis is not able to remove all acetate, a large recycle is needed to remove most acetate, so using distillation is the preferred option. Almost all acetate leaves at the bottom of the column together with some water and ethanol, n-propanol, and the remainder water comes out at the top of the column. The design specifications of the column are shown in Table 4.6 and Figure 4.9.

Table 4.6: Specifications of the distillation column to separate acetate from the liquid product stream

| | |
|---|---|
| Condenser duty | -325.382 $MW$ |
| Reboiler duty | 325.394 $MW$ |
| Tray height | 0.6096 $m$ |
| Tray diameter | 12.128 $m$ |

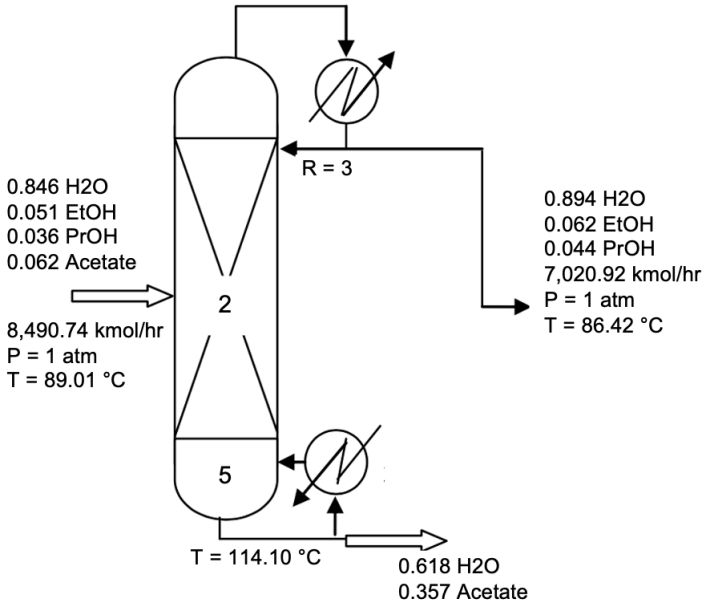


Figure 4.9: Distillation column to separate acetate from ethanol, n-propanol, and water

The bottom exit stream of the distillation column contains acetate and water. The desired product acetic acid can easily be separated from water using distillation, but the compound is present as acetate. Acetate first needs to be protonated to be used in a distillation column. Two options are able to do this; the addition of an acid to lower the pH or electrodialysis. Adding an acid is not desirable, since it dilutes the stream and acids are hazardous compounds, so it is desirable to use as less acids as possible. Using an electro-electrodialysis with a recycle is found to be an effective method to obtain a protonated acetic acid stream. The applied potential in the elctro-electrodialysis unit is 4.3 $V$ and has a removal efficiency of 40.47%.[168] An electro-electrodialysis unit consists of three compartments separated by ion exchange membranes. The carrier in all streams is $H_2O$, so the protonated acetic acid leaves the electrodialyser still dissolved in $H_2O$. The stream containing acetate that is not converted is recycled to reduce the loss of the product.

After the electro-electrodialyser, acetic acid is separated from water using a distillation column. The required purity of acetic acid is 80 mole% and the column is designed so that acetic acid has the desired purity. The column specifications are shown in Figure 4.10 and Table 4.7.

Table 4.7: Specifications of the distillation column to separate acetic acid from $H_2O$ to the desired purity

| | |
|---|---|
| Condenser duty | -33.763 $MW$ |
| Reboiler duty | 33.719 $MW$ |
| Tray height | 0.6096 $m$ |
| Tray diameter | 2 to 17: 3.799 $m$<br>18 to 24: 5.157 $m$ |

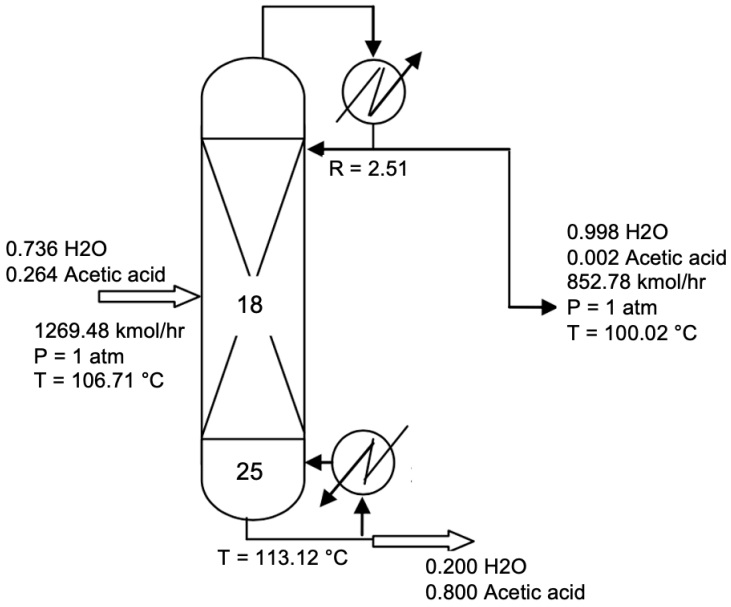


Figure 4.10: Distillation column to isolate acetic acid from water

### 4.4.4. Ethanol

The top exit stream of the first distillation column contains ethanol, n-propanol, and water. This mixture forms an azeotrope, so with normal distillation, the compounds can not be separated to the required purities. Two separation techniques are considered to separate the compounds; pervaporation and extractive distillation. With pervaporation, it is hard to effectively remove one of the compounds, since not much study is performed on the separation of ethanol, n-propanol, and water mixtures. With extractive distillation, ethanol can be easily separated from n-propanol and water using ethylene glycol as an entrainer[169]. A 1:1 flow rate ratio of water and alcohol mixture to ethylene glycol is used to reach the desired purity. With this method, ethanol leaves on the top of the column with a purity of 99 mole%, and ethylene glycol, n-propanol, and water emerge from the bottom of the column. In Figure 4.11 and Table 4.8 the design specifications for the extractive distillation column are shown. Ethanol does not require further purification, since it already meets the required purity for it to be used in the industry.

Table 4.8: Specifications of the extractive distillation column to isolate ethanol

| | |
|---|---|
| Condenser duty | -33.943 $MW$ |
| Reboiler duty | 64.493 $MW$ |
| Tray height | 0.6096 $m$ |
| Tray diameter | 2 to 27: 5.608 $m$<br>18 to 24: 5.550 $m$ |

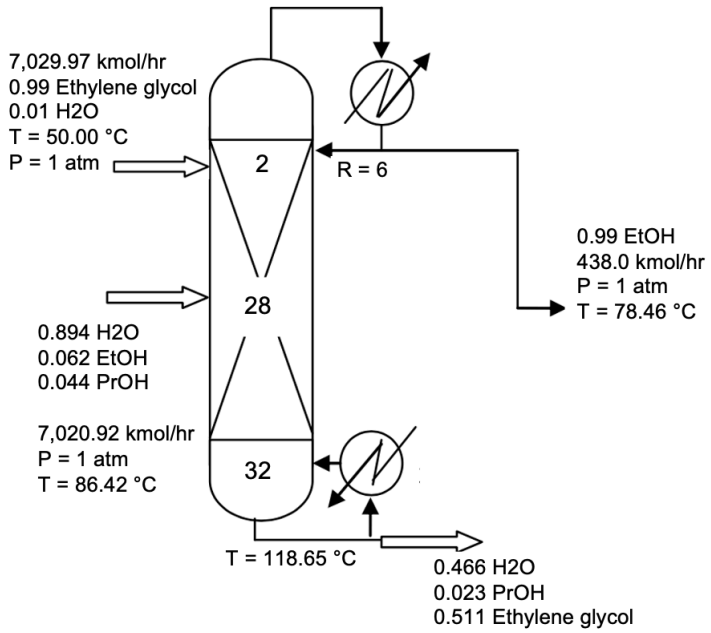


Figure 4.11: Extractive distillation column to isolate ethanol with ethylene glycol as entrainer

After the ethanol extraction column, ethylene glycol is recovered to be reused in the ethanol extraction column. Ethylene glycol, n-propanol, and water do not form an azeotrope, so normal distillation can be used to recover ethylene glycol. n-Propanol and water leave the column on the top and ethylene glycol leaves at the bottom. Ethylene glycol is recycled with a purge, so only a small fresh ethylene glycol stream is needed. The column specifications are shown in Figure 4.12 and Table 4.9.

Table 4.9: Specifications of the distillation column to recover ethylene glycol

| | |
|---|---|
| Condenser duty | -81.153 $MW$ |
| Reboiler duty | 110.248 $MW$ |
| Tray height | 0.6096 $m$ |
| Tray diameter | 2: 5.192 $m$<br>3 to 15: 5.183 $m$<br>16 to 63: 7.336 $m$ |

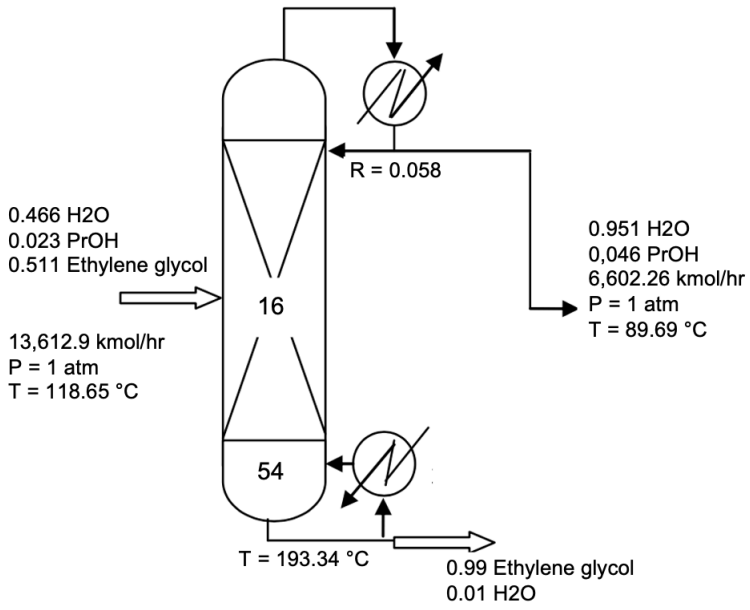


Figure 4.12: Distillation column to recover ethylene glycol

### 4.4.5. n-Propanol

At last, n-propanol needs to be separated from water. n-Propanol and the water form an azeotrope with the azeotropic point at an n-propanol concentration of 71.7 wt%. The boiling point of the mixture is 87.7°C[170]. Due to the fact that distillation is an efficient way of separating, the mixture is first separated with a distillation column to increase the n-propanol concentration close to the azeotropic point. With the column specifications as shown in Figure 4.13 and Table 4.10, n-Propanol leaves the column in the top stream with a purity of 39.9 mole% (68.7 wt%) which is nearly at the azeotropic point.

Table 4.10: Specifications of the distillation column to increase the n-propanol concentration

| | |
|---|---|
| Condenser duty | -21.764 $MW$ |
| Reboiler duty | 23.257 $MW$ |
| Tray height | 0.6096 $m$ |
| Tray diameter | 2 to 3: 3.144 $m$<br>4 to 7: 3.289 $m$ |

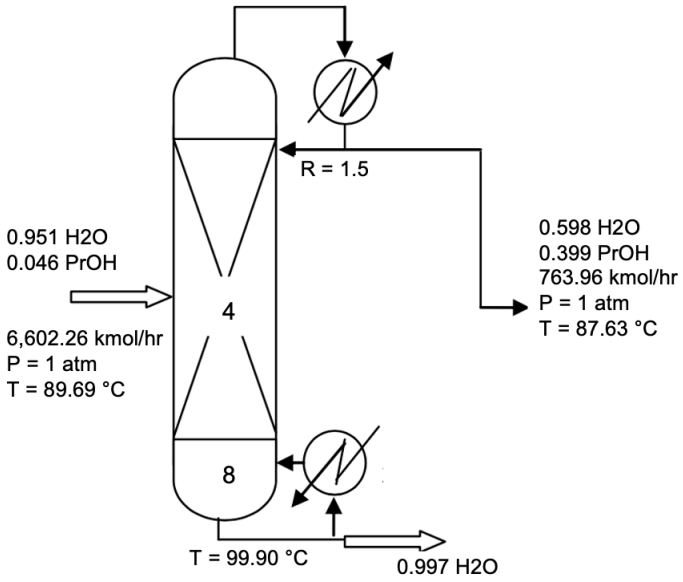


Figure 4.13: Distillation column to increase the n-propanol fraction

n-Propanol is further purified using pervaporation to the desired purity. The used membrane is a hydrophilic polymeric membrane that consists of a polyvinylalcohol active layer on a support of polyacrilonitrile. The flux through this membrane is 1.2 $kg\ m^{-2}\ hr^{-1}$, so the pervaporation membrane has a calculated area of 6,872.04 $m^2$ as shown in Appendix B.4[170]. Water diffuses through this membrane and most n-propanol is stopped. It is assumed that 98% of the water in the feed stream passes through the membrane. With an n-propanol feed concentration of 68.7 wt%, the separation factor of the membrane is 100, so 0.98% of the n-propanol also diffuses through the membrane. After the pervaporation unit, the n-propanol stream has a flow rate of 313.22 $kmol\ hr^{-1}$ with a purity of 96.4 mole%. It is chosen not to further increase the purity of n-propanol, since the conclusion from Greenblatt et al.[165] is not met. The separation energy of n-Propanol is already greater than half of its lower heating value, which is shown in Section 5.3.1. For most applications, n-propanol requires a higher purity, so finding more efficient separation methods or a different order of separating the liquid products with different separation techniques is recommended.

## 4.5. Heat Integration

A significant amount of energy is required for the heating and cooling of the streams. This is done by using heaters and coolers, but the heat of one stream can also be used to heat another stream. This is done to reduce the cost and the emission of $CO_2$. In the process, heat exchangers are used, wherever possible, to exchange energy from a heat stream to a cold stream. A minimum temperature approach of 10°C is used to model the heat exchangers. The heat exchange network of the process can be found in Appendix G.

The bottom stream of the ethylene glycol recovery column has a temperature of 193.34°C. This stream is recycled and needs a temperature of 50°C, so this heat can be used to heat other streams and other streams can cool down ethylene glycol. Therefore this stream is used in four heat exchangers. The four streams that are heated up to the required temperature are the feed stream of the acetate removal column, the feed stream of the acetic acid removal column, the exit stream of the $SO_2$ removal column, and the ethylene product stream leaving electrolyzer 5. The order in which both column feed streams are heated up does not matter, since they will be both heated to the required temperature without surpassing the minimum temperature approach. The other two streams both do not need to be heated, but are only used to cool down the ethylene glycol stream because it needs to be 50°C to be used again. The heat exchangers have an exchanger area of 133.5, 31.6, 884.3, and 62.7 $m^2$, respectively, for heat exchangers 1, 2, 3, and 6.

The other two heat exchangers are used to cool down the bottom stream of the acetate removal column, so the stream can be used in the electro-electrodialyser. In heat exchanger 4, the uncondensable gas stream leaving the ethylene separation column is used for cooling and has an exchanger area of 7.8 $m^2$. Condensed ethylene from the ethylene separation column is used in heat exchanger 5 to cool down the feed stream of the electro-electrodialyser to the required temperature. The exchange area of heat exchanger 5 is 11.8 $m^2$.

Not all streams have the required temperature using the heat exchangers. There are four streams that need extra cooling. Therefore utility stream available in ASPEN PLUS V12 are used to cool the stream to the required temperature. A stream that is cooled is the ethylene glycol recycle stream to reach a temperature of 50°C. To cool this stream, cooling water is used that enters the cooler at 20°C and leaves the cooler at 25°C. Two streams in the gas feed stream purification part need to be cooled to 15 and 25°C. Cooling with cooling water is not possible, since the minimum approach temperature is then crossed. So a refrigerant called refrigerant 1 is used that has a begin temperature of -25°C and a end temperature of -24°. The last stream that requires cooling is the gas stream containing ethylene and non-condensable gasses and this stream is cooled to -80°C using refrigerant 4. This refrigerant has a begin temperature of -103°C and an end temperature of -102 °C.

# 5

# Results and Discussion

## 5.1. Liquid and gas feed stream purification

The liquid and gas feed streams are purified using multiple separation techniques. The concentrations of the ions and oxygen after the liquid feed stream purification part are given in Appendix H.

The requirements for ultrapure water can be found in Table 2.1. The concentrations of each cation should be lower than 0.01 $\mu g\ L^{-1}$. $Na^+$ has the highest concentration, however, the concentration of $Na^+$ is below the maximum concentration, so the requirements for ultrapure water are met. Besides that, the concentration of heavy metal ions $Fe^{2+}$, $Pb^{2+}$, and $Zn^{2+}$ should be very low to prevent poisoning the catalyst.[61] The concentrations of $Pb^{2+}$ and $Zn^{2+}$ after purification are too low for ASPEN PLUS V12 to be considered and are therefore automatically set to 0 $\mu g\ L^{-1}$. The lowest concentration of $Fe^{2+}$ researched by Hori et al.[61] is 0.05 $\mu M$ and the concentration of $Fe^{2+}$ after the liquid feed stream purification part is in the order of $10^{-}5\ \mu M$. The concentrations of the heavy metal ions that deactivate the catalyst are much lower than researched and therefore it is assumed that the heavy metals do not poison the catalyst.

For the anions, $HCO_3^-$ has the highest concentration after all purification units with a concentration of 0.004708 $\mu g\ L^{-1}$. This is below the maximum concentration allowed for anions of 0.05 $\mu g\ L^{-1}$. $O_2$ is also removed sufficiently from the liquid feed stream with a concentration of 2.442 $\mu g\ L^{-1}$ where the maximum allowed concentration for dissolved oxygen is 10 $\mu g\ L^{-1}$.

The concentrations of the gas impurities after the gas purification part are given in Appendix H. The target was to decrease the concentrations of these compounds to an acceptable level. The target for $H_2S$ is to have a concentration below 10 ppm and this target is reached. However, as explained later in Section 5.2.2, another separation technique for $H_2S$ should be used to make the process economically feasible. For the other compounds, it is assumed that the concentrations are low enough to not deactivate the catalyst.

The specifications of the separation techniques are obtained from literature data, but the specifications might change when the process operates at a large scale which can cause the concentrations to increase. More research on the up-scaling of the purification techniques is recommended to validate the performance of the individual separation units.

## 5.2. Techno-Economical Analysis

In this section, the techno-economical analysis is done where the CapEx and OpEx are calculated using a base case. Later a sensitivity analysis is done with two different cases to get an insight into what factors most influence the economics of the process.

### 5.2.1. Total Capital Investment

To calculate the CapEx of each unit, the equations for the capital cost of a single unit from Seider et al. are used[117]. For units that are not present in the book, other references are used to determine the price of the unit as can be seen in Appendix C. All the calculated and prices are later corrected for inflation using method explained in Section 2.4. The process consists of five parts. These five parts are the liquid feed stream purification (Section 4.1), gas feed stream purification (Section 4.2), electrolyzers (Section 4.3), liquid product separation, and gas product separation (Section 4.4). The price without the correction for inflation of each unit in these parts can be found in Tables C.16 to C.21 and is summary shown in Table 5.1. The prices are based on the flow rate and size of each unit. The price calculations can be found in Appendix C.1.1. When calculating the prices of each unit, the following assumptions are made:

- The concentration of ions in the liquid feed stream to the liquid feed stream purification section is constant
- The gas feed composition entering the gas purification part is constant
- The free on board purchase price for all PSA units are based on the price of a $H_2$ PSA unit[171]
- Flash drums are pressurized vessels
- COS to $H_2S$ reactor is an autoclave
- Adsorber columns are distillation columns
- Heaters and coolers are heat exchangers
- Pressure drop in the liquid product separation process and gas stream are neglected
- Electrolyzer costs are calculated using equations from Jouny et al.[54]

Table 5.1: Total f.o.b. price of all parts of the process

| Unit | F.o.b. price ($) | Contribution to total |
|---|---|---|
| Liquid feed stream purification | 82,893,379.63 | 18.2% |
| Gas feed stream purification | 21,827,817.11 | 4.8% |
| Electrolyzers | 317,205,343.11 | 69.5% |
| Liquid product separation | 21,763,719.27 | 4.8% |
| Gas product separation | 11,737,798.88 | 2.6% |
| Heat exchangers | 905,439.54 | 0.2% |
| **Total** | **456,333,497.53** | |

The total CapEx without the correction for inflation is $456,333,497.53. The f.o.b prices obtained from Seider et al.[117] have a CE index of 567, but the value is outdated and has increased since. Currently, the CE index has a value of 808.7.[172] To calculate the total investment, Equation 2.29 is used. From this equation, it is calculated that the total capital investment (TCI) of this process is $4,053,574,120.98 as shown in Table 5.2. The price of the TCI for each part is also shown in the same table. The TCI contains all costs that come with designing, constructing, and starting up a new plant.

The largest contributors to the CapEx are the electrolyzers and the liquid feed stream purification. The cost of the electrolyzers will increase when the electrolyzers operate at higher current densities or potentials. The cost of the electrolyzers is based on the price per $kW$, applied voltage, and current density[44]. Research needs to be performed on more efficient catalysts to reduce the applied potential and reducing the cost per $kW$ to compensate for the increase in the CapEx due to a higher CD. Increasing the recycling of the electrolytes helps to reduce the size of the liquid feed stream purification part which results in a lower CapEx. Therefore, influence of the electrolyte recycle on the electrolyzer performance needs to be researched.

Table 5.2: Total capital investment of all parts of the process

| Unit | TCI ($) |
|---|---|
| Liquid feed stream purification | 736,335,290.46 |
| Gas feed stream purification | 194,071,739.31 |
| Electrolyzers | 2,817,709,803.89 |
| Liquid product separation | 193,325,385.23 |
| Gas product separation | 104,265,932.80 |
| Heat exchangers | 8,042,947.31 |
| **Total** | **4,053,574,120.98** |

### 5.2.2. Operating Cost

Operating costs are the ongoing expenses required to maintain the daily operations of the process. These costs consists of the costs to operate each unit, the costs of all materials, and the maintenance of the units that the process uses. The OpEx of each unit are shown in Tables C.29 to C.35. All calculations for the OpEx can be found in Appendix C.2. A summary of the OpEx are shown in Table C.36.

The total OpEx for the base case is $71,754,164.89 (See Appendix C.2.2) per day. This is mainly due to the cost of the materials and especially the cost of methyl diethanolamine (MDEA). The daily cost of the MDEA consumption is $64,350,720.00 (See Appendix C.2.2). Since this amount is too high for the process to be economically feasible in any way, the cost of MDEA is neglected and it is recommended to use a different compound or technique to remove $H_2S$. In Table 5.3, the OpEx is shown where the cost for MDEA is neglected. Now the OpEx is $7,403,444.89. When calculating the prices of each unit, the following assumptions are taken:

- Maintenance costs are 2.5% of the CapEx each year, except for units in the UPW production
- An electricity price of $0.19 per kWh is used[173]
- For CO PSA, the same separation energy is used as for $CO_2$
- Cost for MDEA is neglected
- The prices from Aspen PLUS V12 are used for different heat sources
- A reference cost of $0.40 per $m^3$ of volumetric flow is used for the electrodeionization[174]

When the cost for MDEA is neglected, the largest contributors to the OpEx are the daily cost of the electrolyzers and materials. The daily electrolyzers cost is cost for the electricity needed to convert $CO_2$ and CO in high value compounds. Decreasing the energy consumption will almost always lead to a decrease in product formation. Therefore the electrolyzers need a high faradaic efficiency towards the desired or most valuable product. Moreover, the cell also needs a high energy efficiency, so most of the energy consumed will be stored in newly formed chemical bonds. The material cost mainly consists of the cost of KOH and $KHCO_3$. These compounds are used in the electrolytes. Researching the effect of reducing the molarity or using a different salt on the electrolyzer performance helps to find the optimum molarity and compound which can result in a lower daily cost.

Table 5.3: Summary of all operating cost of different parts of the process with the cost of MDEA neglected

| Unit | Operating cost ($\$\ day^{-1}$) |
|---|---|
| Liquid feed stream purification | 40,836.69 |
| Gas feed stream purification | 337,985,84 |
| Electrolyzers | 4,794,046.27 |
| Liquid product separation | 108,411.08 |
| Gas product separation | 103,351.39 |
| Heat exchangers | 62.02 |
| Materials | 2,018,751.60 |
| **Total** | **7,403,444.89** |

### 5.2.3. Income

The five formed products are sold after they are separated. The income from selling these products is shown in Table 5.4. The income of each product is calculated in Appendix C.3. Next to selling products, the process also consumes $CO_2$. Nowadays companies have to pay a $CO_2$ tax for every ton of $CO_2$ they emit. The current $CO_2$ tax is \$60.78 per ton $CO_2$ and this tax increases with \$12.55 per ton each year.[175] As can be seen in Section 5.3.2, if solar, wind, or nuclear energy sources are used as an energy source, the process is $CO_2$ negative. Since the $CO_2$ feed stream already exists and does not need to be produced, money is saved when the process consumes $CO_2$ and the net $CO_2$ emission is negative. For the calculation of how much $CO_2$ tax is saved, it is assumed that wind energy is used as an energy source. The income from the process is \$2,362,629.35 a day.

The income of each product is based on how much is produced and the price of the produced compound. The amount produced of a product is based on the faradaic efficiency of the compound and the number of electrons needed to form the products. Acetic acid and ethanol both require 4 electrons, ethylene 8 electrons, and n-propanol 12 electrons to be formed. For each product, the income per mole electrons consumed can be used to determine from an income point of view which product is most desired to produce. The income per mole electrons consumed is calculated in Appendix C.3. The highest income per mole electrons consumed is generated by acetic acid, followed by ethanol. Ethylene has the lowest income per mole electrons consumed. The highest income can be generated when the faradaic efficiency towards acetic acid is the highest. The influence on the CapEx and OpEx of a high faradaic efficiency towards acetic acid is not known, but the income per mole electrons consumed for acetic acid is almost 3.5 times higher than for ethylene and the cost for electricity is independent of the produced compound. Developing a catalyst with a high faradaic efficiency towards acetic acid is recommended to increase the income from the process.

Table 5.4: Total income from selling the products

| **Product** | **Income (\$ $day^{-1}$)** |
|---|---|
| Acetic acid | 418,290.48 |
| Ethanol | 349,578.54 |
| Ethylene | 885,993.60 |
| Hydrogen | 20,001.21 |
| n-Propanol | 567,710.43 |
| $CO_2$ tax saving | 121,055.09 |
| **Total** | **2,362,629.35** |

### 5.2.4. Net Present Value

From the previous sections, the NPV can be calculated by using the TCI, OpEx, and income. The OpEx is higher than the income, so the daily profit is -\$5,040,815.54. To calculate the NPV, an interest rate of 10%, average inflation of 2.0%, and a plant lifetime of 15 years are used.[118, 176, 177] The profit tax for corporations in the Netherlands is 25.8%, but this only apply when a profit is made, so for the base case this does not have to be paid. For the calculations of the NPV, the cost for MDEA is also neglected. The NPV is calculated to be almost -19.4 billion dollars for the base case after 15 years as shown in Appendix C.4. This high loss is due to a higher OpEx than income as well as the high TCI. The designed process and the current market for energy and product prices result in an economically unfeasible process. When MDEA is considered and no other separation technique for $H_2S$ is used, the NPV decreases to more than -210 billion dollars in 15 years.

### 5.2.5. Sensitivity Analysis

In the previous section, the base case is elaborated where current parameters are used. A sensitivity analysis is performed where the variables in the base case are compared with a better and an optimistic case to see which variables are needed for an economically feasible process. The variables are chosen, so the most optimistic case has a positive NPV. The chosen variables are shown in Table 5.5. Mostly parameters that depend on market developments are changed. Changing the electrolyzer parameters for lower electricity costs will decrease the formation of $C_{2+}$ products, which are the target products

in this process. For the electricity price and material cost, only 65% and 30% of the base price are used for the better and optimistic cases, respectively. Next to lower costs for electricity and materials, higher selling prices of 35% and 70% for the formed products are assumed for the better and optimistic cases, respectively. A higher price of the products is feasible in the future, since the formed products nowadays are mainly obtained from fossil fuels, which become scarce in the future. The $CO_2$ tax is also varied with the tax two and three times the current amount because this tax will increase in the coming years with $12.59 each year. The only technology development parameter that is changed for this analysis is the applied voltage because this can be improved with the development of a better and more efficient catalyst and electrolyzer cell.

Table 5.5: Sensitivity parameters with the base, better and optimistic case

| | **Base** | **Better** | **Optimistic** |
|---|---|---|---|
| Electricity Price ($\$\ kWh^{-1}$) | 0.190 | 0.124 | 0.057 |
| Selling Price Products ($\$\ kg^{-1}$) | 0% | 35% | 70% |
| Voltage ($V$) | 3.2 | 2.8 | 2.5 |
| Material cost ($) | 100% | 65% | 30% |
| $CO_2$ tax ($\$\ ton^{-1}$) | 60.78 | 121.56 | 182.34 |

The NPV for the better and optimistic scenario is calculated in Appendix C.5. Even with the better parameters the NPV is -8,010.48 million dollars. The optimistic case however, has a postive NPV of 433.36 million dollar after 15 years. Because the net profit in the optimistic case is positive, 25.8% corporate tax has to be paid on this profit. The NPV becomes positive in year 12 in the optimistic case, so after 12 years the process has earned itself back.

Next to knowing what the parameters need to be to have a positive NPV, the influence of the different parameters on the NPV is shown in Figure 5.1. At $\$ = 0$, the NPV of the better scenario is given and the bars show the difference of one parameter compared to the better scenario. As can be seen from the figure, the $CO_2$ tax has the least influence on the NPV. However, the electricity price does have a large influence on the NPV and this parameter will have the biggest influence in the future for this process to become economically feasible.[44, 178] The electricity price will even have a larger influence on the process than currently shown because a current density of 300 $mA\ cm^{-2}$ is used. In the future, it is planned to increase the CD to increase the product formation, but this will also increase the electricity cost. Large-scale state-of-the-art hydrogen electrolyzers have current densities of over 1,000 $mA\ cm^{-2}$, so the influence of the electricity price on the NPV will increase in the future.[179] The two other market-based parameters almost have an equal and quite large influence on the NPV. The influence of the selling price is also dependent on the FE towards the different compounds, since the selling price of the different compounds are different and some products require more electrons to be formed. The only technology-based parameter is the applied voltage and as can be seen, it does influence the NPV. The market-based parameters, however, have a larger influence on the NPV. This shows that the process is not limited by technological progress, but mainly by market conditions.

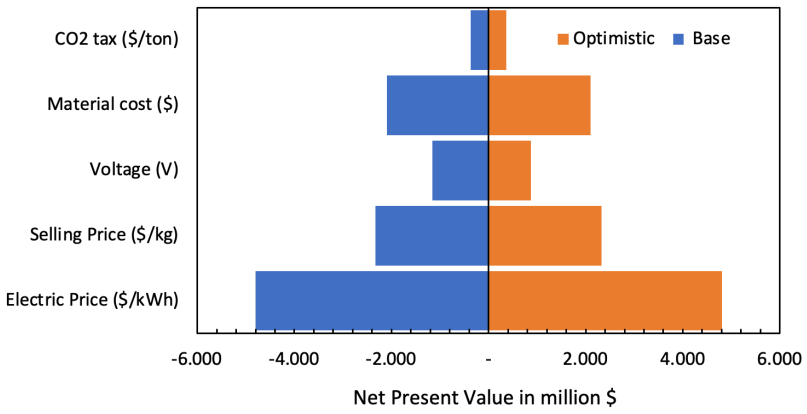


Figure 5.1: Influence of different parameters on the NPV with the better scenario as reference

## 5.3. Energy Analysis

In this section, the energy requirements of the process are analysed. First, it is checked if the energy requirement from the article of Greenblatt et al.[165] is met. Later, it is analysed if the process is carbon-neutral using different energy sources.

### 5.3.1. Product Separation Energy

As mentioned in the previous section, the energy to isolate each product should cost no more than about half of the enthalpy of combustion or lower heating value as stated by Greenblatt et al.[165]. The enthalpy of combustion, the amount produced, and the total energy content of the products are listed in Table D.1. In Tables D.2 to D.6, the energy required to isolate the product is shown. The energy consumption is the total energy that is consumed for every unit a compound passes through and the relative energy consumption is the energy a unit uses multiplied by the molar feed fraction of that unit for the relevant compound.

As can be seen from Tables D.2 and D.6, the maximum energy consumption to isolate acetic acid and n-propanol is exceeded. A higher recycle ratio is needed to meet this requirement, but the assumption that the electrolyzers specifications do not change is harder to validate if the $H_2O$ fraction drops even lower. Another solution to solve this is to find more efficient separation methods, but normally distillation is one of the most efficient separation method. Separating the products in a different order could also possibly reduce the energy consumption, but more research needs to be done on separating acetic acid, ethanol, n-propanol, and water mixtures. This is because the influence of the other products on some separation techniques, such as pervaporation, is not known.

### 5.3.2. $CO_2$ Analysis

One of the main objectives of this process is to reduce the emission of $CO_2$ and look if it is possible to use $CO_2$ as a source for carbon-based products. This process consumes $CO_2$ by using electricity, but all units in this process also require energy. Generating this energy will also emit $CO_2$. In this part, it is analysed if the process is $CO_2$ negative. For the energy analysis the parameters from the base case are used. As can be seen from Table 5.6, all used energy sources emit energy. This is because the total life cycle assessment of these different energy sources is used and $CO_2$ emissions involved in the production of each energy source is also taken into account.

The process consumes almost 2.4 million $kg$ $CO_2$ each day and the relative emission in Table 5.6 shows how much $CO_2$ the process emits compared to how much $CO_2$ is consumed. The process is only carbon negative when nuclear, wind, or solar energy is used as an energy source. When these sources are used only 18.16, 18.16, and 62.04% of the $CO_2$ that is consumed, is emitted by the process. This shows that the process is only carbon negative when a sustainable energy source is used as an energy source. When carbon-based sources are used, more $CO_2$ is emitted than without the use of this process. There is also a difference in which sustainable energy source is used. When nuclear and wind energy are used as energy source, less $CO_2$ is emitted compared to solar energy, so nuclear and wind energy should be used as energy source for this process to maximise the reduction of $CO_2$ emissions.

As shown in Table E.2, the biggest contributor to the total $CO_2$ emission is the second electrolyzer with 64.7% of the total emission. It is expected that this unit will consume the most energy and as a result the most $CO_2$, because molecular bonds have to be broken and formed which costs a lot of energy. For this electrolyzer, it is planned to increase the current density and this will also increase the $CO_2$ emission. This will result in a higher product formation rate, but the relationship between the extra $CO_2$ emitted and consumed should be investigated from a $CO_2$ point of view.

Other large contributors to the total $CO_2$ emissions are the first electrolyzer, the first distillation column, and the ethylene glycol recovery column. For the first electrolyzer, the high emission is due to the same reason as for the other electrolyzer, because a certain amount of energy to convert molecules is always needed. The first distillation column contributes 10.4% of the total $CO_2$ emissions because most of the stream leaves the unit on the top. This requires a lot of energy to evaporate a large part of the stream. Separating the products in a different order could possibly reduce the energy consumed

in such units. Also, the ethylene glycol recovery column consumes a lot of energy, which is the main reason why the conclusion from the research from Greenblatt et al.[165] can not be met for n-propanol. Finding alternate separation techniques that require lesser energy could help meet the requirements suggested by Greenblatt et al.[165] for the separation of alcohols.

For this process to run on large-scale, a stable, reliable, and large enough renewable energy source is needed. The total capacity of all nuclear, solar, and wind energy that is currently produced in the Netherlands is 426, 18,849, and 13,950 $MW$, respectively.[180–183] The designed large-scale CO2 electrolyzer plant requires a total power of 1,496.38 $MW$, thus requiring a considerable investment and scale-up in the renewable energy and storage sector to ensure a continuous supply of energy for the operation of the plant. This means that next to the technical and economical challenges, there also is a challenge in producing and storing the required energy from a sustainable energy source.

Table 5.6: $CO_2$ emissions from the different parts in the process based on different energy sources[54]

| **Section** | **$CO_2$ emmision with gas ($kg\ day^{-1}$)** | **Coal** | **Nuclear** | **Wind** | **Solar** | **Coal with CCS** |
|---|---|---|---|---|---|---|
| Liquid feed stream purification | 31,850.32 | 53,300.54 | 780.01 | 780.01 | 2,665.03 | 13,000.13 |
| Gas feed stream purification | 2,088,908.06 | 3,465,492.87 | 50,714.53 | 50,714.53 | 173,274.64 | 845,242.16 |
| Electrolyzers | 12,307,561.78 | 20,596,327.88 | 301,409.68 | 301,409.68 | 1,029,816.39 | 5,023,494.60 |
| Liquid product separation | 3,124,325.20 | 5,228,462.58 | 76,514.09 | 76,514.09 | 261,423.13 | 1,275,234.78 |
| Gas product separation | 234,757.53 | 392,859.54 | 5,749.16 | 5,749.16 | 19,642.97 | 95,819.40 |
| **Total** | **17,772,193.89** | **29,710,991.61** | **434,795.00** | **434,795.00** | **1,485,549.58** | **7,246,583.33** |
| Relative emission | 742.16% | 1,240.72% | 18.16% | 18.16% | 62.04% | 302.61% |

# 6

# Conclusions

A low-temperature, electrochemical $CO_2$ reduction process was designed with the required upstream and downstream processing of the gas and liquid streams in this work. The process is considered to be located in an average steel-producing plant in Europe where the flue gas stream of the plant is used as the gas feed stream and the liquid feed stream is obtained from the river Rhine. In this process, $CO_2$ is converted to $C_{2+}$ products in two steps. In the first step, $CO_2$ is converted to CO using a silver catalyst in an MEA flow cell with a current density (CD) of 300 $mA\ cm^{-2}$. The faradaic efficiency (FE) to CO is 96% with a single pass conversion of $CO_2$ of 50%. The MEA electrolyzer has an applied potential of 3.2 $V$ and uses 1M KOH anolyte. The anolyte is recycled 3,500 times to reduce the cost of the liquid feed stream purification. In the second step, CO is converted to $C_{2+}$ products using a copper catalyst. The electrolyzer type is a GDE flow cell with a CD of 300 $mA\ cm^{-2}$. The FE to acetic acid, ethanol, ethylene, n-propanol, and hydrogen is 9.35, 15.49, 45.57, 16.38, and 10.92%, respectively with a single pass conversion of 43% of CO. The catholyte is 1M $KHCO_3$ and the anolyte is 2.5M KOH.

Electrolyzers require ultrapure water, so ions and other compounds present in the liquid feed stream need to be removed. The purification of the liquid feed stream, i.e., water that is obtained from the river Rhine, is performed in seven steps to meet the specifications of ultrapure water. These purification steps are ultrafiltration, UV treatment, activated carbon, softener, reverse osmosis, degasser, and electrodeionization. To achieve the desired level of purity, multiple units of certain purification steps are needed. Therefore, two active carbon filters and four reverse osmosis units are used. The flue gas contains multiple sulfur and nitrogen compounds and these can harm the electrolyzers and other downstream processes. These compounds are removed using selective catalytic reduction, hydrolysis, and absorption columns. After the impurities are removed to the desired level, both CO and $CO_2$ are separated further using pressure swing adsorption (PSA) units. The anolyte is recycled 3,500 times to reduce the size and cost of the liquid feed stream purification part and the catholyte is recycled 2,000 times to increase the liquid product concentration. The liquid products, acetic acid, ethanol, and n-propanol, are separated to the desired purities using distillation, extractive distillation, pervaporation, and electro-electrodialysis. Recycle streams are used to recover the entrainer used in the extractive distillation column and to increase the recovery of acetate in the electro-electrodialyser. For the separation of the gas products, $H_2$ and ethylene, PSA and cryogenic distillation units are used.

The identified pre-treatment and post-treatment steps are modelled in ASPEN PLUS V12 and integrated into one model. The model consists of five different parts including the liquid feed stream purification, gas feed stream purification, electrolyzers, liquid products separation, and gas product separation. The sequence of purification units in the liquid feed stream is in the order: ultrafiltration, UV treatment, activated carbon, softener, reverse osmosis, degasser, and electrodeionization. In the gas feed stream purification part, $NO_x$ is removed first, followed by the removal $SO_2$, then the conversion of COS into $H_2S$, and finally, the removal of $H_2S$. $CO_2$ is firstly separated from the purified gas feed stream to reach a high $CO_2$ concentration and is converted to CO in the first electrolyzer. Unreacted $CO_2$ is separated from the formed CO and then recycled. The formed CO is mixed with the $CO_2$-lean purified gas feed stream and fed to the CO PSA, where a stream of concentrated CO is obtained for use

in the second electrolyzer. Unreacted CO is separated from the gaseous exit stream of second electrolyzer and recycled. The electrolyte leaving the second electrolyzer has a liquid product concentration of 20 mole%. First, acetate is removed from the other liquid products and water using distillation, and is then converted into acetic acid and purified using electro-electrodialysis and distillation. Ethanol is secondly removed using extractive distillation with ethylene glycol as entrainer and ethylene glycol is recovered and recyled using distillation. At last, n-propanol is separated from water using distillation and pervaporation.

From the techno-economical analysis, it is calculated that the free on board purchase price of the process is 456.33 million dollars. Using the Lang method, the total capital investment of the process is calculated to be 4,053.57 million dollars. This cost mainly consists of the cost of the electrolyzers and liquid feed stream purification. The cost to operate this process is 7.403 million dollars per day, which mainly consists of the cost of electricity and materials. For the calculation of the operating expenses, the cost for methyl diethanolamine was neglected, since it is too high. The income of the process is generated by selling the formed products and saving on the $CO_2$ tax. The total income is 2.263 million dollars a day, which results in a negative daily income of 5.041 million dollars. It is found that the income can be increased when the faradaic efficiency towards acetic acid is increase, since the income per mole electrons is the highest for acetic acid and the lowest for ethylene glycol. The net present value (NPV) of the current design process is calculated to be -19.38 billion dollars. A sensitivity analysis is performed on the process using three scenarios to see what the influences of different parameters are on the economic feasibility. The three scenarios include a base, better, and an optimistic scenario. The market-based parameters that are changed include the electricity price, selling price of the products, cost of materials, and $CO_2$ tax while the only technology-based parameter which is considered is the cell voltage. The NPV of the better case is negative, but the optimistic case has a positive NPV. It is concluded that the price of electricity has the biggest influence on the NPV and this influence will increase in the future if the electrolyzers operate at higher current densities. Two other parameters with a large influence are the cost of materials and the selling price of the products. The $CO_2$ tax has the lowest influence on the feasibility of the process. The conclusion from the sensitivity analysis is that the feasibility of the process is determined mainly by market-based parameters and not by technological-based parameters, so the process is currently not economically feasible due to market limitations.

The main purpose of this process is to reduce the emission of $CO_2$ in the atmosphere. All the units in the process require a form of energy that causes an emission of $CO_2$. The second electorlyzer and the distillation column to separate acetic acid from ethanol, n-propanol, and water consume the most energy. To minimize the use of energy, heat exchangers are used wherever possible for utilizing the waste heat available in the process. From the $CO_2$ analysis, it is concluded that the process is only carbon negative when a sustainable energy source is used. When the energy generated comes from nuclear or wind, then the net $CO_2$ consumption is the highest. This, however, brings an extra challenge to generate all energy required for the system sustainably, since current supplies of electricity from these renewable sources fall short of delivering the high energy requirements for these processes in the Netherlands.

# 7

# Recommendations

Based on the results from the designed process and analysis in the previous chapters, some recommendations are provided to improve the process and try to make it economically feasible.

Firstly, finding a different technique to effectively remove $H_2S$ from the gas feed stream without using MDEA is recommended. A cheaper alternative needs to be used that can decrease the $H_2S$ concentration to the desired level. The techno-economical analysis will also be more realistic when another separation technique is used since all costs are included then and nothing is neglected anymore.

Additionally, a research needs to be performed to determine the effect of change in composition of the gas and liquid feed streams on the purification process and electrolyzers. In this research, the composition and flow rate of both feed streams are assumed to be constant, but this will not be the case in reality. For the composition of the liquid feed stream, water from the river Rhine is assumed near Niewegein, The Netherlands. Water concentrations in rivers change constantly and depend on multiple factors, such as the distance from the rivers mouth to the sea and the presence of industries upstream. The composition of the gas feed stream varies depending on the energy source.

Furthermore, researching the influence of the electrolyte recycle on performance of electrolyzers is crucial. Gaining a better understanding of how the recycle affects the performance can help design and improve the electrolyzer and increase the amount of electrolyte that is recycled, which reduces the cost for materials, purification of the liquid feed stream, and product separation. The cost for materials will be lower since less fresh electrolyte is needed and as a consequence less KOH or $KHCO_3$ is required. When less fresh electrolyte is needed, also the purification of the liquid feed stream can be smaller, which saves costs. At last, with a larger recycle, the product concentration in the CO to $CO_2$ electrolyzer will be higher which results in a smaller and cheaper to operate product separation part. It has to be noted that, next to the increase in product concentration, also the concentration of ions that are still present in the ultrapure water accumulate. The influence of this ion accumulation also needs to be researched.

Next to researching the influence of the recycling of the electrolyte, more research has to be done on finding an optimal catalyst used in the electrolyzer. The targets for an optimal catalyst are that it has a high faradaic efficiency to the desired products and it can operate at lower potentials. From an income point of view, acetic acid generates the highest income per mole electrons consumed. Doing research in increasing the faradaic efficiency to acetic acid will increase the income when the same amount of electricity is used.

In the cryogenic distillation column, ethylene is separated from uncondensable gasses. These uncondensable gases primarily consist of CO, which is currently not recycled back to the electrolyzers. However, in order to fully maximize the use of the available feedstock and minimize waste, the CO can be purified, if necessary, and recycled. This leads to an increased formation of high-value products,

which increases the income from the process.

The energy required to separate acetic acid and n-propanol is more than half of the enthalpy of combustion of these products. This is mainly due to the energy consumption of the first distillation column where acetic acid is removed from ethanol, n-propanol, and water. More efficient separation techniques are needed to reduce the energy consumption or the order in which the products are separated should be changed. Therefore, more research needs to be done on separating techniques for the separation of acetic acid, ethanol, n-propanol, and water mixtures.

Currently, oxygen is purged as a product. Oxygen has a lot of applications in the industry and healthcare industry. Researching the composition of the gaseous exit stream can help to know and later model this stream. With this knowledge, the required purification steps can be determined and oxygen can be sold as a product which increases the income of the process.

For the calculation of the free on board purchase price, operating cost, and energy consumption of the pressure swing adsorption (PSA) units, assumptions are made because of lack of information. Additional research needs to be performed on the cost and the energy consumption of pressure swing adsorption units. Furthermore, more research needs to be done to know what the influences of the impurities are on the PSA units.

This process is found to be only carbon negative when the energy used is generated from sustainable sources. The energy consumption of this process is extremely large and a lot of extra sustainable energy sources need to be built and placed. It needs to be investigated how the energy required for the system can be generated using only sustainable sources, so this process can operate continuously and constantly.

Since the electrochemical $CO_2$ reduction process is not yet commercialized or scaled-up to industrially relevant sizes, there is insufficient data available in the literature or real-life to validate the developed large-scale process model. Hence, it is desirable to set up pilot plants and scale-up projects to obtain the required data for the validation and for further optimization of the process model.

# Reference list


[1] R. A. J. Bogan, S. Ohde, T. Arakaki, I. Mori, and C. W. McLeod, *Changes in rainwater ph associated with increasing atmospheric carbon dioxide after the industrial revolution,* Water, Air, and Soil Pollution **196**, 263 (2008).

[2] S. Manabe and R. J. Stouffer, *Sensitivity of a global climate model to an increase of co2 concentration in the atmosphere,* Journal of geophysical research **85**, 5529 (1980).

[3] S. Manabe, R. Wetherald, and R. Stouffer, *Summer dryness due to an increase of atmospheric co2 concentration,* Climatic Change **3**, 347 (1981).

[4] W. Thomson, *Xxxv. polar ice-caps and their influence in changing sea levels,* Transactions of the Geological Society of Glasgow **8**, 322 (2022).

[5] *Paris agreement,* https://unfccc.int/sites/default/files/english_paris_agreement.pdf (2015), accessed: 2022-9-15.

[6] E. Alper and O. Yuksel Orhan, *CO2 utilization: Developments in conversion processes,* Petroleum **3**, 109 (2017).

[7] R. S. Norhasyima and T. M. Mahlia, *Advances in CO2 utilization technology: A patent landscape review,* Journal of CO2 Utilization **26**, 323 (2018).

[8] M. Pérez-Fortes, J. C. Schöneberger, A. Boulamanti, G. Harrison, and E. Tzimas, *Formic acid synthesis using CO2 as raw material: Techno-economic and environmental evaluation and market potential,* International Journal of Hydrogen Energy **41**, 16444 (2016).

[9] M. S. Maru, S. Ram, R. S. Shukla, and N. u. H. Khan, *Ruthenium-hydrotalcite (Ru-HT) as an effective heterogeneous catalyst for the selective hydrogenation of CO2 to formic acid,* Molecular Catalysis **446**, 23 (2018).

[10] N. Yan and K. Philippot, *Transformation of CO2 by using nanoscale metal catalysts: cases studies on the formation of formic acid and dimethylether,* Current Opinion in Chemical Engineering **20**, 86 (2018).

[11] B. Hu, C. Guild, and S. L. Suib, *Thermal, electrochemical, and photochemical conversion of CO2 to fuels and value-added products,* Journal of CO2 Utilization **1**, 18 (2013).

[12] T. M. Suzuki, T. Takayama, S. Sato, A. Iwase, A. Kudo, and T. Morikawa, *Enhancement of CO2 reduction activity under visible light irradiation over Zn-based metal sulfides by combination with Ru-complex catalysts,* Applied Catalysis B: Environmental **224**, 572 (2018).

[13] H. R. M. Jhong, S. Ma, and P. J. Kenis, *Electrochemical conversion of CO2 to useful chemicals: Current status, remaining challenges, and future opportunities,* Current Opinion in Chemical Engineering **2**, 191 (2013).

[14] D. R. Kauffman, J. Thakkar, R. Siva, C. Matranga, P. R. Ohodnicki, C. Zeng, and R. Jin, *Efficient Electrochemical CO2 Conversion Powered by Renewable Energy,* ACS Applied Materials & Interfaces **7**, 15626 (2015).

[15] W. Sun, X. Wang, J. Yang, J. Lu, H. Han, Y. Zhang, and J. Wang, *Pervaporation separation of acetic acid-water mixtures through Sn-substituted ZSM-5 zeolite membranes,* Journal of Membrane Science **335**, 83 (2009).

[16] K. Roh, J. H. Lee, and R. Gani, *A methodological framework for the development of feasible CO2 conversion processes,* International Journal of Greenhouse Gas Control **47**, 250 (2016).

[17] S. Perdan, C. R. Jones, and A. Azapagic, *Public awareness and acceptance of carbon capture and utilisation in the UK,* Sustainable Production and Consumption **10**, 74 (2017).

[18] A. Dominguez-Ramos, B. Singh, X. Zhang, E. G. Hertwich, and A. Irabien, *Global warming footprint of the electrochemical reduction of carbon dioxide to formate,* Journal of Cleaner Production **104**, 148 (2015).

[19] O. S. Bushuyev, P. De Luna, C. T. Dinh, L. Tao, G. Saur, J. van de Lagemaat, S. O. Kelley, and E. H. Sargent, *What Should We Make with CO2 and How Can We Make It?* Joule **2**, 825 (2018).

[20] *Evonik and siemens to generate high-value specialty chemicals from carbon dioxide and eco-electricity,* https://corporate.evonik.com/en/media/press-releases/corporate/evonik-and-siemens-to-generate-high-value-specialty-chemica\ls-from-carbon-dioxide-and-eco-electricit-106259.html (2018), accessed: 2023-01-10.

[21] Y. Hori, *'deactivation of copper electrode' in electrochemical reduction of CO2,* Electrochim. Acta **50**, 5354 (2005).

[22] T. E. Graedel, G. W. Kammlott, and J. P. Franey, *Carbonyl sulfide: Potential agent of atmospheric sulfur corrosion,* Science **212**, 663 (1981).

[23] S. Liang, N. Altaf, L. Huang, Y. Gao, and Q. Wang, *Electrolytic cell design for electrochemical CO2 reduction,* Journal of CO2 Utilization **35**, 90 (2020).

[24] Q. Chen, P. Tsiakaras, and P. Shen, *Electrochemical Reduction of Carbon Dioxide: Recent Advances on Au-Based Nanocatalysts,* Catalysts **12** (2022), 10.3390/catal12111348.

[25] A. Mohammadi and M. Mehrpooya, *A comprehensive review on coupling different types of electrolyzer to renewable energy sources,* Energy **158**, 632 (2018).

[26] D. Gao, P. Wei, H. Li, L. Lin, G. Wang, and X. Bao, *Designing Electrolyzers for Electrocatalytic CO2 Reduction,* ACTA PHYSICO-CHIMICA SINICA **37**, 2009021 (2021).

[27] E. Ruiz-López, J. Gandara-Loe, F. Baena-Moreno, T. R. Reina, and J. A. Odriozola, *Electrocatalytic CO2 conversion to C2 products: Catalysts design, market perspectives and techno-economic aspects,* Renewable and Sustainable Energy Reviews **161** (2022), 10.1016/j.rser.2022.112329.

[28] S. Shironita, K. Karasuda, M. Sato, and M. Umeda, *Feasibility investigation of methanol generation by CO2 reduction using Pt/C-based membrane electrode assembly for a reversible fuel cell,* Journal of Power Sources **228**, 68 (2013).

[29] S. Pérez-Rodríguez, F. Barreras, E. Pastor, and M. J. Lázaro, *Electrochemical reactors for CO2 reduction: From acid media to gas phase,* International Journal of Hydrogen Energy **41**, 19756 (2016).

[30] Y. C. Li, D. Zhou, Z. Yan, R. H. Gonçalves, D. A. Salvatore, C. P. Berlinguette, and T. E. Mallouk, *Electrolysis of CO2 to Syngas in Bipolar Membrane-Based Electrochemical Cells,* ACS Energy Letters **1**, 1149 (2016).

[31] Y. Wu, S. Garg, M. Li, M. N. Idros, Z. Li, R. Lin, J. Chen, G. Wang, and T. E. Rufford, *Effects of microporous layer on electrolyte flooding in gas diffusion electrodes and selectivity of CO2 electrolysis to CO,* Journal of Power Sources **522**, 230998 (2022).

[32] N. S. Spinner, J. A. Vega, and W. E. Mustain, *Recent progress in the electrochemical conversion and utilization of CO2,* Catal. Sci. Technol. **2**, 19 (2012).

[33] S. R. Narayanan, B. Haines, J. Soler, and T. I. Valdez, *Electrochemical Conversion of Carbon Dioxide to Formate in Alkaline Polymer Electrolyte Membrane Cells,* Journal of The Electrochemical Society **158**, A167 (2011).

[34] C. Chen, J. F. Khosrowabadi Kotyk, and S. W. Sheehan, *Progress toward Commercial Application of Electrochemical Carbon Dioxide Reduction,* Chem **4**, 2571 (2018).

[35] K. Wu, E. Birgersson, B. Kim, P. J. A. Kenis, and I. A. Karimi, *Modeling and Experimental Validation of Electrochemical Reduction of CO 2 to CO in a Microfluidic Cell* , Journal of The Electrochemical Society **162**, F23 (2015).

[36] A. J. Bard and L. R. Faulkner, *Electrochemical Methods: Fundamentals and Applications, 2nd Edition*, Vol. 2 (John wiley & sons, 2000) p. 864.

[37] P. H. Bigg, *The International System of Units (SI Units),* British Journal of Applied Physics **15**, 1243 (1964).

[38] E. M. Gutman, *Can the Tafel equation be derived from first principles?* Corrosion Science **47**, 3086 (2005).

[39] *Universal gas constant value,* https://physics.nist.gov/cgi-bin/cuu/Value?r (2019), accessed: 2022-09-27.

[40] T. Shinagawa, A. T. Garcia-Esparza, and K. Takanabe, *Insight on Tafel slopes from a microkinetic analysis of aqueous electrocatalysis for energy conversion,* Scientific Reports **5**, 1 (2015).

[41] A. M. Appel and M. L. Helm, *Determining the Overpotential for a Molecular Electrocatalyst,* ACS Catalysis **4**, 630 (2014).

[42] R. Lin, J. Guo, X. Li, P. Patel, and A. Seifitokaldani, *Electrochemical reactors for CO2 conversion*, Vol. 10 (Catalysts, 2020) pp. 27–30.

[43] N. Perez, *Electrochemistry and Corrosion Science: Second Edition* (Springer, 2016) pp. 1–455.

[44] M. Jouny, W. Luc, and F. Jiao, *General Techno-Economic Analysis of CO2 Electrolysis Systems,* Industrial and Engineering Chemistry Research **57**, 2165 (2018).

[45] J. A. Rogers, A. A. Maznev, M. J. Banet, and K. A. Nelson, *Optical generation and characterization of acoustic waves in thin films: Fundamentals and applications*, Vol. 30 (Annual Review of Materials Science, 2000) pp. 117–157.

[46] S. Nitopi, E. Bertheussen, S. B. Scott, X. Liu, A. K. Engstfeld, S. Horch, B. Seger, I. E. Stephens, K. Chan, C. Hahn, J. K. Nørskov, T. F. Jaramillo, and I. Chorkendorff, *Progress and Perspectives of Electrochemical CO2 Reduction on Copper in Aqueous Electrolyte,* Chemical Reviews **119**, 7610 (2019).

[47] V. Sumit, K. Byoungsu, H.-R. M. Jhong, M. Sichao, and P. J. A. Kenis, *A gross-margin model for defining technoeconomic benchmarks in the electroreduction of co2,* ChemSusChem **9**, 1972 (2016).

[48] Z. Sun, T. Ma, H. Tao, Q. Fan, and B. Han, *Fundamentals and Challenges of Electrochemical CO2 Reduction Using Two-Dimensional Materials,* Chem **3**, 560 (2017).

[49] S. Park, D. T. Wijaya, J. Na, and C. W. Lee, *Towards the large-scale electrochemical reduction of carbon dioxide,* Catalysts **11**, 1 (2021).

[50] P. W. Atkin, *Physical Chemistry*, 1 (Oxford University Press, 1998).

[51] X. Han, H. Sheng, C. Yu, T. W. Walker, G. W. Huber, J. Qiu, and S. Jin, *Electrocatalytic Oxidation of Glycerol to Formic Acid by CuCo2O4Spinel Oxide Nanostructure Catalysts,* ACS Catalysis **10**, 6741 (2020).

[52] D. Higgins, C. Hahn, C. Xiang, T. F. Jaramillo, and A. Z. Weber, *Gas-Diffusion Electrodes for Carbon Dioxide Reduction: A New Paradigm,* ACS Energy Letters **4**, 317 (2019).

[53] E. A. Hernández-Pagán, N. M. Vargas-Barbosa, T. Wang, Y. Zhao, E. S. Smotkin, and T. E. Mallouk, *Resistance and polarization losses in aqueous buffer-membrane electrolytes for water-splitting photoelectrochemical cells,* Energy and Environmental Science **5**, 7582 (2012).

[54] M. Jouny, W. Luc, and F. Jiao, *General Techno-Economic Analysis of CO2 Electrolysis Systems,* Industrial and Engineering Chemistry Research **57**, 2165 (2018).

[55] J. M. Spurgeon and B. Kumar, *A comparative technoeconomic analysis of pathways for commercial electrochemical CO2 reduction to liquid products,* Energy and Environmental Science **11**, 1536 (2018).

[56] M. Rumayor, A. Dominguez-Ramos, P. Perez, and A. Irabien, *A techno-economic evaluation approach to the electrochemical reduction of CO2 for formic acid manufacture,* Journal of CO2 Utilization **34**, 490 (2019).

[57] Y. Hori, H. Wakebe, T. Tsukamoto, and O. Koga, *Electrocatalytic process of CO selectivity in electrochemical reduction of CO2 at metal electrodes in aqueous media,* Electrochimica Acta **39**, 1833 (1994).

[58] A. Bagger, W. Ju, A. S. Varela, P. Strasser, and J. Rossmeisl, *Electrochemical CO2 Reduction: A Classification Problem,* Electrochimica Acta **18**, 3266 (2017).

[59] C. W. Li, J. Ciston, and M. W. Kanan, *Electroreduction of carbon monoxide to liquid fuel on oxide-derived nanocrystalline copper,* Nature **508**, 504 (2014).

[60] C. H. Bartholomew, *Mechanisms of catalyst deactivation,* Applied Catalysis A: General **212**, 17 (2001).

[61] Y. Hori, H. Konishi, T. Futamura, A. Murata, O. Koga, H. Sakurai, and K. Oguma, *"deactivation of copper electrode" in electrochemical reduction of CO2,* Electrochimica Acta **50**, 5354 (2005).

[62] K. J. P. Schouten, Y. Kwon, C. J. M. van der Ham, Z. Qin, and M. T. M. Koper, *A new mechanism for the selectivity to C1 and C2 species in the electrochemical reduction of carbon dioxide on copper electrodes,* Chem. Sci. **2**, 1902 (2011).

[63] A. Wuttig and Y. Surendranath, *Impurity Ion Complexation Enhances Carbon Dioxide Reduction Catalysis,* ACS Catalysis **5**, 4479 (2015).

[64] M. Dunwell, Q. Lu, J. M. Heyes, J. Rosen, J. G. Chen, Y. Yan, F. Jiao, and B. Xu, *The Central Role of Bicarbonate in the Electrochemical Reduction of Carbon Dioxide on Gold,* Journal of the American Chemical Society **139**, 3774 (2017).

[65] T. E. Graedel, J. P. Franey, and G. W. Kammlott, *The corrosion of copper by atmospheric sulphurous gases,* Corrosion Science **23**, 1141 (1983).

[66] J. P. Franey, G. W. Kammlott, and T. E. Graedel, *The corrosion of silver by atmospheric sulfurous gases,* Corrosion Science **25**, 133 (1985).

[67] A. Poullikkas, *Review of Design, Operating, and Financial Considerations in Flue Gas Desulfurization Systems,* Energy Technology & Policy **2**, 92 (2015).

[68] V. v. R. RIWA, *Jaarraport 2021 De Rijn*, Tech. Rep. (RIWA, 2021).

[69] C. S. Chen, A. D. Handoko, J. H. Wan, L. Ma, D. Ren, and B. S. Yeo, *Stable and selective electrochemical reduction of carbon dioxide to ethylene on copper mesocrystals,* Catal. Sci. Technol. **5**, 161 (2015).

[70] N. Hoshi, M. Kato, and Y. Hori, *Electrochemical reduction of CO2 on single crystal electrodes of silver Ag(111), Ag(100) and Ag(110),* Journal of Electroanalytical Chemistry **440**, 283 (1997).

[71] W. Zhu, R. Michalsky, Ö. Metin, H. Lv, S. Guo, C. J. Wright, X. Sun, A. A. Peterson, and S. Sun, *Monodisperse Au nanoparticles for selective electrocatalytic reduction of CO2 to CO.* Journal of the American Chemical Society **135**, 16833 (2013).

[72] S. Zhang, P. Kang, S. Ubnoske, M. K. Brennaman, N. Song, R. L. House, J. T. Glass, and T. J. Meyer, *Polyethylenimine-enhanced electrocatalytic reduction of CO□ to formate at nitrogen-doped carbon nanomaterials.* Journal of the American Chemical Society **136**, 7845 (2014).

[73] J. L. DiMeglio and J. Rosenthal, *Selective Conversion of CO2 to CO with High Efficiency Using an Inexpensive Bismuth-Based Electrocatalyst,* Journal of the American Chemical Society **135**, 8798 (2013).

[74] L. Duan, R. Fu, B. Zhang, W. Shi, S. Chen, and Y. Wan, *An Efficient Reusable Mesoporous Solid-Based Pd Catalyst for Selective C2 Arylation of Indoles in Water,* ACS Catalysis **6**, 1062 (2016).

[75] D. H. Won, H. Shin, J. Koh, J. Chung, H. S. Lee, H. Kim, and S. I. Woo, *Highly Efficient, Selective, and Stable CO2 Electroreduction on a Hexagonal Zn Catalyst.* Angewandte Chemie (International ed. in English) **55**, 9297 (2016).

[76] A. S. Varela, N. Ranjbar Sahraie, J. Steinberg, W. Ju, H.-S. Oh, and P. Strasser, *Metal-Doped Nitrogenated Carbon as an Efficient Catalyst for Direct CO2 Electroreduction to CO and Hydrocarbons.* Angewandte Chemie (International ed. in English) **54**, 10758 (2015).

[77] Airgas, *Material Safety Data Sheet Hydrogen Sulfide,* Exposure , 8 (2010).

[78] M. Jitaru, D. A. Lowy, M. Toma, B. C. Toma, and L. Oniciu, *Electrochemical reduction of carbon dioxide on flat metallic cathodes,* Journal of Applied Electrochemistry **27**, 875 (1997).

[79] C. M. Sánchez-Sánchez, V. Montiel, D. A. Tryk, A. Aldaz, and A. Fujishima, *Electrochemical approaches to alleviation of the problem of carbon dioxide accumulation,* Pure and Applied Chemistry **73**, 1917 (2001).

[80] K. P. Kuhl, E. R. Cave, D. N. Abram, and T. F. Jaramillo, *New insights into the electrochemical reduction of carbon dioxide on metallic copper surfaces,* Energy Environ. Sci. **5**, 7050 (2012).

[81] N. Weinhart, *Evaluation of a Novel Concept for Combined $NO_x$ and $SO_x$ Removal,* (2015).

[82] R. K. Srivastava and W. Jozewicz, *Flue Gas Desulfurization: The State of the Art,* Journal of the Air & Waste Management Association **51**, 1676 (2001).

[83] A. Poullikkas, *Review of Design, Operating, and Financial Considerations in Flue Gas Desulfurization Systems,* Energy Technology & Policy **2**, 92 (2015).

[84] H. Akiho, S. Ito, and H. Matsuda, *Effect of oxidizing agents on selenate formation in a wet FGD,* Fuel **89**, 2490 (2010).

[85] Y. Zhang, Z. Xiao, and J. Ma, *Hydrolysis of carbonyl sulfide over rare earth oxysulfides,* Applied Catalysis B: Environmental **48**, 57 (2004).

[86] D. Mamrosh, K. McIntush, and K. Fisher, *Caustic scrubber designs for H2S removal from refinery gas streams,* American Fuel and Petrochemical Manufacturers, AFPM - AFPM Annual Meeting 2014 , 671 (2014).

[87] J. Bobek, D. Rippel-Pethő, É. Molnár, and R. Bocsi, *Selective Hydrogen Sulphide Removal from Acid Gas by Alkali Chemisorption in a Jet Reactor,* Hungarian Journal of Industry and Chemistry **44**, 51 (2016).

[88] H. T. Madsen, *Water treatment for green hydrogen: what you need to know,* https://hydrogentechworld.com/water-treatment-for-green-hydrogen-what-you-need-to-know (2022), accessed: 2022-11-24.

[89] H. Lee, Y. Jin, and S. Hong, *Recent transitions in ultrapure water (UPW) technology: Rising role of reverse osmosis (RO),* Desalination **399**, 185 (2016).

[90] R. Singh, *Chapter 13 - Development of Hybrid Processes for High Purity Water Production,* in *Emerging Membrane Technology for Sustainable Water Treatment*, edited by N. P. Hankins and R. Singh (Elsevier, Boston, 2016) pp. 327–357.

[91] H. Basri, A. F. Ismail, M. Aziz, K. Nagai, T. Matsuura, M. S. Abdullah, and B. C. Ng, *Silver-filled polyethersulfone membranes for antibacterial applications - effect of PVP and TAP addition on silver dispersion,* Desalination **261**, 264 (2010).

[92] A. Moslehyani, M. Mobaraki, A. F. Ismail, T. Matsuura, S. A. Hashemifard, M. H. Othman, A. Mayahi, M. Rezaei Dashtarzhandi, M. Soheilmoghaddam, and E. Shamsaei, *Effect of HNTs modification in nanocomposite membrane enhancement for bacterial removal by cross-flow ultrafiltration system,* Reactive and Functional Polymers **95**, 80 (2015).

[93] A. W. Zularisam, A. F. Ismail, and R. Salim, *Behaviours of natural organic matter in membrane filtration for surface water treatment — a review,* Desalination **194**, 211 (2006).

[94] A. W. Zularisam, A. F. Ismail, M. R. Salim, M. Sakinah, and O. Hiroaki, *Fabrication, fouling and foulant analyses of asymmetric polysulfone (PSF) ultrafiltration membrane fouled with natural organic matter (NOM) source waters,* Journal of Membrane Science **299**, 97 (2007).

[95] M. C. Collivignarelli, A. Abbà, M. C. Miino, F. M. Caccamo, V. Torretta, E. C. Rada, and S. Sorlini, *Disinfection of Wastewater by UV-Based Treatment for Reuse in a Circular Economy Perspective. Where Are We at?* International Journal of Environmental Research and Public Health **18** (2021), 10.3390/ijerph18010077.

[96] W. C. Award, D. Byrne, and M. Adams, *NIOSH Science Blog r2p Corner State-based Occupational Health updates,* Niosh eNews **5** (2008).

[97] A. B. K. dos Santos, E. M. T. Claro, R. N. Montagnolli, J. M. Cruz, P. R. M. Lopes, and E. D. Bidoia, *Electrochemically assisted photocatalysis: Highly efficient treatment using thermal titanium oxides doped and non-doped electrodes for water disinfection,* Journal of Environmental Management **204**, 255 (2017).

[98] W. Qi, W. Li, J. Zhang, X. Wu, J. Zhang, and W. Zhang, *Effect of biological activated carbon filter depth and backwashing process on transformation of biofilm community,* Frontiers of Environmental Science and Engineering **13**, 1 (2019).

[99] N. R. C. U. S. D. W. Committee, *Drinking Water and Health*, Vol. 2 (National Academies Press (US), 1980").

[100] I. Ion, *Ion Exchange Treatment of Drinking Water,* Cycle (2009).

[101] U. Baruah, A. Konwar, and D. Chowdhury, *A sulphonated carbon dot-chitosan hybrid hydrogel nanocomposite as an efficient ion-exchange film for Ca2+ and Mg2+ removal,* Nanoscale **8**, 8542 (2016).

[102] Z. Yang, Y. Zhou, Z. Feng, X. Rui, T. Zhang, and Z. Zhang, *A Review on Reverse Osmosis and Nanofiltration Membranes for Water Purification.* Polymers **11** (2019), 10.3390/polym11081252.

[103] A. Physicochemical and T. Technologies, *Advanced Physicochemical Treatment Technologies* (2007).

[104] Lenntech, *Oxygen (o) and water,* (2023).

[105] H. Togawa, T. Okubo, Y. Nonaka, T. Yamaguchi, and S. Obika, *Retention behavior of short double-stranded oligonucleotide and its potential impurities by anion-exchange chromatography under non-denaturing conditions,* Journal of Chromatography A **1691**, 463808 (2023).

[106] M. Enmark, J. Samuelsson, and T. Fornstedt, *Development of a unified gradient theory for ion-pair chromatography using oligonucleotide separations as a model case,* **1691** (2023), 10.1016/j.chroma.2023.463823.

[107] B. S. Rathi, P. S. Kumar, and R. Parthiban, *A review on recent advances in electrodeionization for various environmental applications,* Chemosphere **289**, 133223 (2022).

[108] B. S. Rathi and P. S. Kumar, *Electrodeionization theory, mechanism and environmental applications. A review,* Environmental Chemistry Letters **18**, 1209 (2020).

[109] L. Handojo, A. K. Wardani, D. Regina, C. Bella, M. T. Kresnowati, and I. G. Wenten, *Electromembrane processes for organic acid recovery,* RSC Advances **9**, 7854 (2019).

[110] R. Yang, *Chemical Engineering Science*, Vol. 43 (1988) p. 985.

[111] Z. Guo, S. Deng, S. Li, Y. Lian, L. Zhao, and X. Yuan, *Entropy Analysis of Temperature Swing Adsorption for CO(2) Capture Using the Computational Fluid Dynamics (CFD) Method.* Entropy (Basel, Switzerland) **21** (2019), 10.3390/e21030285.

[112] X. Zhang, T. Zhou, and K. Sundmacher, *Integrated metal-organic framework (MOF) and pressure/vacuum swing adsorption process design: MOF matching,* AIChE Journal **68**, 1 (2022).

[113] D. M. Ruthven, *Principles of Adsorption and Adsorption Processes*, Wiley-Interscience publication (Wiley, 1984).

[114] C. Font-Palma, D. Cann, and C. Udemu, *Review of Cryogenic Carbon Capture Innovations and Their Potential Applications,* Journal of Carbon Research **7** (2021), 10.3390/c7030058.

[115] Arjoso, *Air Separation Unit with Pure Argon Recovery (Simplified),* Occupational Medicine **53**, 130 (2006).

[116] V. Gerbaud and Rodriguez-Donis, *Review of Extractive Distllation.* (2019).

[117] W. D. Seider, D. R. Lewin, J. D. Seader, S. Widagdo, R. Gani, and K. M. Ng, *Product and Process Design Principles: synthesis, analysis and evaluation*, 4th ed. (John Wiley & Sons Inc., 2017).

[118] R. Hillebrand, *Life Cycle Management and Service,* , 8 (2007).

[119] Danilo Gomes de Arruda, *FAQs on 1G Bio-Ethanol*, Tech. Rep. March (2021).

[120] *Beverage & industrial use: Ethanol,* https://www.epure.org/about-ethanol/beverage-industrial-use/ (2022), accessed: 2023-03-04.

[121] *Nedstar: industrial ethanol,* https://www.nedstar.com/industries/industrial-ethanol (2023), accessed: 2023-03-04.

[122] ClassNK, *Lemnis public lighting*, Tech. Rep. 0715 (1998).

[123] *Vedanta,* https://www.vedantu.com/chemistry/uses-of-propanol (2023), accessed: 2023-03-03.

[124] *Indiamart: N-propanol, 95% purity, 200 liters drum for paint industry,* https://www.indiamart.com/proddetail/n-propanol-22958662288.html (2023), accessed: 2022-03-03.

[125] *Penta italia export srl: Acetic acid 80%,* https://www.pentaitalia.com/trading (2022), accessed: 2022-12-15.

[126] *Yigitoglu kimya: Acetic acid 80%,* https://www.yigitoglu.com.tr/product-category/204/asitler (2022), accessed: 2022-12-15.

[127] *Vivochem: Acetic acid 80%,* https://www.vivochem.nl/nl/p/azijnzuur (2022), accessed: 2022-12-15.

[128] *Dow: ethylene,* https://www.dow.com/en-us/pdp.ethylene.31681z.html#overview (2023), accessed: 2023-07-04.

[129] Y. Yang, G. Wang, L. Zhang, S. Zhang, and L. Lin, *Comparison of hydrogen specification in national standards for china,* E3S Web of Conferences **118**, 03042 (2019).

[130] *Linde: methane 99.5% k,* https://www.lindedirect.com/store/product-detail/methane_ch4_methane_99_5_k (2023), accessed: 2023-07-04.

[131] *Praxair: methane,* https://www.lindeus.com/-/media/corporate/praxairus/documents/specification-sheets-and-brochures/gases/methane-ch4-spec-sheet-ss-p4618.pdf?la=en (2023), accessed: 2023-07-04.

[132] *Air products: Industrial and medical gas specifications (u.s.),* https://www.airproducts.com/gases/gas-facts/industrial-and-medical-gas-specifications (2023), accessed: 2023-07-04.

[133] J. Cromphout, J. Coemelck, W. Closset, and L. Verdickt, *Design and operation of an ultrafiltration plant for the production of drinking water out of the river Scheldt SCIENCE Design and Operation of an Ultrafiltra-tion Plant for the Production of Drinking Water out of the River Scheldt Ultrafi ltration, drinking water treatment, membrane fouling,* (2011).

[134] A. Moslehyani, A. F. Ismail, T. Matsuura, M. A. Rahman, and P. S. Goh, *Chapter 3 - Recent Progresses of Ultrafiltration (UF) Membranes and Processes in Water Treatment,* in *Membrane Separation Principles and Applications*, Handbooks in Separation Science, edited by A. F. Ismail, M. A. Rahman, M. H. D. Othman, and T. Matsuura (Elsevier, 2019) pp. 85–110.

[135] B. Wise, W. Shih, and Smith Stanton, *Ceramic Ultrafiltration Membranes with Improved Economics, Operability, and Process Design Flexibility,* Nanostone Water, Inc. (2019).

[136] X. Li, L. Jiang, and H. Li, *Application of Ultrafiltration Technology in Water Treatment,* IOP Conference Series: Earth and Environmental Science **186** (2018), 10.1088/1755-1315/186/3/012009.

[137] C. COTTON, D. OWEN, G. CLINE, and T. BRODEUR, *Uv disinfection costs for inactivating cryptosporidium,* Journal - American Water Works Association **93**, 82 (2001).

[138] M. Jern, *What does activated carbon filters remove from tap water?* https://tappwater.co/en/what-activated-carbon-filters-remove/ (2022).

[139] M. Karnib, A. Kabbani, H. Holail, and Z. Olama, *Heavy metals removal using activated carbon, silica and silica activated carbon composite,* Energy Procedia **50**, 113 (2014).

[140] *Promac water technologies: Activated carbon,* https://www.promacwt.com/activated-carbon.html (2023), accessed: 2023-02-22.

[141] L. Zhou, Q. Yu, Y. Cui, F. Xie, W. Li, Y. Li, and M. Chen, *Adsorption properties of activated carbon from reed with a high adsorption capacity,* Ecological Engineering **102**, 443 (2017).

[142] *Jacobi service: Design and selection of activated carbon air and gas treatment systems,* https://services.jacobi.net/design-selection-of-air-gas-treatment-with-industrial-filters/ (2023), accessed: 2023-09-02.

[143] W. R. Ebenezer, *Dangers of using activated carbon past its lifespan,* https://chemistry.stackexchange.com/questions/117597/dangers-of-using-activated-carbon-past-its-lifespan (2019).

[144] J. Woodard, *Activated Carbon Filters 101,* https://www.freshwatersystems.com/blogs/blog/activated-carbon-filters-101 (2019).

[145] Y. N. Wang and R. Wang, *Membrane Separation Principles and Applications: From Material Selection to Mechanisms and Industrial Uses* (Elsevier Inc., 2018) pp. 1–45.

[146] I. Nancrede Engineering Company, *Industrial Water & High Purity Lab Water Systems, Service and Equipment,* https://industrialwatersoftener.com/water-treatment-equipment/industrial-water-softeners/analysis-ion-exchange-vs-lime-softening/ (2022).

[147] *How does ion exchange resin work, and how long does it last?* https://mlball.com/2019/11/how-does-ion-exchange-resin-work-and-how-long-does-it-last/ (2019), accessed: 2023-02-02.

[148] *Ion exchange plant design,* http://dardel.info/IX/processes/design_principles.html (2022), accessed: 2023-16-02.

[149] Y. N. Wang and R. Wang, *Membrane Separation Principles and Applications: From Material Selection to Mechanisms and Industrial Uses* (Elsevier Inc., 2018) pp. 1–45.

[150] U. W. Systems, *When do i change my ro membrane?* https://www.uswatersystems.com/blog/when-do-i-change-my-ro-membrane (2023), accessed: 2023-02-23.

[151] A. S. Tyusenkov and S. E. Cherepashkin, *Scale inhibitor for boiler water systems,* Russian Journal of Applied Chemistry **87**, 1240 (2014).

[152] D. W. Solutions, *DuPont ™ Ligasep ™ Degasification Modules Technical Manual,* (2020).

[153] D. W. Solutions, *Product Data Sheet: DuPont ™ Ligasep ™ Degasification Modules,* (2020).

[154] I. G. Wenten, Khoiruddin, F. Arfianto, and Zudiharto, *Bench scale electrodeionization for high pressure boiler feed water,* Desalination **314**, 109 (2013).

[155] B. Tilly, A. Griffiths, and A. Golland, *Flue gas desulphurisation at Longannet Power Station, Scotland: a regulators view of the BPEO assessment,* (Institute of Energy, London (United Kingdom), United Kingdom, 1995).

[156] R. Fiedorow, R. Léauté, and I. Lana, *A study of the kinetics and mechanism of COS hydrolysis over alumina,* Journal of Catalysis **85**, 339 (1984).

[157] J. Bachelier, A. Aboulayt, J. C. Lavalley, O. Legendre, and F. Luck, *Activity of different metal oxides towards COS hydrolysis. Effect of SO2 and sulfation,* Catalysis Today **17**, 55 (1993).

[158] C. Y. Yang, H. G. Chang, J. L. He, C. R. Wen, H. Yi, C. Y. Tu, and S. S. Qu, *Selective Absorption of H2S from Gas Mixtures Contains CO2 into New Sterically Hindered Amine DTBP for Natural Gas Purification,* , 456 (2018).

[159] T.-L. Chen, Y.-X. Xiong, Y.-H. Chen, P.-C. Chiang, and Y.-H. Chen, *Performance evaluation and process simulation for synergetic removal of NOx, CO2 and PM using green alkaline solution in a high-gravity rotating packed bed,* Fuel **280**, 118643 (2020).

[160] L.-q. Zhu, J.-l. Tu, and Y.-j. Shi, *Separation of CO, CO2, N2 gas mixture for high-purity CO by pressure swing adsorption,* Gas Separation & Purification **5**, 173 (1991).

[161] C. G. Morales-Guio, E. R. Cave, S. A. Nitopi, J. T. Feaster, L. Wang, K. P. Kuhl, A. Jackson, N. C. Johnson, D. N. Abram, T. Hatsukade, C. Hahn, and T. F. Jaramillo, *Improved CO2 reduction activity towards C2+ alcohols on a tandem gold on copper electrocatalyst,* Nature Catalysis **1**, 764 (2018).

[162] T. Akter, H. Pan, and C. J. Barile, *Tandem Electrocatalytic CO2 Reduction inside a Membrane with Enhanced Selectivity for Ethylene,* The Journal of Physical Chemistry C **126**, 10045 (2022).

[163] R. Wang, H. Haspel, A. Pustovarenko, A. Dikhtiarenko, A. Russkikh, G. Shterk, D. Osadchii, S. Ould-Chikh, M. Ma, W. A. Smith, K. Takanabe, F. Kapteijn, and J. Gascon, *Maximizing Ag Utilization in High-Rate CO2 Electrochemical Reduction with a Coordination Polymer-Mediated Gas Diffusion Electrode,* ACS Energy Letters **4**, 2024 (2019).

[164] N. S. Romero Cuellar, C. Scherer, B. Kaçkar, W. Eisenreich, C. Huber, K. Wiesner-Fleischer, M. Fleischer, and O. Hinrichsen, *Two-step electrochemical reduction of CO2 towards multi-carbon products at high current densities,* Journal of CO2 Utilization **36**, 263 (2020).

[165] J. B. Greenblatt, D. J. Miller, J. W. Ager, F. A. Houle, and I. D. Sharp, *The Technical and Energetic Challenges of Separating (Photo)Electrochemical Carbon Dioxide Reduction Products,* Joule **2**, 381 (2018).

[166] W. Jud, C. O. Kappe, and D. Cantillo, *Development and Assembly of a Flow Cell for Single□Pass Continuous Electroorganic Synthesis Using Laser□Cut Components,* Chemistry–Methods **1**, 36 (2021).

[167] H. Du, J. Li, J. Zhang, G. Su, X. Li, and Y. Zhao, *Separation of Hydrogen and Nitrogen Gases with Porous Graphene Membrane,* The Journal of Physical Chemistry C **115**, 23261 (2011).

[168] H. Du, L. Xie, J. Liu, and S. Xu, *Concentration of mixed acid by electrodialysis for the intensification of absorption process in acrylic acid production,* Chinese Journal of Chemical Engineering **36**, 10 (2021).

[169] I. D. Gil, A. M. Uyazán, J. L. Aguilar, G. Rodríguez, and L. A. Caicedo, *Separation of ethanol and water by extractive distillation with salt and solvent as entrainer: Process Simulation,* Brazilian Journal of Chemical Engineering **25**, 207 (2008).

[170] D. Teleman, P. Kreis, and S. Lauterbach, *Optimal operational conditions for the pervaporation of a binary combination of water/ 1-propanol and water/1-propanol/propionic acid ternary combination,* Periodico **91**, 30 (2022).

[171] *Price of an psa unit,* https://cdtcwy.en.alibaba.com/product/60722023694-807844848/Cost_efficient_hydrogen_generation_unit_PSA_hydrogen_purification_system_hydrogen_generator_for_sale.html (2023), accessed: 2023-07-03.

[172] *Ce index cost indices,* https://toweringskills.com/financial-analysis/cost-indices/ (2022), accessed: 2023-03-04.

[173] *Cbs: aardgas en elektriciteit, gemiddelde prijzen van eindverbruikers,* https://opendata.cbs.nl/statline/#/CBS/nl/dataset/81309NED/table?fromstatweb (2023), accessed: 2023-22-02.

[174] S. Y. Pan, S. W. Snyder, H. W. Ma, Y. J. Lin, and P. C. Chiang, *Energy-efficient resin wafer electrodeionization for impaired water reclamation,* Journal of Cleaner Production **174**, 1464 (2018).

[175] *Dutch emission authority: Tarieven co2-heffing,* https://www.emissieautoriteit.nl/onderwerpen/tarieven-co2-heffing (2023), accessed: 2023-03-04.

[176] *indeflatie.nl: Inflatie afgelopen 10 jaar in nederland (in grafiek en tabel),* https://indeflatie.nl/inflatie-afgelopen-10-jaar/ (2023), accessed: 2023-11-04.

[177] *Average cost of equity per industry,* https://pages.stern.nyu.edu/~adamodar/New_Home_Page/datafile/wacc.htm (2023), accessed: 2023-11-04.

[178] J. Na, B. Seo, J. Kim, C. W. Lee, H. Lee, Y. J. Hwang, B. K. Min, D. K. Lee, H. S. Oh, and U. Lee, *General technoeconomic analysis for electrochemical coproduction coupling carbon dioxide reduction with organic oxidation,* Nature Communications **10** (2019), 10.1038/s41467-019-12744-y.

[179] L. Zhang, Z. Shi, Y. Lin, F. Chong, and Y. Qi, *Design Strategies for Large Current Density Hydrogen Evolution Reaction,* Frontiers in Chemistry **10** (2022), 10.3389/fchem.2022.866415.

[180] *Cbs: Elektriciteit en warmte; productie en inzet naar energiedrager,* https://opendata.cbs.nl/statline/#/CBS/nl/dataset/80030NED/table (2022), accessed: 2023-06-04.

[181] *Cbs: Hernieuwbare elektriciteit; productie en vermogen,* https://opendata.cbs.nl/#/CBS/nl/dataset/82610NED/table (2023), accessed: 2023-06-04.

[182] *Rijksoverheid regionale klimaatmonitor: Gerealiseerd en gepland vermogen wind op land,* https://klimaatmonitor.databank.nl/dashboard/klimaatbeleid/gerealiseerd-en-gepland-vermogen-wind-op-land (2023), accessed: 2023-06-04.

[183] *Tennet: 29 terawattuur windopbrengst in de nederlandse en duitse noordzee in 2022,* https://www.tennet.eu/nl/nieuws/29-terawattuur-windopbrengst-de-nederlandse-en-duitse-noordzee-2022 (2023), accessed: 2023-06-04.

[184] *Price of an uv treatment unit,* https://www.indiamart.com/proddetail/industrial-uv-water-treatment-22295143948.html (2023), accessed: 2023-24-02.

[185] *Price of a softener unit,* https://samcotech.com/how-much-does-it-cost-to-buy-maintain-and-o (2023), accessed: 2023-24-02.

[186] *Price of a degasser unit,* https://beyond-machinery.en.made-in-china.com/product/XZCTiydjGLhA/China-New-arrival-vacuum-pump-and-condensing-part-vacuum-dega.html (2023), accessed: 2023-24-02.

[187] *Price of an electrodeionization unit,* https://dir.indiamart.com/impcat/electro-deionizer.html (2023), accessed: 2023-24-02.

[188] *Price of an electrodialyser unit,* https://crownmachine.en.made-in-china.com/product/zxsYVNyrbAkD/China-Hot-Sale-Electrodialysis-Pure-Mineral-Small-Water-Treat.htmll (2023), accessed: 2023-07-03.

[189] S. Actions, *Utilize Ultraviolet Lamps for Disinfection,* U.S. Department of Energy **53** (2021).

[190] *Price of active carbon per ton,* https://www.indexbox.io/blog/activated-carbon-price-per-ton-june-2022/ (2022), accessed: 2023-23-02.

[191] L. Riboldi and O. Bolland, *Overview on Pressure Swing Adsorption (PSA) as CO2 Capture Technology: State-of-the-Art, Limits and Potentials,* Energy Procedia **114**, 2390 (2017).

[192] A. El-Gendi, H. Abdallah, and A. Amin, *Economic study for blend membrane production,* Bulletin of the National Research Centre **45**, 126 (2021).

[193] M. Nordio, S. A. Wassie, M. Van Sint Annaland, D. A. Pacheco Tanaka, J. L. Viviente Sole, and F. Gallucci, *Techno-economic evaluation on a hybrid technology for low hydrogen concentration separation and purification from natural gas grid,* International Journal of Hydrogen Energy **46**, 23417 (2021).

[194] *Globe newswire: Eu potassium hydroxide market report: Suppliers, buyers, prices and forecast - indexbox,* https://www.globenewswire.com/en/news-release/2022/06/09/2459386/0/en/EU-Potassium-Hydroxide-Market-Report-Suppliers-Buyers-Prices-and-Forecast-IndexBox.html (2023), accessed: 2023-31-03.

[195] *Alibaba: Hot sale 99% price potassium bicarbonate khco3 cas 298-14-6,* https://www.alibaba.com/product-detail/Hot-Sale-99-Price-Potassium-Bicarbonate_1600221272985.html?s=p (2023), accessed: 2023-31-03.

[196] *Statistica: Price of ethylene worldwide from 2017 to 2022,* https://www.statista.com/statistics/1170573/price-ethylene-forecast-globally/ (2023), accessed: 2023-31-03.

[197] *Alibaba: Best price per ton calcium carbonate for food,* https://www.alibaba.com/product-detail/Best-Price-Per-Ton-Calcium-Carbonate_60669977553.html?s=p (2023), accessed: 2023-31-03.

[198] J. Park, L. Seok Young, J. Kim, and Y.-S. Yoon, *Efficiency, Economic, Energy, and Safety (3ES) Analyses on Different Configurations of MDEA Absorption Process for Coke Oven Gas Desulfurization,* Chemical Engineering Journal Advances **10**, 100281 (2022).

[199] *Indexbox: U.s. - acetic acid - market analysis, forecast, size, trends and insights,* https://www.indexbox.io/blog/acetic-acid-price-per-ton-june-2022/ (2022), accessed: 2023-22-02.

[200] *Market insider: Ethanol price,* https://markets.businessinsider.com/commodities/ethanol-price (2023), accessed: 2023-22-02.

[201] *Statista: Price of ethylene worldwide from 2017 to 2022,* https://www.statista.com/statistics/1170573/price-ethylene-forecast-globally/ (2022), accessed: 2023-22-02.

[202] *Iea: Global hydrogen review 2021,* https://www.iea.org/reports/global-hydrogen-review-2021/executive-summary (2021), accessed: 2023-22-02.

[203] *Alibaba: Propanol,* https://www.alibaba.com/product-detail/CAS-71-23-8-Best-Price_1600609166497.html?spm=a2700.7724857.0.0.6a52331d7mGi9Z (2023), accessed: 2023-22-02.

[204] *The engineering toolbox: Combustion heat,* https://www.engineeringtoolbox.com/standard-heat-of-combustion-energy-content-d_1987.html (2023), accessed: 2023-03-04.

[205] D. Arbeidsomstandigheden, *Wijziging Arbeidsomstandighedenregeling,* **120**, 1 (2005).

[206] *Pubchem compound summary for cid 280, carbon dioxide,* https://pubchem.ncbi.nlm.nih.gov/compound/Carbon-dioxide (2022), accessed: 2022-09-30.

[207] *The national institute for occupational safety and health (niosh), carbon monoxide,* https://www.cdc.gov/niosh/idlh/630080.html (2022), accessed: 2022-09-30.

[208] C. Identity and C. Properties, *4. CHEMICAL AND PHYSICAL INFORMATION of carbon monoxide,* , 2006 (2006).

[209] *Pubchem compound summary for cid 284, formic acid,* https://pubchem.ncbi.nlm.nih.gov/compound/Formic-acid (2022), accessed: 2022-09-30.

[210] *Rivm stofgegevens mierenzuur,* https://rvszoeksysteem.rivm.nl/stof/detail/952 (2022), accessed: 2022-09-30.

[211] *Pubchem compound summary for cid 712, formaldehyde,* https://pubchem.ncbi.nlm.nih.gov/compound/Formaldehyde (2022), accessed: 2022-10-03.

[212] *Center for disease control and prevention, formaldehyde,* https://www.cdc.gov/niosh/npg/npgd0293.html (2019), accessed: 2022-10-03.

[213] *Cbm, milieu en mvo, formaldehyde,* https://www.cbm.nl/dienstverlening/milieu-mvo/formaldehyde/ (2022), accessed: 2022-10-03.

[214] Alliance Consulting International, *Methanol Safe Handling Manual,* Methanol Institute **5**, 1 (2008).

[215] *Center for disease control and prevention, methanol,* https://www.cdc.gov/niosh/idlh/67561.html (2014), accessed: 2022-10-03.

[216] *Rijksinstituut voor volksgezondheid en milieu, index stoffen, methanol,* https://rvszoeksysteem.rivm.nl/stof/detail/917 (2022), accessed: 2022-10-03.

[217] A. H. Johnstone, *CRC Handbook of Chemistry and Physics-69th Edition Editor in Chief R. C. Weast, CRC Press Inc., Boca Raton, Florida, 1988, pp. 2400, price £57.50. ISBN 0-8493-0369-5,* Journal of Chemical Technology & Biotechnology **50**, 294 (2007).

[218] G. H. S. L. Elements, *Material Name,* Definitions , 1 (2020).

[219] W. M. Haynes, *CRC Handbook of Chemistry and Physics*, Vol. 97 (CRC press, 2016) p. 2670.

[220] *Cameo chemicals, oxalic acid,* https://cameochemicals.noaa.gov/chemical/8966 (1999), accessed: 2022-10-03.

[221] C. Identification, N. Hazardous, and O. Acid, *Oxalic Acid Oxalic Acid,* **393**, 6 (2018).

[222] *Engineering toolbox, gases explosion and flammability concentration limits,* https://www.engineeringtoolbox.com/explosive-concentration-limits-d_423.html (2003), accessed: 2022-10-03.

[223] I. I. für Arbeitsschutz der Deutschen Gesetzlichen Unfallversicherung, *Code, Substance Group and Aggregation, State O F and Characterisation, Chemical, Ethylene,* **1**, 1 (2022).

[224] I. I. für Arbeitsschutz der Deutschen Gesetzlichen Unfallversicherung, *Code, Substance Group and Aggregation, State O F and Characterisation, Chemical, Ethanol,* **1**, 1 (2022).

[225] I. I. für Arbeitsschutz der Deutschen Gesetzlichen Unfallversicherung, *Code, Substance Group and Aggregation, State O F and Characterisation, Chemical, Ethane,* **1**, 1 (2022).

[226] Thermo Fisher Scientific, *Safety Data Sheet, Ethane,* Material Safety Data Sheet **4(2)**, 8 (2012).

[227] *Center for disease control and prevention, n-propanol,* https://www.cdc.gov/niosh/npg/npgd0533.html\#print (2019), accessed: 2022-10-03.

[228] J. L. Unmack, *n-Propanol Health-Base Assessment and Recommendation for HEAC,* (2011).

[229] J. Gummer and S. Hawksworth, *Spontaneous ignition of hydrogen Literature Review,* Health (San Francisco) (2008).

[230] W. L. Jolly, *Britannica, hydrogen,* https://www.britannica.com/science/hydrogen (2022), accessed: 2022-10-03.

[231] *Beleidsregel 4.2-1 bijlage 6,* http://www.libre-net.nl/Arbo/Wetgeving/docs/arbobrb6.htm (2022), accessed: 2022-10-03.

[232] M. Bransby, *Explosive lessons,* Computing and Control Engineering Journal **9**, 57 (1998).

[233] LabChem, *Water Safety Data Sheet,* LabChem **4**, 8 (2020).

[234] A. M. Helmenstine, *Thoughtco, water chemistry definition and properties,* https://www.thoughtco.com/definition-of-water-in-chemistry-605946 (2020), accessed: 2022-10-03.

[235] *Universal industrial gases inc., material safety data sheet gaseous oxygen,* http://www.uigi.com/MSDS_gaseous_O2.html (2015), accessed: 2022-10-03.

[236] S. Asphyxiants, *Safety data sheet,* , 1 (2021).

[237] Risk Management Technologies, *Argon, Compressed. Safety Data Sheet #004,* **2.4**, 1 (2017).

[238] *Pubchem compound summary for cid 10039, carbonyl sulfide,* https://pubchem.ncbi.nlm.nih.gov/compound/Carbonyl-sulfide (2022), accessed: 2022-10-04.

[239] Praxair Inc., *Carbonyl sulfide Safety Data Sheet,* , 1 (2016).

[240] Airgas, *Safety Data Sheet - Carbonyl Sulphide,* Material Safety Data Sheet , 1 (2017).

[241] H. Services, *ATSDR's Toxicological Profiles*, December (2002).

[242] S. C. Gad, *Sulfur dioxide,* Encyclopedia of Toxicology , 115 (2005).

[243] S. G. Code, S. O. F. Aggregation, and C. Characterisation, *Sulfur Dioxide,* , 1 (2022).

[244] *Centers for disease control and prevention, nitrogen oxide,* https://www.cdc.gov/niosh/npg/npgd0454.html (2019), accessed: 2022-10-03.

[245] *Centers for disease control and prevention, idlh values nitrogen oxide,* https://www.cdc.gov/niosh/idlh/10102440.html (2014), accessed: 2022-10-03.

[246] S. van Sociale Zaken en Werkgelegenheid, *Arbeidsomstandighedenregeling in verband met de implementatie van Richtlijn 2017/164 in Bijlage XIII,* Staatscourant , 1 (2018).

[247] Thermo Fisher Scientific, *Safety Data Sheet Safety Data Sheet,* Material Safety Data Sheet **4(2)**, 8 (2012).

# A

# Appendix A

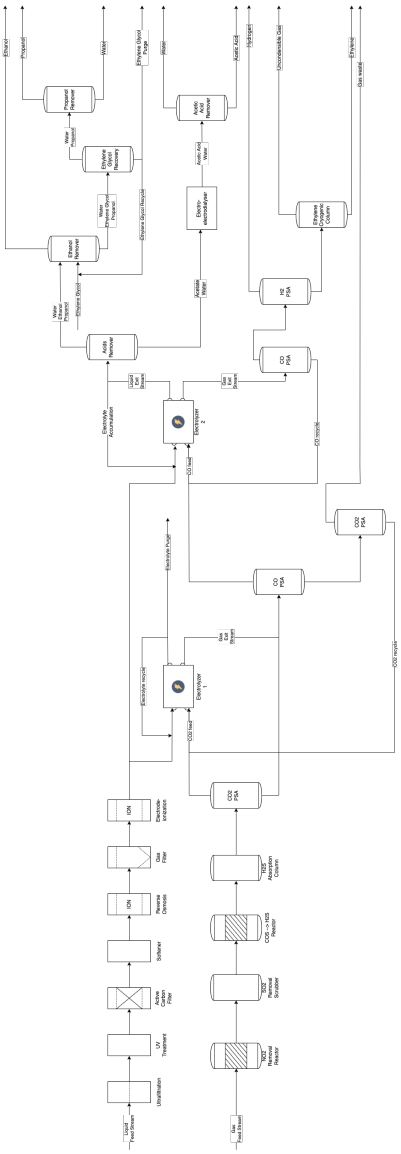


Figure A.1: Model scheme of the designed process

# B

# Appendix B

## B.1. Ultrapure water

### Ultrafiltration

The flux through an UF membrane is 381 $L\ m^{-2}\ hr^{-1}$ according to the article used. The flow rate through the UF membrane is 1,179,517.33 $L/hr^{-1}$. The UF membrane surface area is calculated in Equation B.1.

$$UF\ membrane\ area = \frac{1,179,517.33}{381} = 3,095.85\ m^2 \tag{B.1}$$

### Activated Carbon

AC can adsorb 704,23 $mg\ g^{-1}$ and has a density of 650 $kg\ m^{-3}$. $Pb^{2+}$, $Zn^{2+}$ and $Cl^{-1}$ are adsorbed by active carbon. In the first AC filter, 0.0265926, 0.188122, 2047.48 $kg\ day^{-1}$ of $Pb^{2+}$, $Zn^{2+}$ and $Cl^{-1}$ are adsorbed, respectively. In the second filter, the ions have an adsorption rate of 0.00452, 0.0309 and 102.374 $kg\ day^{-1}$, respectively. The volumes of active carbon beds are calculated in Equations B.2 and B.3.

$$AC\ bed\ volume = \frac{(0.0265926 + 0,188122 + 2047,48) * 183 * 1000}{704,23 * 650} = 818.63\ m^3 \tag{B.2}$$

$$AC\ bed\ volume = \frac{(0.00452 + 0.0309 + 102.374) * 183 * 1000}{704,23 * 650} = 40.94\ m^3 \tag{B.3}$$

### Reverse Osmosis

Four RO units are required to meet the specifications for ultrapure water. The volumetric flow rate through each membrane is 24,690.9, 22,230.3, 20,015.4 and 18,021.2 $m^3\ day^{-1}$. The used membrane has a water permeability of 41.6 $m^3\ day^{-1}$ for a 37 $m^2$ membrane. The surface area of the membranes are:

$$RO\ membrane\ 1\ surface\ area = \frac{24,690.9}{41.6} * 37 = 21,960.7\ m^2 \tag{B.4}$$

$$RO\ membrane\ 2\ surface\ area = \frac{22,230.3}{41.6} * 37 = 19,772.1\ m^2 \tag{B.5}$$

$$RO\ membrane\ 3\ surface\ area = \frac{20,015.4}{41.6} * 37 = 17,802.2\ m^2 \tag{B.6}$$

$$RO\ membrane\ 4\ surface\ area = \frac{18,021.2}{41.6} * 37 = 16,028.5\ m^2 \tag{B.7}$$

### Storage Tank

An one day volume tank is needed to cope with small maintenance stops. The UPW production is 736.018 $m^3\ hr^{-1}$, so shown in Equation B.8 a storage tank of 17,664.4 $m^3$ is needed to store UPW.

$$Storage\ tank\ volume = 736.018 * 24 = 17,664.4\ m^3 \tag{B.8}$$

## B.2. Gas Purification

All flash drums are assumed to be pressurize vessels with a height 4 times its diameter and an average residence time of 5 $min$. The volumes of each flash drum is calculated in Equations B.9 to B.11. The flow rate through each flash drum is 89.409, 82.290, 0.376 $m^3\ min^{-1}$, respectively. With the assumption that the height is 4 times the diameter, the diameter and height can be calculated using Equation B.12. The height and diameters are 5.22 and 20.88, 5.08 and 20.31 and 0.84 and 3.37, respectively, for flash drum 1, 2, and 3.

$$Flash\ drum\ 1\ volume = 89.409 * 5 = 447.04\ m^3 \tag{B.9}$$

$$Flash\ drum\ 2\ volume = 82.290 * 5 = 411.45\ m^3 \tag{B.10}$$

$$Flash\ drum\ 3\ volume = 0.376 * 5 = 1.88\ m^3 \tag{B.11}$$

$$V_{cylinder} = \frac{1}{4}\pi D^2 H \tag{B.12}$$

## B.3. Electrolyzers

### First Electrolyzer

From the used literature and the mentioned flow rate and electrode surface area, the total electrode surface area is calculated. The used article for the first electrolyzer said they used an electrode surface area of 1.9 $cm^2$ with a gas flow rate of 40 $mL\ min^{-1}$. The gas flow in this process for the first electrolyzer is 1,524,101.84 $L\ min^{-1}$. As can be seen from Equations B.13 and B.14, the electrode surface area needs to be 7,239.48 $m^2$.

$$Electrode\ surface\ area = \frac{1,524,101.84}{0.040} * 1.9 = 72,394,837.40\ cm^2 \tag{B.13}$$

$$Electrode\ surface\ area = \frac{72,394,837.40}{10000} = 7,239.48\ m^2 \tag{B.14}$$

### Second Electrolyzer

The article used as a reference for the second electrolyzer mentioned an electrode surface area of 10 $cm^2$ and a gas flow rate of 50 $mL\ min^{-1}$. The gas flow of the second electrolyzer is 5,088,866.48 $L\ min^{-1}$. Equations B.15 and B.16 show that the electrode surface area needs to be 101,777.33 $m^2$.

$$Electrode\ surface\ area = \frac{5,088,866.48}{0.050} * 10 = 1,017,773,296.0\ cm^2 \tag{B.15}$$

$$Electrode\ surface\ area = \frac{1,017,773,296.0}{10000} = 101,777.33\ m^2 \tag{B.16}$$

### Storage Tank

The average residence time in an electrolyzer is 1 $min$. A tank volume of two times the volume of anolyte that passes through the electrolyzer every minute is assumed to be adequate. The anolyte flow rate through the first electrolyzer is 468.87 $m^3\ min^{-1}$, so from Equation B.17, it is known that the volume of the storage tank needs to be 937.75 $m^3$. The flow rate of the anolyte in the second electrolyzer is 10.183.1 $m^3\ min^{-1}$, so as calculated in Equation B.18, this storage tank needs a volume of 20,366.2 $m^3$.

$$Storage\ tank\ 1\ anolyte\ = 2 * 468.87 = 937.75\ m^3 \tag{B.17}$$

$$Storage\ tank\ 2\ anolyte\ = 2 * 10,183,1 = 20,366.2\ m^3 \tag{B.18}$$

It is assumed that the catholyte storage tank should contain an extra volume of 1 day of downstream production besides the volume of two times the average residence time. Every day a volume of 7,402.12 $m^3$ flows to the liquid product separation. Since the catholyte and anolyte flow are equal for the second electrolyzer, the catholyte storage tank has a calculated volume of 27,768,32 $m^3$.

$$Storage\ tank\ catholyte\ = 20,366.2 + 7,402.12 = 27,768.32\ m^3 \tag{B.19}$$

## B.4. Propanol Pervaporation

The flux through the membrane is 1.2 $kg\ m^{-2}\ hr^{-1}$ and the flow rate through the membrane is 8,246.45 $kg\ hr^{-1}$.

$$Pervaporation\ membrane\ area = \frac{8,246.45}{1.2} = 6,872.04\ m^2 \tag{B.20}$$

# C

# Appendix C

## C.1. Capital Cost

### C.1.1. Calculations

The prices for the units used for the production of UPW are calculated in Table C.1.

**Ultrapure Water**

Table C.1: Calculations for the f.o.b. purchase prices for the unit to produce UPW

| Unit | Formula | Symbol | Value (imperial) | Value (metric) | Cp ($) | Quantity | Total ($) | |
|---|---|---|---|---|---|---|---|---|
| Ultrafiltration | Cp = 25A | A=membrane area ($ft^2$) | 33,323.42 | 3,095.85 | 833,085.50 | 1 | 833,085.50 | |
| UV treatment | 1 unit for 20,000 to 100,000 $L\ hr^{-1}$ | | | 1.14 million $L\ hr^{-1}$ | 1,185.45 | 12 | 14,225.40 | [184] |
| Active Carbon Filter 1 | Cp = 41S | S=Bulk volume ($ft^3$) | 28,909.72 | 818.63 | 1,185,298.67 | 1 | 1,185,298.67 | |
| Active Carbon Filter 2 | Cp = 41S | S=Bulk volume ($ft^3$) | 1,445.83 | 40.94 | 59,279.19 | 1 | 59,279.19 | |
| Softener | 40 to 200 dollar per cubic foot | | 1,615.70 | 45.76 | 177,759.91 | 1 | 177,759.91 | [185] |
| Reverse Osmosis 1 | Cbm=3.1Q | Q=water volume ($gal\ day^{-1}$) | 7,254,190.97 | 27,460.10 | 22,487,991.99 | 1 | 22,487,991.99 | |
| Reverse Osmosis 2 | Cbm=3.1Q | Q=water volume ($gal\ day^{-1}$) | 6,525,261.02 | 24,700.80 | 20,228,309.17 | 1 | 20,228,309.17 | |
| Reverse Osmosis 3 | Cbm=3.1Q | Q=water volume ($gal\ day^{-1}$) | 5,875,001.52 | 22,239.30 | 18,212,504.70 | 1 | 18,212,504.70 | |
| Reverse Osmosis 4 | Cbm=3.1Q | Q=water volume ($gal\ day^{-1}$) | 5,289,649.08 | 20,023.50 | 16,397,912.16 | 1 | 16,397,912.16 | |
| Degasser | one unit for 15 $ton\ hr^{-1}$ | | | | 36,900.00 | 51 | 1,881,900.00 | [186] |
| EDI | One unit for max 100 $m^3\ hr^{-1}$ | | | | 6,647.97 | 8 | 53,183.76 | [187] |
| Storage tank | Cp= 475 $V^{0.507}$ | V=tank volume ($gal$) | 4,666,440.80 | 17,664.40 | 1,142,534.68 | 1 | 1,142,534.68 | |

The formula for the calculation of the price of the pumps is given in Equation C.1 with $F_t$ the motor type factor and $C_B$ the base cost. The type factor for an open, drip-proof enclosure is 1 and the base cost is calculated using Equations C.2 and C.3 with $P_B$ and $Q$ the break power of the pump in $Hp$ and Q the flow rate in $gal\ min^{-1}$. The prices are calculated in Table C.2.

$$C_P = F_t * C_B \tag{C.1}$$

$$C_B = exp5.9332 + 0.16829ln(P_C) - 0.1100568ln(P_C)^2 + 0.071413ln(P_C)^3 - 0.0063788ln(P_C)^4 \tag{C.2}$$

$$P_C = \frac{P_B}{-0.316 + 0.24015ln(Q) - 0.01199ln(Q)^2} \tag{C.3}$$

Table C.2: Calculations for the f.o.b. purchase prices for the pumps used in the UPW production

| **Unit** | $C_B$ | $P_C$ | **Pb** ($Hp$) | **Q** ($gal\ min^{-1}$) | $C_P$ **(\$)** |
|---|---|---|---|---|---|
| Pump 1 | 22,153.94 | 356.25 | 306.71 | 5,192.4 | 22,153.94 |
| Pump 2 | 2,547.00 | 57.67 | 49.59 | 5,037.46 | 2,547.00 |
| Pump 3 | 2,546.37 | 57.66 | 49.58 | 5,036.27 | 2,546.37 |
| Pump 4 | 2,546.35 | 57.66 | 49.58 | 5,036.21 | 2,546.35 |
| Pump 5 | 47,222.03 | 835.99 | 718.84 | 5035,61 | 47,222.03 |
| Pump 6 | 44,326.31 | 758.66 | 649.38 | 4,529.61 | 44,326.31 |
| Pump 7 | 41,373.68 | 689.73 | 587.51 | 4,078.21 | 41,373.68 |
| Pump 8 | 38,398.51 | 627.49 | 531.73 | 3,671.87 | 38,398.51 |
| Pump 9 | 16,568.82 | 275.78 | 232.41 | 3,306.04 | 16,568.82 |
| Pump 10 | 1,711.49 | 39.40 | 33.21 | 3,306.63 | 1,711.49 |

## Gas Purification

The price for the absorber columns for the gas purification are calculated in Table C.3 using Equations C.4 to C.14.

$$P_D = exp(0.60608 + 0.91615ln(P_G) + 0.0015655ln(P_G)^2) \tag{C.4}$$

$$t_p = \frac{\frac{D_i * P_d}{2*S*E-1.2*P_d}}{12} \tag{C.5}$$

$$W = \pi * (D_i + t_p) * (L + 0.8 * D_i) * t_p * \rho \tag{C.6}$$

$$C_V = exp(10.5449 - 0.4672ln(W) + 0.05482ln(W)^2) \tag{C.7}$$

$$C_{PL} = 341 * D_i^{0.633316} * L^{0.80161} \tag{C.8}$$

$$F_{nt} = \frac{2.25}{1.0414^{N_T}} \quad for \quad N_T < 20 \tag{C.9}$$

$$F_{nt} = 1 \quad for \quad N_T > 20 \tag{C.10}$$

$$F_{tm} = 1.87 + 0.0577 * D_i \tag{C.11}$$

$$C_{bt} = 468 * exp(0.1482 * D_i) \tag{C.12}$$

$$C_t = C_{bt} * F_{tm} * F_{tt} * F_{nt} * N_t \tag{C.13}$$

$$C_p = C_{pl} + F_m * C_V + C_t \tag{C.14}$$

Table C.3: Calculations for the f.o.b. purchase prices for the columns used for the gas cleaning

| **Unit** | $D_i$ $(ft)$ | **L** $(ft)$ | **Pressure** $(psig)$ | $P_D$ | **E** | **Max Stress (S)** $(psi)$ | $t_p$ $(ft)$ | **Density** $(lb\ ft^3)$ | **Weight** $(lb)$ | $C_v$ | $C_{pl}$ | $F_m$ | $N_t$ | $F_{nt}$ | $F_{tt}$ | **Material Type** | $F_{tm}$ | $C_{bt}$ **(\$)** | $C_t$ **(\$)** | $C_P$ **(\$)** |
|---|---|---|---|---|---|---|---|---|---|---|---|---|---|---|---|---|---|---|---|---|
| $SO_2$ scrubber | 34.878 | 12 | 10 | 15.24 | 1 | 15,000 | 0.00148 | 499.4 | 3,226.14 | 31,211 | 23,701 | 1.7 | 6 | 1.76 | 1 | 303 Stainless Steel | 3.88247681 | 82,242.67 | 3,379,359.46 | 3,456,118.75 |
| $H_2S$ srubber | 29.451 | 10 | 10 | 15.24 | 1 | 15,000 | 0.00125 | 499.4 | 1,934.74 | 25,561 | 18,398 | 1.7 | 5 | 1.84 | 1 | 303 Stainless Steel | 3.5693483 | 36,797.02 | 1,206,330.41 | 1,268,182.34 |

The price for the flash drums in the gas purification part are calculated in Table C.4 using Equations C.15 to C.20.

$$P_D = exp(0.60608 + 0.91615ln(P_G) + 0.0015655ln(P_G)^2) \tag{C.15}$$

$$t_p = \frac{\frac{D_i * P_d}{2 * S * E - 1.2 * P_d}}{12} \tag{C.16}$$

$$W = \pi * (D_i + t_p) * (L + 0.8 * D_i) * t_p * \rho \tag{C.17}$$

$$C_V = exp(7.139 + 0.18255ln(W) + 0.02297ln(W)^2) \tag{C.18}$$

$$C_{PL} = 410.3 * D_i^{0.7396} * D21^{0.70648} \tag{C.19}$$

$$C_p = C_{pl} + F_m * C_V \tag{C.20}$$

Table C.4: Calculations for the f.o.b. purchase prices for the flash drums used for the gas cleaning

| Unit | Type | Di ($ft$) | L ($ft$) | Pressure ($psig$) | Pd | E | S | tp ($ft$) | Density ($lb\ ft^3$) | Weight ($lb$) | Cv ($) | Cpl ($) | Fm | Cp ($) |
|---|---|---|---|---|---|---|---|---|---|---|---|---|---|---|
| Flash drum 1 | vertical vessel | 17.128 | 68.514 | 10 | 15.24 | 1 | 15,000 | 0.00073 | 490 | 1,572.9 | 16,767 | 66,451 | 1 | 83,217.83 |
| Flash drum 2 | vertical vessel | 16.661 | 66.645 | 10 | 15.24 | 1 | 15,000 | 0.00071 | 490 | 1,447.6 | 16,061 | 63,846 | 1 | 79,906.57 |
| Flash drum 3 | vertical vessel | 2.765 | 11.060 | 10 | 15.24 | 1 | 15,000 | 0.00012 | 490 | 6.6 | 1,931 | 4,755 | 1 | 6,686.21 |

For the price of the coolers, Equations C.21 to C.23 with $F_L$ equal to 1 and $F_P$ equal to 0.9803 and A the area in $ft^2$ are used. The calculations for the price of the coolers are shown in Table C.5

$$F_m = 2.7 + \frac{A}{100}^{0.07} \tag{C.21}$$

$$C_b = exp(12.031 - 0.8709ln(A) + 0.09005ln(A)^2) \tag{C.22}$$

$$C_p = F_m * F_l * F_P * C_b \tag{C.23}$$

Table C.5: Calculations for the f.o.b. purchase prices for the coolers used for the gas cleaning

| Unit | A ($ft^2$) | Fm | Fl | Fp | Cb ($) | Cp ($) |
|---|---|---|---|---|---|---|
| Cooler 1 | 7,548.97 | 4,053480923 | 1 | 0.9803 | 92,436.45 | 367,307.99 |
| Cooler 2 | 12,591.8 | 4,102833561 | 1 | 0.9803 | 138,005.39 | 555,058.75 |

The price for the other units used in gas purification process are calculated in Table C.6.

Table C.6: Calculations for the f.o.b. purchase prices of the remaining units for the gas cleaning section

| Unit | Formula | Symbol | Value (imperial) | Value (metric) | Cp ($) | Quantity | Total ($) | |
|---|---|---|---|---|---|---|---|---|
| COS to H2S reactor | CP = 2.245S^0.58 | S = vessel volume (gal) | 2,251,368.427 | 8,522.36 | 11,338.66 | 1 | 11,338.66 | |
| CO2 PSA | 2 million $ for 200k m3/hr | | | 296,166 | 2,000,000.00 | 2 | 4,000,000.00 | [171] |
| CO2 PSA recycle | 2 million $ for 200k m3/hr | | | 211,873 | 2,000,000.00 | 2 | 4,000,000.00 | [171] |
| CO PSA | 2 million $ for 200k m3/hr | | | 353,225 | 2,000,000.00 | 2 | 4,000,000.00 | [171] |
| CO PSA recycle | 2 million $ for 200k m3/hr | | | 220,405 | 2,000,000.00 | 2 | 4,000,000.00 | [171] |

### Electrolyzers

The prices of the electrolyzers are based on the price per $kW$ for a hydrogen electrolyzer. The cost for the electrolyzers per $m^2$ are calculated using Equation C.24 using a price of $250.25 per $kW$.[54] The calculations for the cost per $m^2$ are shown in Table C.7. The first and second electrolyzer both have a CD of 300 $mA\ cm^{-2}$, so using the total electrode area, the total current, power and cost are calculated as shown in Tables C.8 and C.9. The power of the electrolyzer is calculated using Equation C.25.

$$Price\ per\ m^2 = \frac{\frac{Voltage * CD}{1000}}{1000} * 10^4 * 250.25 * 1.2 \tag{C.24}$$

$$Power = Voltage * total\ current \tag{C.25}$$

Table C.7: Calculations for the price of the electrolyzer per $m^2$ with an applied voltage of 3.2 $V$ and a current density of 300 $mA\ cm^{-2}$

| | | |
|---|---|---|
| Cost for electrolyzer | 250.25 | $\$\ kW^{-1}$ |
| Electrolyzer Voltage | 3.2 | $V$ |
| Current Density | 300 | $mA\ cm^{-2}$ |
| Installed Cost | 2,882.9 | $\$\ m^{-2}$ |

Table C.8: Capex, current and power calculation for the first electrolyzer

| | | |
|---|---|---|
| Current Density: | 300.00 | $mA\ cm^{-2}$ |
| Cell Voltage: | 3.20 | $V$ |
| Current Needed: | 21,718,440.00 | $A$ |
| Electrolyzer area: | 7,239.48 | $m^2$ |
| Power Needed: | 69.50 | $MW$ |
| Total cost: | 20,870,552.10 | $ |

Table C.9: Capex, current and power calculation for the second electrolyzer

| | | |
|---|---|---|
| Current Density: | 300.00 | $mA\ cm^{-2}$ |
| Cell Voltage: | 3.20 | $V$ |
| Current Needed: | 305,331,990.00 | $A$ |
| Electrolyzer area: | 101,777.33 | $m^2$ |
| Power Needed: | 977.06 | $MW$ |
| Total cost: | 293,411,829.11 | $ |

## Liquid Product Separation

In the liquid product separation section, a lot of distillation columns are used. The same equations as for the calculations of the CapEx for the absorber columns are used for these distillation columns, so Equations C.4 to C.14. The calculations are shown in Table C.10. The price of the cooler used is calculated using Equations C.21 to C.23 and the calculations are shown in Table C.11. The prices for the remaining units are calculated in Table C.12.

Table C.10: Calculations for the f.o.b. purchase prices for the columns used for the liquid product separation

| Unit | $D_i$ $(ft)$ | L $(ft)$ | Pressure $(psig)$ | $P_D$ | E | Max Stress (S) $(psi)$ | $t_p$ $(ft)$ | Density $(lb\ ft^3)$ | Weight $(lb)$ | $C_v$ | $C_{pl}$ | $F_m$ | $N_t$ | $F_{nt}$ | $F_{tt}$ | Material Type | $F_{tm}$ | $C_{bt}$ ($) | $C_t$ ($) | $C_P$ ($) |
|---|---|---|---|---|---|---|---|---|---|---|---|---|---|---|---|---|---|---|---|---|
| Acetate removal column | 39.790 | 12 | 10 | 15.24 | 1 | 15,000 | 0.00169 | 499.4 | 4,401.79 | 35,735 | 22,260 | 1.7 | 5 | 1.84 | 1 | 303 Stainless Steel | 4.16588452 | 170,305.68 | 6,516,299.01 | 6,599,308.30 |
| Ethanol removal column | 18.399 | 64 | 10 | 15.24 | 1 | 15,000 | 0.00078 | 499.4 | 1,771.03 | 24,765 | 60,481 | 1.7 | 32 | 1.00 | 1 | 303 Stainless Steel | 2.93160617 | 7,152.08 | 670,946.74 | 773,528.63 |
| Ethylene glycol recovery column | 24.068 | 108 | 10 | 15.24 | 1 | 15,000 | 0.00102 | 499.4 | 4,899.18 | 37,533 | 109,057 | 1.7 | 54 | 1.00 | 1 | 303 Stainless Steel | 3.25872239 | 16,569.90 | 2,915,821.19 | 3,088,684.25 |
| Propanol removal column | 10.790 | 16 | 10 | 15.24 | 1 | 15,000 | 0.00046 | 499.4 | 190.60 | 14,811 | 14,198 | 1.7 | 8 | 1.63 | 1 | 303 Stainless Steel | 2.49259398 | 2,315.95 | 75,112.52 | 114,488.38 |
| Acetic acid separation column | 16.921 | 50 | 10 | 15.24 | 1 | 15,000 | 0.00072 | 499.4 | 1,209.01 | 21,818 | 47,059 | 1.7 | 25 | 1.00 | 1 | 303 Stainless Steel | 2.84632073 | 5,745.12 | 408,811.58 | 492,961.23 |

Table C.11: Calculations for the f.o.b. purchase prices for the cooler used for the liquid products separation

| Unit | A ($ft^2$) | Fm | Fl | Fp | Cb ($) | Cp ($) |
|---|---|---|---|---|---|---|
| Cooler 3 | 1,599.65 | 3,91417629 | 1 | 0.9803 | 36,576.11 | 140,344.98 |

Table C.12: Calculations for the f.o.b. purchase prices for the remaining unit for the liquid products separation

| Unit | Formula | Symbol | Value (imperial) | Value (metric) | Cp ($) | Quantity | Total ($) | |
|---|---|---|---|---|---|---|---|---|
| n-Propanol pervaporation | Cp = 43A | A=membrane area (ft2) | 242,683.80 | 6,872.04 | 10,435,403.49 | 1 | 10,435,403.49 | |
| Electro-electrodialyser | One unit for 20 $tonne\ hr^{-1}$ | | | 261 | 8,500.00 | 14 | 119,000.00 | [188] |

## Gas Product Separation

A cryogenic distillation column is used to separate ethylene from non-condensable gasses. The price of this unit is calculated using Equations C.4 to C.14 and shown in Table C.13. It should be noted that the gauge pressure in this unit is negative, but for gauge pressures of 0 $psi$ or lower, a gauge pressure of 10 $psi$ should be used for price calculations.[117]

Table C.13: Calculation for the f.o.b. purchase prices for the column used to separate ethylene

| Unit | $D_i$ ($ft$) | L ($ft$) | Pressure ($psig$) | $P_D$ | E | Max Stress (S) ($psi$) | $t_p$ ($ft$) | Density ($lb\ ft^3$) | Weight ($lb$) | $C_v$ | $C_{pl}$ | $F_m$ | $N_t$ | $F_{nt}$ | $F_{tt}$ | Material Type | $F_{tm}$ | $C_{bt}$ ($) | $C_t$ ($) | $C_P$ ($) |
|---|---|---|---|---|---|---|---|---|---|---|---|---|---|---|---|---|---|---|---|---|
| Ethylene separation column | 4.272 | 58 | 10 | 15.24 | 1 | 15,000 | 0.00018 | 499.4 | 74.48 | 14,039 | 22,167 | 1.7 | 29 | 1.00 | 1 | 303 Stainless Steel | 2,1164763 | 881.42 | 54,099.52 | 100,133.14 |

The f.o.b. purchase price of the compressor is calculated using Equations C.26 and C.27 with $F_D$ the turbine drive factor, $F_M$ the material factor, and $P_C$ the consumed power in $Hp$. $F_D$ has a value of 1.5 for a gas turbine drive and the compressor is made of stainless steel, so $F_M$ equals 2.5. The compressor has a power of 7,591.19 $Hp$, so the $C_P$ is $9,491,852.29.

$$C_P = F_D * F_M * C_B \tag{C.26}$$

$$C_B = exp9.1553 + 0.63ln(P_C) \tag{C.27}$$

The price of the cooler used is calculated using Equations C.21 to C.23 and the calculations are shown in Table C.14.

Table C.14: Calculations for the f.o.b. purchase prices for the cooler used for the gas products separation

| Unit | A ($ft^2$) | Fm | Fl | Fp | Cb ($) | Cp ($) |
|---|---|---|---|---|---|---|
| Cooler 3 | 1,730.37 | 3.920870861 | 1 | 0.9803 | 37,936.39 | 145,813.45 |

The only remaining unit is the $H_2$ PSA and this unit has a price of $2,000,000.00.[171]

## Heat Exchangers

Just as the coolers, the price of the heat exangers are calculated using Equations C.21 to C.23 with $F_L$ equal to 1 and $F_P$ equal to 0.9803, and A the area in $ft^2$. The prices are shown in Table C.15

Table C.15: Calculations for the f.o.b. purchase price for the heat exchangers used in the process

| | A ($ft_2$) | Fm | Fl | Fp | Cb ($) | Cp ($) |
|---|---|---|---|---|---|---|
| Heat exchanger 1 | 1,436.83 | 3.90508693 | 1 | 0.9803 | 34,858.28 | 133,442.96 |
| Heat exchanger 2 | 340.181 | 3.78948111 | 1 | 0.9803 | 22,342.81 | 82,999.71 |
| Heat exchanger 3 | 9,518.38 | 4.07562295 | 1 | 0.9803 | 110,196.30 | 440,270.92 |
| Heat exchanger 4 | 84.2534 | 3.68807775 | 1 | 0.9803 | 20,740.77 | 74,986.67 |
| Heat exchanger 5 | 126.743 | 3.71672775 | 1 | 0.9803 | 20,441.48 | 74,478.70 |
| Heat exchanger 6 | 674.899 | 3.84300128 | 1 | 0.9803 | 26,347.98 | 99,260.59 |

### C.1.2. Table Summaries

Table C.16: Price of each individual unit for the UPW production

| **Unit** | **Price ($)** | |
|---|---|---|
| Ultrafiltration | 833,085.50 | |
| UV treatment | 14,225.40 | [184] |
| Active carbon filter 1 | 1,185,298.67 | |
| Active carbon filter 2 | 59,279.19 | |
| Softener | 177,759.91 | [185] |
| Reverse osmosis 1 | 22,487,991.99 | |
| Reverse osmosis 2 | 20,228,309.17 | |
| Reverse osmosis 3 | 18,212,504.70 | |
| Reverse osmosis 4 | 16,397,912.16 | |
| Degasser | 1,881,900.00 | [186] |
| Electrodeionization | 53,183.76 | [187] |
| Storage tank | 1,142,534,68 | |
| Pump 1 | 22,153.94 | |
| Pump 2 | 2,547.00 | |
| Pump 3 | 2,546.37 | |
| Pump 4 | 2,546.35 | |
| Pump 5 | 47,222.03 | |
| Pump 6 | 44,326.31 | |
| Pump 7 | 41,373.68 | |
| Pump 8 | 38,398.51 | |
| Pump 9 | 16,568.82 | |
| Pump 10 | 1,711.49 | |
| **Total** | **82,893,379.63** | |

Table C.17: Price of each individual unit for the gas cleaning process

| **Unit** | **Price ($)** | |
|---|---|---|
| $SO_2$ scrubber | 3,456,118.75 | |
| Cooler 1 | 367,307.99 | |
| Flash drum 1 | 83,217.83 | |
| COS reactor | 11,388.66 | |
| $H_2S$ scrubber | 1,268,182.34 | |
| Flash drum 2 | 79,906.57 | |
| Cooler 2 | 555,058.75 | |
| Flash drum 3 | 6,686.21 | |
| $CO_2$ PSA | 4,000,000.00 | [171] |
| CO PSA | 4,000,000.00 | [171] |
| $CO_2$ recycle PSA | 4,000,000.00 | [171] |
| CO recycle PSA | 4,000,000.00 | [171] |
| **Total** | **21,827,817.11** | |

Table C.18: Price of each electrolyzer with storage tanks

| Unit | Price ($) | |
|---|---|---|
| Electrolyzer 1 | 20,870,552,10 | [44] |
| Storage tank 1 | 257,892.26 | |
| Electrolyzer 2 | 293,411,829.11 | [44] |
| Storage tank anolyte | 1,228,026.18 | |
| Storage tank catholyte | 1,437,043.46 | |
| **Total** | **317,205,343.11** | |

Table C.19: Price of each liquid product separation unit

| Unit | Price ($) | |
|---|---|---|
| Acetate removal column | 6,599,308.30 | |
| Electro-electrodialyser | 119,000.00 | [188] |
| Acetic acid separation column | 492,961.23 | |
| Ethanol removal column | 773,528.63 | |
| Ethylene glycol recovery column | 3,088,684.25 | |
| Propanol removal column | 114,488.38 | |
| Propanol pervaporation | 10,435,403.49 | |
| Cooler 3 | 140,344.98 | |
| **Total** | **21,763,719.27** | |

Table C.20: Price of each gas product separation unit

| Unit | Price ($) | |
|---|---|---|
| $H_2$ PSA | 2,000,000.00 | [171] |
| Compressor | 9,491,852.29 | |
| Cooler 4 | 145,813.45 | |
| Ethylene separation column | 100,133.14 | |
| **Total** | **11,737,798.88** | |

Table C.21: Price of each heat exchanger

| Unit | Price ($) |
|---|---|
| Heat exchanger 1 | 133,442.96 |
| Heat exchanger 2 | 82,999.71 |
| Heat exchanger 3 | 440,270.92 |
| Heat exchanger 4 | 74,986.67 |
| Heat exchanger 5 | 74,478.70 |
| Heat exchanger 6 | 99,260.59 |
| **Total** | **905,439.54** |

## C.2. Operating Cost

### C.2.1. Calculations

For the calculations of the OpEx, an electricity price of $0.19 is used and all units operate 24 $hr$ a day.[173]. The operating cost are divided in to parts. One is the cost to run the unit and the other is the average cost for maintains. For all units a maintenance cost of 2.5% of the CapEx is assumed each year, except for the ultrapure water units, where units require different maintenance and regeneration procedures which changes the maintenance cost.

### Ultrapure Water

In the first table, all operating cost for all non-pump units are calculated. In the second table, the OpEx for the pumps are calculated.

Table C.22: Calculations of the operating cost of all non pump units for the production of ultrapure water

| Units | Value | Costs ($\$\ day^{-1}$) | | |
|---|---|---|---|---|
| Ultrafiltration | $833,085.50 CapEx | 0.00 | Pump is used | |
| Ultrafiltration maintenance | | 57.06 | 2.5% of CapEx each year | [135] |
| UV treatment | 7.253 million gallon/day | 241.19 | 175 kWh/million gallon | [189] |
| UV treatment maintenance | $14,225.40 CapEx | 0.97 | 2.5% of CapEx each year | |
| Active carbon filter 1 | | 0.00 | Pump | |
| Active carbon filter 1 maintenance | 818.63 $m^3$ bed | 7,900.23 | Replace bed every 6 months with an AC price of $2,717 per ton | [190] |
| Active carbon filter 2 | | 0.00 | Pump | |
| Active carbon filter 2 maintenance | 40.94 $m^3$ bed | 395.09 | Replace bed every 6 months with an AC price of $2,717 per ton | [190] |
| Softener | | 0.00 | Pump | |
| Softener maintenance | 1616 $ft^3$ bed | 20.66 | Replace resins after 8 years and $70 per $ft^3$ | [185] |
| RO 1 | | 0.00 | Pump | |
| RO 2 | | 0.00 | Pump | |
| RO 3 | | 0.00 | Pump | |
| RO 4 | | 0.00 | Pump | |
| RO maintenance | 21,960.7, 19,772.1, 17,802.2, 16,028.5 $m^2$ membranes | 8,837.31 | Replace membrane every 4 years and membrane cost is $170.75 per $m^2$ | [150] |
| Degasser | 51 units | 5,116.32 | 22 kW per unit | [186] |
| Degasser maintenance | $1,881,900.00 CapEx | 128.90 | 2.5% of CapEx each year | |
| Electrodionizer | 18,024.9 $m^3$ per day | 7,209.96 | $0.40 per $m^3$ | [174] |
| Electrodionizer maintenance | $53,183.76 CapEx | 3.64 | 2,5% of CapEx each year | |

Table C.23: Calculations of the operating cost of all pumps used for the production of ultrapure water

| Pumps | Pressure increase ($bar$) | Power ($kW$) | Costs ($\$\ day^{-1}$) | Maintenance cost ($\$\ day^{-1}$) |
|---|---|---|---|---|
| Pump 1 | 6 | 228.717 | 1,042.95 | 1.52 |
| Pump 2 | 1 | 36.9814 | 168.64 | 0.17 |
| Pump 3 | 1 | 36.9732 | 168.60 | 0.17 |
| Pump 4 | 1 | 36.9728 | 168.60 | 0.17 |
| Pump 5 | 14.5 | 536.042 | 2,444.35 | 3.23 |
| Pump 6 | 14.5 | 484.242 | 2,208.14 | 3.04 |
| Pump 7 | 14.5 | 438.109 | 1,997.78 | 2.83 |
| Pump 8 | 14.5 | 396.513 | 1,808.10 | 2.63 |
| Pump 9 | 7 | 173.305 | 790.27 | 1.13 |
| Pump 10 | 1 | 24.7621 | 112.92 | 0.12 |

### Gas Purification

All operating expenses for the absorber columns, coolers, and flash drums are obtained from ASPEN PLUS V12. The costs for the PSA units are calculated in Table C.24.

Table C.24: Operating and maintenance costs of each unit for the gas cleaning process

| Unit | | Value | Operating cost ($\$\ day^{-1}$) | |
|---|---|---|---|---|
| $CO_2$ PSA | 560 $kJ/mol^{-1}$ per $kg$ $CO_2$ | 31.0762 $kg\ s^{-1}$ | 79,356.18 | [191] |
| CO PSA | 560 $kJ/mol^{-1}$ per $kg$ CO | 46.6879 $kg\ s^{-1}$ | 119.222,22 | [191] |
| $CO_2$ recycle PSA | 560 $kJ/mol^{-1}$ per $kg$ $CO_2$ | 30.5158 $kg\ s^{-1}$ | 77.925,15 | [191] |
| CO recycle PSA | 560 $kJ/mol^{-1}$ per $kg$ CO | 55.72 $kg\ s^{-1}$ | 142,286.59 | [191] |
| Maintenance | | $21,827,817.11 total CapEx | 1,495.06 | |

### Electrolyzers

Table C.25: Operating costs of both electrolyzers

| Unit | Value | Operating cost ($\$\ day^{-1}$) |
|---|---|---|
| Electrolyzer 1 | 69.50 $MW$ | 316,915.48 |
| Electrolyzer 2 | 977.06 $MW$ | 4,455,404.40 |
| Maintenance | $317,205,343.11 CapEx | 21,726.39 |

### Liquid Product Separation

The utilities and condenser and reboiler duties are obtained from ASPEN PLUS V12.

Table C.26: OpEx of the distillation columns used for liquid product separation

| Units | Condenser duty (MW) | Condenser untility | Condenser cost ($/day) | Reboiler duty (MW) | Reboiler utility | Reboiler cost ($/day) | Total cost ($) |
|---|---|---|---|---|---|---|---|
| Acetate removal column | -325.382 | Cooling water (20-25) | 5,959.95 | 325.394 | LPS | 53,416.7 | 59,376.65 |
| Ethanol removal column | -33.9425 | Cooling water (20-25) | 621.719 | 64.4928 | MPS | 12,258.8 | 12,880.52 |
| Ethylene glycol revocery column | -81.1534 | Cooling water (20-25) | 1,486.47 | 110.248 | HPS | 23,813.5 | 25,299.97 |
| Propanol removal column | -21.7641 | Cooling water (20-25) | 398.649 | 23.2565 | LPS | 3,817.78 | 4,216.43 |
| Propanol pervaporation | | | | 5.01199 | LPS | 822.769 | 822.77 |
| Acetic acid separation column | -33.7479 | Cooling water (20-25) | 618.154 | 20.9731 | LPS | 3,442.94 | 4,061.09 |
| Cooler 3 | -4.1739 | Cooling water (20-25) | 76.45 | | | | 76.45 |

THe power of the electro-electrodialyser is 35 $kW$ per 30 ton and the flow rate through this unit is 225 ton each hour. The power of 8 units are needed, so the electicity consumption is 6,720 $kWh$. Multiplied with the electricity price gives an OpEx of $1,276.80 per day.

### Gas Product Separation

The operating cost for the $H_2$ PSA unit is $5 per $kg$ of $H_2$. With a total flow of 17,969.13 $kg\ day^{-1}$, the OpEx of the $H_2$ PSA is $89,845.63 per day. The power of the compressor before the ethylene separation column is 1,908.87 $kW$ which operates 24 hours a day. Using the electricity price, the OpEx is $8,704.45. The operating cost for the cooler is obtained from ASPEN PLUS V12 and is $4,366.08. The OpEx for the ethylene is also obtain from ASPEN PLUS V12, since there is no condenser and that the inlet temperature is so low, a cooling product can be created. This generates a valuable product which earns money, so the OpEx of the ethylene separation column is -$368.73 a day. The total CapEx of this section is $11,737,798.88, so the daily maintenance cost is $803.86.

### Heat Exchangers

The heat exchangers do not have any operating cost, but they require maintenance. The calculation for the OpEx is found in the table below.

Table C.27: Operating cost of the heat exchangers

| Unit | Value | Operating cost ($\$\ day^{-1}$) |
|---|---|---|
| Maintenance | 905,439.54 CapEx | 62.02 |

### Materials

Table C.28: The calculations of the operating cost for the used materials

| Materials | Price ($\$\ ton^{-1}$) | mass flow ($ton\ day^{-1}$) | Price per day ($\$\ day^{-1}$) |
|---|---|---|---|
| KOH | 506 | 1,086.704963 | 549,872.71 |
| $KHCO_3$ | 1,400 | 974.85967 | 1,364,803.54 |
| Ethylene glycol | 1,235 | 81.0366 | 100,080.20 |
| CaCO3 | 330 | 12.1065 | 3,995.15 |
| MDEA | 2,660 | 24,192 | 64,350,720.00 |

## C.2.2. Table Summaries

Table C.29: Operating and maintenance costs of each unit for the UPW production

| **Unit** | **Operating cost ($\$\ day^{-1}$)** | **Maintenance ($\$\ day^{-1}$)** | |
|---|---|---|---|
| Ultrafiltration | 0.00 | 57.06 | |
| UV treatment | 241.19 | 0.97 | [189] |
| Active carbon filter 1 | 0.00 | 7,900.23 | [190] |
| Active carbon filter 2 | 0.00 | 395.09 | [190] |
| Softener | 0.00 | 20.66 | [185] |
| Reverse osmosis 1 | 0.00 | 2,568.35 | [192] |
| Reverse osmosis 2 | 0.00 | 2,312.39 | [192] |
| Reverse osmosis 3 | 0.00 | 2,082.00 | [192] |
| Reverse osmosis 4 | 0.00 | 1,874,57 | [192] |
| Degasser | 5,116.32 | 128.90 | [186] |
| Electrodeionization | 7,209.96 | 3,64 | [174] |
| Pump 1 | 1,042.95 | 1.52 | |
| Pump 2 | 168.64 | 0.17 | |
| Pump 3 | 168.60 | 0.17 | |
| Pump 4 | 168.60 | 0.17 | |
| Pump 5 | 2,444.35 | 3.23 | |
| Pump 6 | 2,208.14 | 3.04 | |
| Pump 7 | 1,997.78 | 2.83 | |
| Pump 8 | 1,808.10 | 2.63 | |
| Pump 9 | 790.27 | 1.13 | |
| Pump 10 | 112.92 | 0.12 | |
| **Total** | **23,477.82** | **17,358.87** | |

Table C.30: Operating and maintenance costs of each unit for the gas cleaning process

| **Unit** | **Operating cost ($\$\ day^{-1}$)** | |
|---|---|---|
| $SO_2$ scrubber | 0.00 | |
| Cooler 1 | 9,075.94 | |
| Flash drum 1 | 0.00 | |
| COS reactor | 4,370.45 | |
| $H_2S$ scrubber | 0.00 | |
| Flash drum 2 | 0.00 | |
| Cooler 2 | 14,790.84 | |
| Flash drum 3 | 7,687.21 | |
| $CO_2$ PSA | 56,017.11 | [191] |
| CO PSA | 86,412.58 | [191] |
| $CO_2$ recycle PSA | 55,006.95 | [191] |
| CO recycle PSA | 103,129.70 | [191] |
| Maintenance | 1,495.06 | |
| **Total** | **337,985.84** | |

Table C.31: Operating costs of both electrolyzers

| **Unit** | **Operating cost ($\$\ day^{-1}$)** |
|---|---|
| Electrolyzer 1 | 316,915.48 |
| Electrolyzer 2 | 4,455,404.40 |
| Maintenance | 21,726.39 |
| **Total** | **4,794,046.27** |

Table C.32: Operating costs of the liquid product separation process

| **Unit** | **Operating cost ($\$\ day^{-1}$)** | |
|---|---|---|
| Acetate removal column | 59,376.65 | |
| Electro-electrodialyser | 901.29 | [188] |
| Acetic acid separation column | 4,061.09 | |
| Ethanol removal column | 12,880.52 | |
| Ethylene glycol recovery column | 25,299.97 | |
| Propanol removal column | 4,216.43 | |
| Propanol pervaporation | 822.77 | |
| Cooler 3 | 76.45 | |
| Maintenance | 775.91 | |
| **Total** | **108,411.08** | |

Table C.33: Operating cost of the gas product separation units

| **Unit** | **Operating cost ($\$\ day^{-1}$)** | |
|---|---|---|
| $H_2$ PSA | 89,845.63 | [193] |
| Compressor | 8,704.45 | |
| Cooler 4 | 4,366.08 | |
| Ethylene separation column | -368.73 | |
| Maintenance | 803.96 | |
| **Total** | **103,351.39** | |

Table C.34: Operating cost of the heat exchangers

| **Unit** | **Operating cost ($\$\ day^{-1}$)** |
|---|---|
| Heat exchanger 1 | 0.00 |
| Heat exchanger 2 | 0.00 |
| Heat exchanger 3 | 0.00 |
| Heat exchanger 4 | 0.00 |
| Heat exchanger 5 | 0.00 |
| Heat exchanger 6 | 0.00 |
| Maintenance | 62.02 |
| **Total** | **62.02** |

Table C.35: Operating cost of the used materials

| **Materials** | **Operating cost ($\$\ day^{-1}$)** | |
|---|---|---|
| KOH | 549,872.71 | [194] |
| KHCO3 | 1,364,803.54 | [195] |
| Ethylene glycol | 100,080.20 | [196] |
| $CaCO_3$ | 3,995.15 | [197] |
| MDEA | 64,350,720.00 | [198] |
| **Total** | **66,369,471.60** | |

Table C.36: Summary of all operating cost of different parts of the process

| **Unit** | **Operating cost ($\$\ day^{-1}$)** |
|---|---|
| Ultrapure water | 40,836.69 |
| Gas feed purification | 337,985.84 |
| Electrolyzers | 4,794,046.27 |
| Liquid product separation | 108,411.08 |
| Gas product separation | 103,351.39 |
| Heat exchangers | 62.02 |
| Materials | 66,369,471.60 |
| **Total** | **71,754,164.89** |

## C.3. Income

The income generated by selling the products is calculated in the table below. The $CO_2$ saving that is saved by not emitting $CO_2$ is also calculted using the net $CO_2$ consumption and the current $CO_2$ tax

Table C.37: Calculations for the total income from selling the products

| **Product** | **amount produced ($kg\ day^{-1}$)** | **Price ($\$\ kg^{-1}$)** | **Income ($\$\ day^{-1}$)** | |
|---|---|---|---|---|
| Acetic acid | 516,408 | 0.810 | 418,290.48 | [199] |
| Ethanol | 483,373 | 0.723 | 349,578.54 | [200] |
| Ethylene | 885,994 | 1.000 | 885,993.60 | [201] |
| Hydrogen | 18,183 | 1.100 | 20,001.21 | [202] |
| n-Propanol | 441,798 | 1.285 | 567,710.43 | [203] |
| $CO_2$ tax saving | 1,964,145 | 0.06078 | 121,055.09 | [175] |
| **Total** | | | **2,362,629.35** | |

The molecular weight of acetic acid, ethanol, ethylene, and n-propanol is 60.05, 46.06, 28.05, and 60.06 $g\ mol^{-1}$, respectively. Acetic acid and ethanol both require 4 electrons, ethylene 8 electrons, and n-propanol 12 electrons to be formed. Using the price per $kg$, amount of electrons needed for formation and how much $mol$ is present in 1 $kg$, the price per mole electrons consumed can be calculated. The calculations are shown in the table below.

Table C.38: Calculations for the income per mole electrons of each product

| | **Molecular weight ($g\ mole^{-1}$)** | **Income per $kg$** | $Mole\ kg^{-1}$ | **Income per mole** | **Electrons required to form** | **Income per mole electrons** |
|---|---|---|---|---|---|---|
| Acetic acid | 60.05 | 0.810 | 16.65 | 0,0486 | 4 | 0.0122 |
| Ethanol | 46.06 | 0.723 | 21.71 | 0,0333 | 4 | 0.0083 |
| Ethylene | 28.05 | 1.000 | 35.65 | 0,0281 | 8 | 0.0035 |
| n-Propanol | 60.06 | 1.285 | 16.64 | 0,0772 | 12 | 0.0064 |

## C.4. Net Present Value

An interest rate of 10% and an inflation of 2% each year is used. When a profit is made, a company has to pay 25.8% tax in The Netherlands. Since the yearly profit is negative, this tax does not have to be paid. The calculations for the base case are shown in Table C.39. The net profit, net earning, cash flow and cumulative present value are calculated using Equations C.28 to C.31. For the calculation of the NPV, the cost of MDEA is neglected, but in Table C.40 the NPV with the cost of MDEA is shown.

$$Net\ profit = (Total\ income - Total\ cost) * (1 + Inflation)^{Year-1} \tag{C.28}$$

$$Net\ earning = Net\ profit * (1 - Tax) \tag{C.29}$$

$$Cash\ flow = \frac{Net\ earning * 1}{(1 + Interest\ rate)^{Year}} \tag{C.30}$$

$$Cumulative\ present\ value\ (year) = Cumulative\ present\ value\ (year-1) + Cash\ flow\ (year) \tag{C.31}$$

Table C.39: Calculations of the Net Present Value in the base case

| Year | Capital Expenses | Net Profit | Net Earning | Cash Flow (Present Value) | Cumulative Present Value |
|---|---|---|---|---|---|
| 0 | -4,053,751,099 | | -4,053,751,099 | -4,053,751,099 | -4,053,751,099 |
| 1 | | -1,808,561,115 | -1,808,561,115 | -1,644,146,468 | -5,697,897,567 |
| 2 | | -1,844,732,338 | -1,844,732,338 | -1,524,572,180 | -7,222,469,747 |
| 3 | | -1,881,626,984 | -1,881,626,984 | -1,413,694,203 | -8,636,163,950 |
| 4 | | -1,919,259,524 | -1,919,259,524 | -1,310,880,079 | -9,947,044,029 |
| 5 | | -1,957,644,714 | -1,957,644,714 | -1,215,543,346 | -11,162,587,376 |
| 6 | | -1,996,797,609 | -1,996,797,609 | -1,127,140,194 | -12,289,727,569 |
| 7 | | -2,036,733,561 | -2,036,733,561 | -1,045,166,361 | -13,334,893,931 |
| 8 | | -2,077,468,232 | -2,077,468,232 | -969,154,262 | -14,304,048,193 |
| 9 | | -2,119,017,597 | -2,119,017,597 | -898,670,316 | -15,202,718,509 |
| 10 | | -2,161,397,949 | -2,161,397,949 | -833,312,475 | -16,036,030,984 |
| 11 | | -2,204,625,908 | -2,204,625,908 | -772,707,931 | -16,808,738,915 |
| 12 | | -2,248,718,426 | -2,248,718,426 | -716,510,991 | -17,525,249,906 |
| 13 | | -2,293,692,794 | -2,293,692,794 | -664,401,101 | -18,189,651,007 |
| 14 | | -2,339,566,650 | -2,339,566,650 | -616,081,021 | -18,805,732,027 |
| 15 | | -2,386,357,983 | -2,386,357,983 | -571,275,128 | -19,377,007,155 |
| | | | | **NPV ($millions)=** | **-19,377.01** |

Table C.40: Calculations of the Net Present Value in the base case with MDEA considered

| Year | Capital Expenses | Net Profit | Net Earning | Cash Flow (Present Value) | Cumulative Present Value |
|---|---|---|---|---|---|
| 0 | -4,053,751,099 | | -4,053,751,099 | -4,053,751,099 | -4,053,751,099 |
| 1 | | -24,331,313,115 | -24,331,313,115 | -22,119,375,559 | -26,173,126,658 |
| 2 | | -24,817,939,378 | -24,817,939,378 | -20,510,693,700 | -46,683,820,359 |
| 3 | | -25,314,298,165 | -25,314,298,165 | -19,019,006,886 | -65,702,827,245 |
| 4 | | -25,820,584,128 | -25,820,584,128 | -17,635,806,385 | -83,338,633,630 |
| 5 | | -26,336,995,811 | -26,336,995,811 | -16,353,202,284 | -99,691,835,914 |
| 6 | | -26,863,735,727 | -26,863,735,727 | -15,163,878,482 | -114,855,714,396 |
| 7 | | -27,401,010,442 | -27,401,010,442 | -14,061,050,956 | -128,916,765,352 |
| 8 | | -27,949,030,651 | -27,949,030,651 | -13,038,429,068 | -141,955,194,420 |
| 9 | | -28,508,011,264 | -28,508,011,264 | -12,090,179,681 | -154,045,374,101 |
| 10 | | -29,078,171,489 | -29,078,171,489 | -11,210,893,886 | -165,256,267,988 |
| 11 | | -29,659,734,919 | -29,659,734,919 | -10,395,556,149 | -175,651,824,137 |
| 12 | | -30,252,929,617 | -30,252,929,617 | -9,639,515,702 | -185,291,339,839 |
| 13 | | -30,857,988,209 | -30,857,988,209 | -8,938,460,015 | -194,229,799,853 |
| 14 | | -31,475,147,973 | -31,475,147,973 | -8,288,390,195 | -202,518,190,049 |
| 15 | | -32,104,650,933 | -32,104,650,933 | -7,685,598,181 | -210,203,788,230 |
| | | | | **NPV ($millions)=** | **-210,203.79** |

## C.5. Sensitivty Analysis

Both the parameters for the better and optimistic case can be found in Table 5.5. The NPV for the better and optimistic case are calculated in Tables C.41 and C.42. Since the net profit in the optimistic case is positive, tax is also included in the calculations for the NPV.

Table C.41: Calculations of the Net Present Value in the better case

| Year | Capital Expenses | Net Profit | Net Earning | Cash Flow (Present Value) | Cumulative Present Value |
|---|---|---|---|---|---|
| 0 | -4,053,751,099 | | -4,053,751,099 | -4,053,751,099 | -4,053,751,099 |
| 1 | | -467,001,532 | -467,001,532 | -424,546,848 | -4,478,297,947 |
| 2 | | -476,341,563 | -476,341,563 | -393,670,713 | -4,871,968,660 |
| 3 | | -485,868,394 | -485,868,394 | -365,040,116 | -5,237,008,776 |
| 4 | | -495,585,762 | -495,585,762 | -338,491,744 | -5,575,500,519 |
| 5 | | -505,497,477 | -505,497,477 | -313,874,162 | -5,889,374,682 |
| 6 | | -515,607,427 | -515,607,427 | -291,046,951 | -6,180,421,632 |
| 7 | | -525,919,575 | -525,919,575 | -269,879,900 | -6,450,301,532 |
| 8 | | -536,437,967 | -536,437,967 | -250,252,271 | -6,700,553,803 |
| 9 | | -547,166,726 | -547,166,726 | -232,052,105 | -6,932,605,908 |
| 10 | | -558,110,061 | -558,110,061 | -215,175,589 | -7,147,781,497 |
| 11 | | -569,272,262 | -569,272,262 | -199,526,455 | -7,347,307,952 |
| 12 | | -580,657,707 | -580,657,707 | -185,015,440 | -7,532,323,392 |
| 13 | | -592,270,861 | -592,270,861 | -171,559,772 | -7,703,883,164 |
| 14 | | -604,116,279 | -604,116,279 | -159,082,697 | -7,862,965,861 |
| 15 | | -616,198,604 | -616,198,604 | -147,513,047 | -8,010,478,908 |
| | | | | **NPV ($millions)=** | **-8,010.48** |

Table C.42: Calculations of the Net Present Value in the optimistic case

| Year | Capital Expenses | Net Profit | Net Earning | Cash Flow (Present Value) | Cumulative Present Value |
|---|---|---|---|---|---|
| 0 | -4.053.751.099 | | -4.053.751.099 | -4.053.751.099 | -4.053.751.099 |
| 1 | | 713.748.437 | 529.601.341 | 481.455.764 | -3.572.295.335 |
| 2 | | 728.023.406 | 540.193.367 | 446.440.799 | -3.125.854.535 |
| 3 | | 742.583.874 | 550.997.235 | 413.972.378 | -2.711.882.158 |
| 4 | | 757.435.552 | 562.017.179 | 383.865.296 | -2.328.016.862 |
| 5 | | 772.584.263 | 573.257.523 | 355.947.820 | -1.972.069.042 |
| 6 | | 788.035.948 | 584.722.673 | 330.060.705 | -1.642.008.337 |
| 7 | | 803.796.667 | 596.417.127 | 306.056.291 | -1.335.952.047 |
| 8 | | 819.872.600 | 608.345.469 | 283.797.651 | -1.052.154.395 |
| 9 | | 836.270.052 | 620.512.379 | 263.157.822 | -788.996.573 |
| 10 | | 852.995.453 | 632.922.626 | 244.019.071 | -544.977.502 |
| 11 | | 870.055.362 | 645.581.079 | 226.272.230 | -318.705.272 |
| 12 | | 887.456.470 | 658.492.701 | 209.816.068 | -108.889.205 |
| 13 | | 905.205.599 | 671.662.555 | 194.556.717 | 85.667.513 |
| 14 | | 923.309.711 | 685.095.806 | 180.407.138 | 266.074.651 |
| 15 | | 941.775.905 | 698.797.722 | 167.286.619 | 433.361.269 |
| | | | | **NPV ($millions)=** | **433,36** |

# D

# Appendix D

## D.1. Energy Analysis

Table D.1: Energy content of the liquid and gas products[204]

| Compound | Lower Heating Value ($MJ\ kg^{-1}$) | Amount produced ($kg\ hr^{-1}$) | Total Energy ($MJ\ hr^{-1}$) | Total energy ($MW$) |
|---|---|---|---|---|
| Acetic acid | 14.55 | 21,517.00 | 313,072.35 | 86.965 |
| Ethanol | 29.67 | 20,140.54 | 597,569.82 | 165.992 |
| Ethylene | 50.29 | 36,916.40 | 1,856,525.76 | 515.702 |
| Hydrogen | 141.58 | 757.62 | 107,263.84 | 29.796 |
| n-Propanol | 33.62 | 18,408.25 | 618,885.37 | 171.913 |

Table D.2: Energy consumption to isolate acetic acid

| **Compound** | **Total Energy ($MW$)** | |
|---|---|---|
| Acetic acid | | 86.965 |
| **Unit** | **Energy consumption ($MW$)** | **Relative energy consumption ($MW$)** |
| Acetic acid separation column | 157.192 | 65.098 |
| Electro-electrodialyser | 0.280 | 0.280 |
| Acetic acid removal column | 10.132 | 10.132 |
| **Total** | **167.604** | **75.510** |

Table D.3: Energy consumption to isolate ethanol

| **Compound** | **Total Energy ($MW$)** | |
|---|---|---|
| Ethanol | | 165.992 |
| **Unit** | **Energy consumption ($MW$)** | **Relative energy consumption ($MW$)** |
| Acetic acid separation column | 157.192 | 54.015 |
| Ethanol isolation column | 31.155 | 18.273 |
| **Total** | **188.348** | **72.288** |

Table D.4: Energy consumption to isolate ethylene

| **Compound** | **Total Energy ($MW$)** | |
|---|---|---|
| Ethylene | | 515.702 |
| **Unit** | **Energy consumption ($MW$)** | **Relative energy consumption ($MW$)** |
| Hydrogen PSA | 14.974 | 11.607 |
| Compressor | 5.660 | 5.660 |
| Cooler 4 | 5.924 | 5.924 |
| Ethylene separation column | -0.647 | -0.647 |
| **Total** | **25.911** | **22.544** |

Table D.5: Energy consumption to isolate hydrogen

| **Compound** | **Total Energy ($MW$)** | |
|---|---|---|
| Hydrogen | | 29.796 |
| **Unit** | **Energy consumption ($MW$)** | **Relative energy consumption ($MW$)** |
| Hydrogen PSA | 14.974 | 3.367 |
| **Total** | **14.974** | **3.367** |

Table D.6: Energy consumption to isolate n-propanol

| **Compound** | **Total Energy ($MW$)** | |
|---|---|---|
| n-Propanol | | 171.913 |
| **Unit** | **Energy consumption ($MW$)** | **Relative energy consumption ($MW$)** |
| Acetic acid separation column | 157.192 | 38.079 |
| Ethanol isolation column | 31.155 | 12.882 |
| Ethylene glycol column | 53.259 | 53.259 |
| n-Propanol separation column | 11.235 | 11.235 |
| n-Propanol pervaporation unit | 2.421 | 2.421 |
| **Total** | **255.262** | **117.876** |

# Appendix E

## E.1. $CO_2$ Emission

Table E.1: $CO_2$ emission from different energy sources[54]

| Source | g CO2/kWh |
|---|---|
| Coal | 820 |
| Nuclear | 12 |
| Wind | 12 |
| Solar | 41 |
| Coal with CCS | 200 |
| Gas | 490 |

Table E.2: $CO_2$ emission of each individual unit from different energy sources

| Unit | CO2 emmision with gas ($kg\ day^{-1}$) | Coal | Nuclear | Wind | Solar | Coal with CCS | Percentage of all |
|---|---|---|---|---|---|---|---|
| Acid removal column | 1.848.580,00 | 3.093.542,04 | 45,271.35 | 45,271.35 | 154,677.10 | 754,522.45 | 10.412% |
| EtOH removal column | 366,387.00 | 613,137.43 | 8,972.74 | 8,972.74 | 30,656.87 | 149,545.71 | 2.064% |
| Ethylene Glycol revoceyr column | 626,322.00 | 1,048,130.69 | 15,338.50 | 15,338.50 | 52,406.53 | 255,641.63 | 3.528% |
| PrOH removal column | 132,121.00 | 221,100.45 | 3,235.62 | 3,235.62 | 11,055.02 | 53,926.94 | 0.744% |
| PrOH pervaporation | 28,473.40 | 47,649.36 | 697.31 | 697.31 | 2,382.47 | 11,621.80 | 0.160% |
| Electrodialyzer | 3,292.80 | 5,510.40 | 80.64 | 80.64 | 275.52 | 1,344.00 | 0.019% |
| Cooler 3 | 0.00 | 0.00 | 0.00 | 0.00 | 0.00 | 0.00 | 0.000% |
| Acid separatsion column | 119,149.00 | 199,392.20 | 2,917.93 | 2,917.93 | 9,969.61 | 48,632.24 | 0.671% |
| Electrolyzer 1 | 817,308.33 | 1,367,740.48 | 20,015.71 | 20,015.71 | 68,387.02 | 333,595.24 | 4.603% |
| Electrolyzer 2 | 11,490,253.45 | 19,228,587.40 | 281,393.96 | 281,393.96 | 961,429.37 | 4,689,899.37 | 64.719% |
| Pumps UPW | 28,137.18 | 47,086.71 | 689.07 | 689.07 | 2,354.34 | 11,484.56 | 0.158% |
| UV treatment | 622.03 | 1,040.94 | 15.23 | 15.23 | 52.05 | 253.89 | 0.004% |
| Electrodionization | 3,091.12 | 5,172.89 | 75.70 | 75.70 | 258.64 | 1,261.68 | 0.017% |
| COS reactor | 237,945.96 | 398,195.28 | 5,827.25 | 5,827.25 | 19,909.76 | 97,120.80 | 1.340% |
| Cooler 1 | 185,129.00 | 309,807.71 | 4,533.77 | 4,533.77 | 15,490.39 | 75,562.86 | 1.043% |
| Cooler 2 | 301,701.60 | 504,888.39 | 7,388.61 | 7,388.61 | 25,244.42 | 123,143.51 | 1.699% |
| Flash 3 | 266,029.00 | 445,191.39 | 6,515.00 | 6,515.00 | 22,259.57 | 108,583.27 | 1.498% |
| CO2PSA | 204,655.42 | 342,484.58 | 5,011.97 | 5,011.97 | 17,124.23 | 83,532.83 | 1.153% |
| CO2PSA recycle | 200,964.85 | 336,308.53 | 4,921.59 | 4,921.59 | 16,815.43 | 82,026.47 | 1.132% |
| COPSA | 315,703.58 | 514,538.01 | 7,529.82 | 7,529.82 | 25,726.90 | 125,497.08 | 1.732% |
| COPSA recycle | 376,778.64 | 614,078.98 | 8,986.52 | 8,986.52 | 30,703.95 | 149,775.36 | 2.067% |
| H2PSA | 176,097.44 | 294,693.67 | 4,312.59 | 4,312.59 | 14,734.68 | 71,876.51 | 0.992% |
| Compressor | 22,448.31 | 37,566.56 | 549.75 | 549.75 | 1,878.33 | 9,162.58 | 0.126% |
| Cooler 4 | 28,607.28 | 47,873.41 | 700.59 | 700.59 | 2,393.67 | 11,676.44 | 0.161% |
| Absorber 1 | 0.00 | 0.00 | 0.00 | 0.00 | 0.00 | 0.00 | 0.000% |
| Absorber 2 | 0.00 | 0.00 | 0.00 | 0.00 | 0.00 | 0.00 | 0.000% |
| Ethylene sep column | -7,604.50 | -12,725.90 | -186.23 | -186.23 | -636.29 | -3,103.88 | -0,43% |
| **Total** | **17,772,193.89** | **29,710,991.62** | **434,795.00** | **434,795.00** | **1,485,549.58** | **7,246,583.32** | |
| Relative emission | 742.16% | 1,240.72% | 18.16% | 18.16% | 62.04% | 302.61% | |

# Appendix F

Table F.1: Pure component properties

| Component Name | | Technological Data | | | | | | | | Health &Safety data | | | | | | Notes |
|---|---|---|---|---|---|---|---|---|---|---|---|---|---|---|---|---|
| Design | Systematic | Formula | Mol. Weight $g/mol$ | Phase | Boiling Point [1] $°C$ | Melting Point [1] $°C$ | Flash Point [1] $°C$ | Liquid Density [2] $kg/m^3$ | Vapour Density [3] $kg/m^3$ | Auto-ignition Temp. [1] $°C$ | Lower Explosion Limit (LEL ) % | Upper Explosion % | MAC Value [4] $mg/m^3$ | LD50 Oral [5] $g$ | Chemical Reactivity | |
| Carbon dioxode | Carbon dioxide | $CO_2$ | 44,009 | V | -78,48 | -56,50 | not flammable | 1101 | 1,977 | n.a. | n.a. | n.a. | 9000 | n.a. | Non reactive | [205, 206] |
| Carbon monoxide | Carbon monoxide | CO | 28,010 | V | -191,50 | -205,02 | -191 | 789 | 1,145 | 609 | 12,5 | 74,2 | 29 | n.a. | Can react with oxygen and water | [207, 208] |
| Formic acid | Methanoic acid | HCOOH | 46,025 | L | 100,80 | 8,30 | 69 | 1220 | n.a. | 601 | 14 | 34 | 10,98 | 280 | Reducing properties | [209, 210] |
| Formaldehyde | Methanal | HCHO | 30,026 | V | -19,00 | 92,00 | 64 | 815,3 | 1,342 | 430 | 7 | 73 | 0,15 | 7 | | [211–213] |
| Methanol | Methyl alcohol | $CH_3OH$ | 32,04 | L | 64,70 | -97,60 | 12 | 792 | n.a. | 385 | 6 | 36 | 133 | 51,5 | Highly flammable | [214–217] |
| Methane | Methane | $CH_4$ | 16,043 | V | -161,50 | -182,46 | -188 | n.a. | 0,717 | 537 | 4,4 | 17 | n.a. | n.a. | Reacts with oxygen | [218, 219] |
| Oxalic acid | Ethanedoic acid | $H_2C_2O_4$ | 90,034 | S | n.a. | 190,00 | 166 | n.a. | n.a. | n.a. | n.a. | n.a. | 1 | 525 | Corrosive | [220, 221] |
| Ethene | Ethene | $C_2H_4$ | 28,054 | V | -103,70 | 169,20 | -136 | n.a. | 1,178 | 542,8 | 2,75 | 28,6 | 11500 | n.a. | Polymerization | [222, 223] |
| Ethanol | Ethyl alcohol | $C_2H_5OH$ | 46,069 | L | 78,20 | -114,10 | 14 | 789,5 | n.a. | 365 | 3,3 | 19 | 960 | 511 | Flammable | [222, 224] |
| Ethane | Ethane | $C_2H_6$ | 30,07 | V | -88,50 | -182,80 | -135 | n.a. | 1,3562 | 472 | 2,9 | 13 | n.a. | n.a. | Highly flammable | [225, 226] |
| n-Propanol | Propan-1-ol | $C_3H_7OH$ | 60,096 | L | 97,50 | -126,00 | 22 | 803 | n.a. | 371 | 2,2 | 13,7 | 500 | 118,9 | Flammable | [227, 228] |
| Hydrogen | Hydrogen | $H_2$ | 2,016 | V | -252,90 | 259,20 | n.a. | n.a. | 0,0899 | 585 | 18,3 | 59 | n.a. | n.a. | Explosive | [229–232] |
| Water | Dihydrogen monoxide | $H_2O$ | 18,015 | L | 99,98 | 0,00 | not flammable | 997 | n.a. | n.a. | n.a. | n.a. | n.a. | 6300 | | [233, 234] |
| Oxygen | Dioxygen | $O_2$ | 15,999 | V | 183,00 | -218,80 | n.a. | n.a. | 1,429 | n.a. | n.a. | n.a. | n.a. | n.a. | Oxidixer | [235] |
| Nitrogen | Dinitrogen | $N_2$ | 28,014 | V | -195,80 | -209,86 | not flammable | n.a. | 1,2506 | n.a. | n.a. | n.a. | n.a. | n.a. | | [236] |
| Argon | Argon | Ar | 39,95 | V | -185,85 | -189,34 | not flammable | n.a. | 1,784 | n.a. | n.a. | n.a. | n.a. | n.a. | | [237] |
| Hydrogen sulfide | Hydrogen sulfide | $H_2S$ | 34,08 | V | -59,55 | 85,50 | 82,4 | n.a. | 1,363 | 232 | 4,3 | 46 | 2,3 | 44,38 | | [77, 219] |
| Carbonyl sulfide | Carbon oxide sulfide | COS | 60,076 | V | -50,20 | -138,80 | n.a. | n.a. | 2,456 | n.a. | 12 | 29 | 12 | 59,5 | Highly flammable | [238–240] |
| Sulfur Dioxide | Sulfur dioxide | $SO_2$ | 64,064 | V | -10,00 | -75,50 | not flammable | n.a. | 2,629 | n.a. | n.a. | n.a. | 5 | 210 | | [241–243] |
| Nitrogen dioxide | Nitrogen dioxide | $NO_2$ | 46,006 | V | 21,15 | -9,30 | not flammable | n.a. | 1,88 | n.a. | n.a. | n.a. | 1,91 | 7000 | Oxidixer | [244–247] |

Notes:
[1] At 101,325 $Pa$
[2] Density at 25 $°C$
[3] At 0 $°C$
[4] According to the Dutch law
[5] Oral ingestion in ($g$) for a male of 70$kg$ weight

# G

# Appendix G

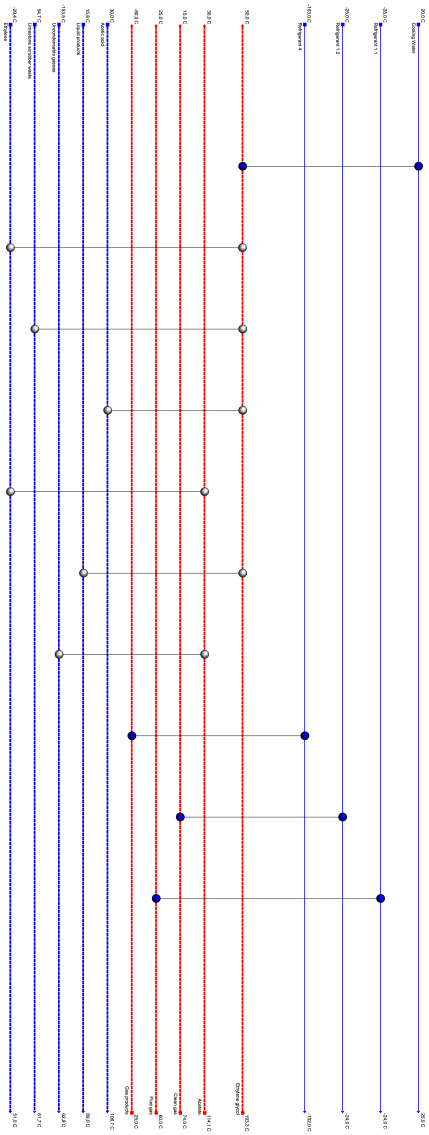

Figure G.1: Heat exchange diagram

# H

# Appendix H

Table H.1: Concentrations of ions and oxygen after the liquid feed stream purification section

| **Compound** | **Concentration ($\mu g\ L^{-1}$)** |
|---|---|
| $Al^{3+}$ | 8.593E-06 |
| $Ba^{2+}$ | 1.838E-06 |
| $Ca^{2+}$ | 8.978E-05 |
| $Fe^{2+}$ | 1.195E-05 |
| $Pb^{2+}$ | 0 |
| $Mg^{2+}$ | 6.753E-05 |
| $Na^{+}$ | 0.002769 |
| $K^{+}$ | 9.273E-05 |
| $Sr^{2+}$ | 9.704E-06 |
| $Zn^{2+}$ | 0 |
| $NH_4^{+}$ | 2.006E-06 |
| $H_3O^{+}$ | 1.307 |
| $OH^{-}$ | 1.168 |
| $Br^{-}$ | 3.976E-06 |
| $Cl^{-}$ | 4.880E-06 |
| $HCO_3^{-}$ | 0.004708 |
| $CO_3^{2-}$ | 6.994E-05 |
| $O_2$ | 2.442 |

Table H.2: Concentrations of gas impurities after the gas feed stream purification section

| **Compound** | **Concentration (ppm)** |
|---|---|
| $NO_2$ | 28 |
| $SO_2$ | 16 |
| COS | 0.74 |
| $H_2S$ | 5.48 |